DISS. ETH NO. 24001

Kinematic and Kinetic Assessments of Upper Limb Function in Patients with Neurological Injury

A thesis submitted to attain the degree of

DOCTOR OF SCIENCES of ETH ZURICH

(Dr. sc. ETH Zurich)

presented by

WERNER LOUIS PAUL POPP

MSc ETH HMS, ETH Zurich

born on 01.10.1982

citizen of Bischofszell (TG), Steinach (SG) and France

accepted on the recommendation of

Prof. Dr. Roger Gassert (examiner)

Prof. Dr. Armin Curt (co-examiner)

Prof. Dr. Christina M. Spengler Walder (co-examiner)

Dr. Michelle Starkey (co-examiner)

2017

Acknowledgement

This thesis is the result of four and half years of research at the Rehabilitation Engineering Lab (RELab) of the ETH Zurich and at the Spinal Cord Injury Center of the University Hospital Balgrist. This thesis would not have been possible without the help from a number of people to which I would like to express my sincerest gratitude.

First of all, to Roger Gassert, who gave me the opportunity to pursue a PhD in such a dynamic lab as the RELab. I am deeply grateful for your motivation, understanding, and the incredibly helpful feedback in an inspiring work atmosphere.

From the Paralab side, I received great support from Michelle Starkey and Armin Curt, who guided me through my PhD, and who made it possible to conduct research in a clinical environment. Thank you.

Thank you also to Christina Spengler, who co-supervised my thesis with insightful inputs, and for making the two energy expenditure experiments possible.

I would like to express my sincere gratitude to Olivier Lambercy for always being available for discussions and for being incredibly supportive. I have learned a lot from you.

A special shout out goes to Mike Domenik Rinderknecht, for enticing discussions about statistics, LabVIEW, and MATLAB, and for critically reviewing this thesis. Thanks as well for the ever-refreshing dry and dark humor during the hard life of a PhD.

Derek Kamper made it possible for me to be part of an exciting and challenging study. Thanks for that and your positive and constructive feedback.

Thank you, Kaspar Leuenberger, fort the ongoing support for the ReSense sensors and for the helpful inputs regarding the design of the algorithms.

I would especially like to thank Mike Brogioli, Sophie Schneider, Urs Albisser and Fabienne Hasler for the precious and fruitful collaboration, and for the many good times we had within our little REACT group.

A very special thanks goes to Lea Richner for being an excellent student and with whom collaborating on various projects was a great pleasure.

Furthermore, I would like to thank all members of the RELab and the Paralab for the fruitful discussions and the good times. I really enjoyed being a part of both labs during work but also during leisure time activities such as the ski weekend, Oktoberfest and various parties. I would especially thank Camila Shirota for the help in the revision of this manuscript and Gunda Johannes for all the spontaneous help during writing. Moreover, I would like to thank Jean-Claude Metzger and Auralius Manurung for the help in improving the ReFlex robot and for the discussions on control and design related aspects. Last but not least I really appreciated the discussions about general aspects of life with Melanie Schmidhalter, Stephanie van der Lely, Eve Huber, Patrick Grabher, Lea Awai, Jenny Haefeli, Julio Duenas, Tobias Bützer, Mike Tucker, Frieder Wittmann, Sven Zwicker, Bogdan Vigaru, Raphael Zimmermann, James Sulzer, Stefan Schrade, Dominic Wyser, Pascal Wespe, Maya Kamber and Raffaele Ranzani.

Moreover, I would like to express my appreciation to all the students who contributed with their work to the success of this thesis: Lara Arcari, Remo Eiholzer, Karin Akermann, Deborah Bergmann, Larissa Angst, Kerrin Weiss, Thi Dao Nguyen, Simone Huber, Franziska Naef, Alina Giger, Ueli Baumgartner and Jasmin Egloff.

This work was supported by the National Center of Competence in Research on Neural Plasticity and Repair (NCCR Neuro) of the Swiss National Science Foundation, by the Clinical Research Priority Program (CRPP) for Neuro-Rehab of the University of Zurich, by the International Foundation for Research in Paraplegia (IRP), and by the Swiss Paraplegic Foundation (SPS). I am grateful for their financial support.

Finally, my sincere thanks go to my family and friends who supported me during all the years and who helped and motivated me in every situation.

Abstract

Standard clinical assessments such as the Fugl-Meyer Assessment or the Graded and Redefined Assessment of Strength, Sensibility and Prehension (GRASSP) are often used as diagnostic tools in clinical routine of stroke and spinal cord injury (SCI) therapy. Even though clinicians can benefit from using them to assess levels of impairment, such clinical assessments have a number of major drawbacks and can therefore only be used in a limited way in research. In order to track functional recovery, level of sensorimotor impairment, degree of compensation, and levels of activity, objective and sensitive assessment tools are needed. In addition to good clinimetric properties, such as high reliability and validity, these assessment tools furthermore should allow for continuous long-term monitoring of physical activity not only during rehabilitation but also outside of the therapy.

Such objective and sensitive assessment tools would allow researchers and clinicians to evaluate the effect of different interventions as well as help gain new insights in biomechanics and neuroscience. Improvements in robotic and sensor technology have created new opportunities for the design of assessment methods beyond what is possible with standardized clinical assessments. The aim of this thesis was to develop objective kinematic and kinetic assessments of the upper-limb function for individuals with a neurological injury. Two assessment tools were developed.

The first assessment tool quantifies the capacity of the upper-limb with kinematic and kinetic measures provided by a robotic system under laboratory settings. A first study was conducted to minimize confounds originating from poor ergonomic design, which in turn could negatively affect muscle activation patterns. Following this step, we used robotic systems with these ameliorated ergonomics to explore the neuronal control of finger and wrist muscles, as a better understanding would help the design of more efficient therapy approaches. We conducted two studies where we investigated the interdependence of wrist and digit control under static condition in healthy subjects and stroke patients with moderate hand impairment. In these experiments, subjects were asked to generate maximum precision grip force at different wrist angles under two wrist stabilization conditions (self- and externally stabilized). The results of these studies showed that both groups were able to benefit from the external wrist stabilization, and that both groups seem to have an optimal but different wrist posture for

generating maximum precision grip force (healthy: 22° of extension, stroke: 3° of extension). Furthermore, strong muscle synergies were found in the healthy group independent of wrist posture or wrist stabilization. Surprisingly, the same muscle synergies were also present in the stroke survivor group, although not as prominent. Stroke survivors additionally showed a strong muscle synergy of their intrinsic hand muscles, which was not found in the healthy group. Together with the relatively high intrinsic muscle activation, this suggests that stroke survivors rely more on the intrinsic muscles for generating force in a precision grip than neurologically intact people. In summary, the robotic systems used can be utilized as an objective kinematic and kinetic assessment tool of wrist and hand function and are a powerful tool to investigate motor control and motor learning, joint properties or proprioception.

The second assessment tool developed within this thesis is a tool for SCI research and can be applied both in daily clinical routine and in the home environment. Its novelty lies in the fact that it is able to continuously and objectively monitor upper-limb activity not only during, but also outside of therapy sessions. This assessment method is based on data provided by wearable inertial measurement units (IMU) and dedicated algorithms, and provides information about general amount and intensity of upper limb activity in the context of different activities of daily living. The first algorithm provides precise and reliable continuous measures of wheel kinematics and type of wheelchair propulsion. The second algorithm provides continuous measures of energy expenditure in wheelchair-bound individuals. These algorithms build a basis for an evaluation framework for upper-limb activity of wheelchair-bound individuals with SCI. The data to develop and evaluate them was collected in two studies. In total, 51 wheelchair-bound subjects with a spinal cord injury at the chronic stage were equipped with wearable sensors. This assessment framework has already been used in two multi-center studies investigating the correlation between sensor metrics and clinical assessment scores, and investigating the change of upper-limb activity during the initial rehabilitation following SCI.

The two novel assessment methods, which resulted from this work, can be used to explore sensorimotor control and the mechanisms underlying sensorimotor impairments. Furthermore, our long-term activity monitoring tool can provide multiple novel insights: Firstly, it can help characterize changes in physical

activity during the course of rehabilitation in general. Secondly, it can elucidate changes in physical activity resulting from one intervention compared to another. Finally, by tracking activity outside of the intervention, it may uncover differences in baseline activity of participants which is believed to be a common confound in otherwise randomized-controlled trials. In summary, both assessment methods provide information beyond what is possible with current standard clinical assessments.

Zusammenfassung

Gängige klinische Assessments, wie zum Beispiel das Fugl-Meyer Assessment oder das GRASSP Assessment (Graded and Redefined Assessment of Strength, Sensibility and Prehension) werden im klinischen Alltag oft im Rahmen der Diagnose und Therapie von Schlaganfall und Rückenmarksverletzung verwendet. Obwohl diese Assessments für Kliniker ein nützliches Werkzeug zur Beurteilung von körperlichen Beeinträchtigungen darstellen, können sie nur begrenzt in der Forschung eingesetzt werden, da sie eine Vielzahl von Limitationen aufweisen. Um das Level der funktionellen Genesung, das Level der sensomotorischen Beeinträchtigung, den Grad der Kompensation und das allgemeine Aktivitätsniveau messen zu können, braucht es sensitive und objektive Assessments. Zusätzlich zu guten Gütekriterien wie Reliabilität und Validität, müssen diese Assessments die physische Aktivität auch kontinuierlich über eine längere Zeitspanne messen können, innerhalb wie auch ausserhalb der Therapiezeiten.

Solche objektiven und sensitiven Assessments könnten von Forschern und Klinikern benutzt werden, um sowohl den Effekt von verschiedenen Interventionen zu untersuchen, als auch um neue Einsichten in die Biomechanik und Neurowissenschaften zu gewinnen. Der technologische Fortschritt hat neue Möglichkeiten für das Entwickeln von Assessmentmethoden eröffnet, welche jenseits der Möglichkeiten von existierenden klinischen Assessments liegen. Das Ziel dieser Dissertation war es, neue objektive kinematische und kinetische Assessmentmethoden für die Evaluation der Funktion der oberen Extremitäten in neurologischen Patienten zu entwickeln. Um dies zu erreichen, wurden zwei separate Methoden entwickelt.

Die erste, im Rahmen dieser Arbeit, entwickelte Assessmentmethode quantifiziert die Kapazität der oberen Extremitäten mit Hilfe von kinematischen und kinetischen Messungen durch den Einsatz eines Roboters. Eine erste Studie wurde durchgeführt, um den Effekt von Störfaktoren, beispielsweise auf die Muskelaktivierung, zu minimieren, welche aus einem nicht optimalen ergonomischen Roboterdesign hervorgerufen werden kann. Anschliessend haben wir Roboter mit ergonomischen Verbesserungen verwendet, um die neuronale Kontrolle der Finger- und Handgelenksmuskulatur zu erforschen, da ein tieferes Verständnis dieser helfen könnte, bessere Therapiemethoden zu entwickeln. Dazu haben wir

zwei Studien durchgeführt, die das Ziel hatten, die gegenseitige Abhängigkeit der muskulären Kontrolle der Finger und des Handgelenks in gesunden Personen sowie in Personen mit einem Schlaganfall, zu untersuchen. In diesen Studien mussten die Teilnehmer ihre Maximalkraft in einem Präzisionsgriff, bei verschiedenen Handgelenkswinkeln und bei zwei Arten der Handgelenksstabilisierung (Eigenstabilisierung und externe Stabilisierung), aufbringen. Die Studie zeigte, dass beide Probandengruppen mehr Kraft mit der externen Stabilisierung aufbringen können und dass beide Gruppen einen optimalen Handgelenkswinkel besitzen (Gesunde: 22° Extension, Schlaganfall: 3° Extension), um die Maximalkraft mit den Fingern erzielen zu können. Des Weiteren wurden starke Muskelsynergien, unabhängig von der Handgelenksstabilisierung, bei der unbeeinträchtigten Probandengruppe gefunden. Überraschenderweise waren diese Synergien auch bei den Probanden mit einem Schlaganfall vorhanden, wenn auch weniger stark ausgeprägt. Zusätzlich zeigte diese Probandengruppe starke Muskelsynergien der intrinsischen Handmuskulatur. Zusammen mit einer erhöhten Aktivität der intrinsischen Muskeln führt dies zum Schluss, dass Personen nach einem Schlaganfall, im Gegensatz zu gesunden Personen, sich stärker auf die intrinsischen Muskeln für die Kraftgenerierung bei den Fingern verlassen müssen. Zusammenfassend kann gesagt werden, dass Roboter für objektive kinematische und kinetische Assessments der Hand und der Finger eingesetzt werden können und dass sie ein vielversprechendes Werkzeug für das Erforschen der motorischeren Kontrolle, des motorischen Lernens, der Gelenkseigenschaften, sowie der Propriozeption sein können.

Das zweite, im Rahmen dieser Arbeit, entwickelte Assessment ist ein Werkzeug für die Forschung im Bereich der Querschnittslähmung, welches sowohl in der Klinik als auch in der Heimumgebung eingesetzt werden kann. Die Stärke dieses Assessments liegt darin, dass es kontinuierliche und objektive Messungen der Armaktivität liefern kann, sowohl während der Therapie, als auch ausserhalb der Therapie. Dieses Assessment basiert auf Daten von tragbaren Inertialsensoren und liefert mithilfe zweier Algorithmen Informationen über die Menge und die Intensität von Armbewegungen im Kontext verschiedener Alltagsaktivitäten. Der erste Algorithmus liefert präzise und reliabel Messwerte über die Radkinematik eines Rollstuhls und über die Art der Rollstuhlfortbewegung. Der zweite Algorithmus liefert kontinuierliche Messwerte bezüglich des Energieverbrauchs der Person im Rollstuhl. Zusammen bilden diese beiden Algorithmen die Grundlage für eine Evaluierung und Quantifizierung der Aktivität

der oberen Extremitäten von Rollstuhlfahrern mit einer Querschnittslähmung. Die beiden Algorithmen wurden mithilfe von Daten aus zwei Studien entwickelt, in denen insgesamt 51 Rollstuhlfahrer mit mehreren Sensoren ausgestattet wurden. Dieser Ansatz wurde bereits in zwei multizentrischen Studien eingesetzt, die einerseits zum Ziel hatten, Sensormessdaten mit klinischen Assessmentwerten zu korrelieren, andererseits die Veränderung der Armaktivität von Patienten während der Erstrehabilitation zu erfassen.

Die beiden, aus dieser Arbeit resultierenden, neuen Assessmentmethoden können für das Erforschen der sensomotorischen Kontrolle sowie grundlegender Mechanismen von sensomotorischen Einschränkungen verwendet werden. Des Weiteren kann das sensoren-basierte Assessment mehrere neue Einsichten liefern: Erstens kann es grundsätzlich eingesetzt werden, um Veränderungen der Aktivität während der Rehabilitation zu erfassen. Zweitens kann es dazu verwendet werden, den Einfluss verschiedener Interventionen auf die physische Aktivität zu untersuchen. Drittens kann das Assessment dazu benutzt werden, die Grundaktivität eines Patienten zu messen, ein Punkt, der bereits als Störfaktor in randomisierten Interventionsstudien bekannt ist. Zusammenfassend kann gesagt werden, dass beide Assessmentmethoden zusätzliche Informationen zu den Ergebnissen gängiger klinischer Assessments generieren können.

Contents

1 General Introduction

Neurological conditions such as stroke, Parkinson's disease (PD), traumatic brain injury (TBI), multiple sclerosis (MS), cerebral palsy (CP), or spinal cord injury (SCI) can lead to severe sensorimotor impairments. Although the resulting motor symptoms may vary between the different neurological conditions, all of them lead to reduced quality of life of the affected person (Wyndaele and Wyndaele, 2006, Cramer et al., 2011, Olanow et al., 2009, Rudick and Miller, 2008).

In more details, sensorimotor impairments of the upper-limb can lead to difficulties in conducting basic activities of daily living such as brushing teeth, self-feeding, dressing or manipulating objects in general. In contrast to neurodegenerative diseases (e.g., MS), functional recovery (e.g. through neuroplasticity supported by intensive therapy) is possible after stroke and SCI. However, the extent of the recovery is highly variable and affected individuals show different levels of sensorimotor impairment. In order to understand the course of recovery, sensitive and objective assessment tools are needed. Current clinical assessments suffer from many disadvantages leading to limited applicability in clinical practice and research.

Therefore, this thesis will focus on improving the assessment of upper-limb function in stroke and SCI using a technology based approach. The algorithms and assessment concepts developed in the context of this thesis could be easily adapted to other neurological conditions.

1.1 Stroke

Stroke is one of the leading causes of long-term disability worldwide (Mozaffarian et al., 2015) and out of the 10 million stroke survivors every year, approximately 60% suffer from severe long-term disabilities (Kwakkel et al., 2003). The worldwide incidence rate of stroke varies from 1.3 to 4.1 per 1000 people (Feigin et al., 2003) and in Switzerland this number lies at 2.96 per 1000 people resulting in approximately 14000 stroke survivors being discharged from the hospital per year (Meyer et al., 2009).

Stroke results from a critical disruption of the blood supply to the brain, which leads to damage of the neurons in the affected brain regions. A stroke can be either the result of a blockage (ischemic stroke) or a rupture (hemorrhagic stroke) of a blood vessel. Ischemic strokes occur in approximately 87% of the cases (Lloyd-Jones et al., 2009) as a result of an obstruction of a blood vessel (thrombosis, embolism, or systemic hypoperfusion) which leads to an undersupply of the brain tissue with blood (Hellier, 2014). Hemorrhagic strokes can further be separated into a cerebral hemorrhage, which is a bleeding within the brain, and subarachnoid hemorrhage, which is a bleeding into the subarachnoid space. In hemorrhagic strokes, the brain tissue is damaged by a hematoma, which is caused by either a brain aneurism or vessel rupture. A hemorrhagic stroke can affect larger brain areas than an ischemic stroke and therefore, the consequences can be more severe (Hellier, 2014). Depending on the brain area, which is damaged, a wide range of impairments can occur. This damage can affect for example vision, hearing, taste, smell, mood, cognition, memory, speech, or behavior. Furthermore, 80% of the stroke survivors suffer from persistent motor deficits such as weakness and hyperexcitability of muscles, loss of interjoint coordination, abnormal movement synergies, tremor, spasticity or loss of control of certain muscle groups (Cirstea and Levin, 2000, Rathore et al., 2002, Kamper et al., 2006). Additionally, 50% of stroke survivors show somatosensory deficits (Carey, 1995) which have been associated with poor prognosis for post-stroke functional recovery (Abela et al., 2012, Sullivan and Hedman, 2015). Hemiparesis is the most common condition in stroke and can affect the motor as well as the sensory system (Cirstea and Levin, 2000). Such sensorimotor deficits often affect the arm and hand of a patient, which in turn can dramatically influence the patient's independence, as human interaction with the environment strongly

relies on upper-limb function. The main reason for reduced independence arises from the deficits in the grasping and manipulation of objects with the hand. At the level of the hand the aforementioned sensorimotor deficits include reduced grip strength (Sunderland et al., 1989), weakness in finger extensors (Kamper et al., 2003, Kamper et al., 2006), hyperexitability of the flexors (Kamper et al., 2003), abnormal muscle activation patterns (Kamper et al., 2003) and the inability to activate fingers individually (Raghavan et al., 2006). Around 40% of chronic stroke survivors have major impairments in hand function (Duncan et al., 2003) and the probability to regain a good level of functional recovery is considered low (Kwakkel et al., 2003). It has been shown that the presence of finger extension at the very acute stage of stroke (72 hours) is a key predictor for functional recovery (Nijland et al., 2010, Stinear et al., 2012).

1.2 Spinal cord injury

SCI results from damage to neurons within the spinal cord. An SCI can either have a traumatic or a non-traumatic cause. Traumatic SCIs most often occur after motor vehicle accidents and falls and involve traumatic contusions or compressions (Stover and Fine, 1987). Non-traumatic SCIs can, for example, result from infections, ischemia or tumors. Worldwide, the annual incidence rate for SCI lies between 10-84 new cases per million people (Wyndaele and Wyndaele, 2006). The estimated prevalence of SCI lies between 223-755 cases per million. On average, a SCI occurs at an age of 33 years, and men are four times more often affected than women (Wyndaele and Wyndaele, 2006). The limited capacity of spontaneous regeneration of axons and the limited fiber growth makes SCI an irreversible injury, which can lead to long-lasting impairments in many cases.

Depending on the neurological level of injury (NLI), the injuries can either be cervical (C1-C8), thoracic (T1-T12), lumbar (L1-L5) or sacral (S1-S5). In case of NLI at T1 or above, a partial or a total loss of control of all four limbs and the trunk can occur, which is called tetraplegia. The partial or total loss of the lower-limb function is called paraplegia. As the spinal cord plays an important role in nearly all body functions, someone suffering an SCI can show a wide range of symptoms, such as muscle paralysis in the arms, trunk and legs, impairments of the somatosensory or the autonomic nervous system (e.g. heart, bladder), the extent of which depend on the NLI and the extent of the lesion. Around 70% of the SCI survivors suffer from persistent motor deficits and almost all tetraplegic individuals show somatosensory deficits of the upper-limb (NSCISC, 2010). The motor deficits in SCI can range from completely paralyzed muscles, to weak muscles, to uncontrollable muscle contractions whereas the sensory deficits range from pain to complete loss of sensation in the related dermatomes (Adams and Hicks, 2005). Similar to stroke, such sensorimotor deficits of the upper-limb can affect the person's ability to grasp and manipulate objects, which is essential for most activities of daily living (Lambercy et al., 2007).

The results of a survey of over 300 participants with a tetraplegia showed that hand and arm function was what most patients would like to regain (Anderson, 2004). Furthermore, Rudhe and van Hedel found a strong correlation between the upper extremity motor score and independence in self-care, which

would imply that improving arm and hand function would increase the patients independence and therefore also his/her quality of life (Rudhe and van Hedel, 2009).

1.3 Functional recovery from neurological injuries

Irrespective of the type of injury or disease, patients receive intensive rehabilitative training following the onset of the neurological condition. The primary goal of the initial rehabilitation is to maximize independence and quality of life of the patient, independent of the type of injury or disease. Independence can be achieved by maximizing the functional recovery or by helping the patient with assistive tools. Functional recovery from neurological injuries (e.g. stroke, SCI) can be divided into two separate mechanisms (Curt et al., 2008, Zeiler and Krakauer, 2013): biological recovery and compensation. In the prior, the patient regains same or similar movement patterns compared to healthy individuals due to axon regeneration or fiber growth (neuroplasticity). In the second, the patient learns to accomplish a motor task by using altered movement patterns. Both mechanisms are currently addressed during rehabilitation. For example, therapists try to reduce impairment by improving the patient's muscle strength, while also trying to improve the skills required to perform activities of daily living with reduced motor function. Several research groups have investigated how sensorimotor impairment can affect the hand and arm function following neurological injuries such as stroke. These different studies have explored for example how muscle activation patterns (Dewald et al., 1995, Seo et al., 2010, Canning et al., 2000), muscle synergies (Roh et al., 2013, Cheung et al., 2012), reflexes (Sangani et al., 2007), or movement coordination (Dewald et al., 1999, Cirstea and Levin, 2000) are changed after stroke. However, the underlying mechanisms of sensorimotor recovery following neurological injury remain unclear. A better understanding of these mechanisms is necessary for the development of effective therapeutic interventions. This includes, on the one hand, a better theoretical understanding by conducting neurophysiological studies and on the other hand practice related experiences about rehabilitation interventions and which parameters of rehabilitative training leads to positive outcomes. These outcomes have to be assessed objectively and sensitive enough to track even small changes.

Huang and Krakauer stated that the biggest impact on impairment reduction is from spontaneous biological recovery (Huang and Krakauer, 2009). This would suggest that rehabilitative training influences the functional recovery mostly by improving compensatory strategies of the patient.

Furthermore, it remains unclear how intensity, duration or type of training influence the overall functional recovery. It is further unclear how the physical activity of the patient outside of the therapy setting influences their functional recovery.

From preclinical studies with rodents in SCI, it is known that rehabilitative training is essential for functional recovery following neurological injury, as severed axons are restricted in their capacity to spontaneously regenerate (Gonzenbach et al., 2010). Starkey and co-workers demonstrated that self-motivated training leads to greater functional recovery following SCI than conventional training paradigms (Starkey et al., 2014). Furthermore, it has been shown that the type of training (Girgis et al., 2007) as well as the intensity of training play an important role in the recovery following SCI in rodents (Multon et al., 2003, Maier et al., 2008, Gonzenbach et al., 2010). Even though the importance of training has been shown in animal studies, there is only limited knowledge in humans SCI, as different intervention studies showed a wide range in the level of improvements and sometimes even contradictory results. For example, some studies were able to show benefits for patients based on specific rehabilitative training, varying in intensity, duration and type. The benefits ranged from improvements in strength (Beekhuizen and Field-Fote, 2005, Beekhuizen and Field-Fote, 2008), arm and hand function (Kowalczewski et al., 2011), and performance of activity of daily living or in general increased quality of life (Hicks et al., 2003). Other studies investigating the effect of specific training on functional recovery, however, were not able to show any significant improvements in the evaluated outcome measures (strength or arm and hand function) between the intervention and the control group (Glinsky et al., 2009, Zariffa et al., 2012, Spooren et al., 2011).

Although, there is a some evidence in stroke that task specificity and intensity play an important role in treatment efficacy (Van Peppen et al., 2004), similar discrepancies between study results on treatment efficacy have also been found (Teasell et al., 2015, Taub et al., 1993, Lincoln et al., 1999, Gelber et al., 1995, Van Peppen et al., 2004, Lang et al., 2016).

The results of training studies are in general difficult to interpret as, besides the diverse training modalities, a wide range of outcome measures are used (Kloosterman et al., 2009, Lu et al., 2015). A further explanation could be that the captured level of improvement beyond the training itself might

depend on the assessment method used for describing the improvements (e.g. compensation vs. impairment reduction). This hypothesis is in line with the work of Duncan and coworkers in which the authors suggested that some clinical trials might have failed to show the efficacy of a treatment due to poor choices of the assessment tools (Duncan et al., 1992).

1.4 Assessment methods used in clinics

Assessments are not only used in research to investigate the effectiveness of a certain treatment or intervention, they are also used as a diagnostic tool in daily clinical routine. Within the initial rehabilitation following a neurological injury, clinical assessments can be used at three different time points to quantify the extent of sensorimotor impairment: prior to the treatment, during the treatment, and after the treatment. Assessments before treatment are used for the diagnosis of a neurological injury, to plan the treatment according to the patient's individual needs, and for the prognosis of the expected level of recovery. During the treatment, assessments are used to objectively report a patient's progress to healthcare specialists, patients and families, and especially to adjust the treatment according to the level of functional recovery of the patient. Assessments after treatment are used to evaluate the effectiveness and retention of a treatment and to select and adapt assistive tools. As neurological injuries such as stroke or SCI produce enormous costs to the health care system, clinical assessments are also often used to justify a certain treatment or intervention to the health insurance companies.

Clinical assessments of neurological conditions generally provide a wide range of outcome measures and therefore, they can address different domains of a patient's health status. The International Classification of Functioning, Disability and Health (ICF), which was introduced in 2001, is a common framework to provide standardized descriptions of function and disability (WHO, 2013). The aim of the ICF is to provide a scientific basis for the description of an individual's health status, in order to make comparisons across countries, health care systems, health care disciplines, and also research disciplines possible. Within the framework of the ICF, health conditions are described with the components "body functions and structures", "activities", and "participation". The component "activities" can, according to the ICF, be further divided into "capacity" and "performance". In this context, capacity describes the highest level of function an individual can achieve in a standardized environment (for example in the lab or in the clinic), and performance describes what an individual is actually achieving in a given environment as for example, the home environment (Lemmens et al., 2012). In the following paragraph some of the well-established sensory and motor assessments of the upper-limb for SCI and stroke patients are presented and assigned to one of the ICF components "body functions and structures",

"activities", and "participation", and in the case of "activities", with a further division into "capacity" and "performance".

One of the most widely used quantitative measures of motor impairment for stroke patients is the Fugl-Meyer assessment (FMA, (Fugl-Meyer et al., 1974, Gladstone et al., 2002)). Although the FMA contains five domains (motor function, sensory function, balance, joint range of motion and joint pain), the motor function subscale of the upper extremity is quite often used without reporting the full test score, especially in research when the intervention targets only the improvement of upper-limb function (e.g. (Klamroth-Marganska et al., 2014)). The upper-extremity motor score contains 33 items which are rated on a 3-point ordinal scale (0 = cannot perform, 1 = preforms partially, 2 = performs fully) with a maximum at 66 points. Items on this subscale contain retraction, elevation, abduction, adduction, and external/internal rotation of the shoulder, elbow flexion and extension as well as pro- and supination of the forearm. Furthermore, the subscale contains items with reflex activities, more complex movements like tapping with the index finger from the knee to the nose, and the grasping of a cylinder or a tennis ball. The FMA provides information on the ICF domain "body functions and structures".

The Chedoke Arm and Hand Activity Inventory (CAHAI) is an assessment of the upper-limb for stroke patients which belongs to ICF domain "activity" (subcomponent "capacity" (Barreca et al., 2005)). The CAHAI consists of 13 functional tasks such as pouring a glass of water or drying the back with a towel, which are rated on an ordinal scale from 0 (no activity) to 7 (complete independence). The CAHAI includes only bimanual tasks, whereby only the affected arm is assessed and evaluated.

The Box and Block Test (BBT) is an assessment which can be administered within 5 minutes (Mathiowetz et al., 1985a). The BBT assesses unilateral gross manual dexterity and belongs to the timed assessments. In this test stroke subjects have to carry as many wooden cubes ($2.5cm^3$, 150 in total) as possible from one side of a box to the other side in 60 seconds. Similar to the CAHAI test, the BBT belongs to ICF domain "activity" (subcomponent "capacity").

The Motor Activity Log (MAL) is a semi-structured interview to assess arm function in stroke and belongs to the ICF domains "activity" and "participation" (Uswatte et al., 2005). Technically speaking the MAL belongs to the group of performance assessments. The MAL contains 30 questions about daily

functional tasks such as object manipulation (e.g. pen, fork) and gross motor activities (e.g. transferring to a car). Participants have to rate for each activity the quality of movement and the amount of movement on an ordinal scale ranging from 0 (not applicable / weaker arm was never used) to 5 (movement of the weaker arm is as good as before the stroke / weaker arm is used as often as before the stroke).

The previously mentioned clinical assessments in stroke are a selection of well-established methodologies to quantify functional deficits and impairment, whereas in SCI only few well generally accepted assessments of sensorimotor function exist:

SCI is often classified using the International Standards of Neurological Classification of SCI (ISNCSCI). The ISNCSCI include a protocol to identify the NLI and a protocol to assess the completeness of a lesion, called ASIA Impairment Scale (AIS). The NLI is determined by the most caudal intact sensory dermatome and myotome (Kirshblum et al., 2011). Dermatomes are assessed by using pinprick and light touch sensation tests and myotomes are assessed by using manual muscle testing. Based on the assessments of all dermatomes and myotomes the completeness of the injury can be classified according to the AIS. A classification of AIS A describes a motor and sensory complete lesion, AIS B describes a motor complete but sensory incomplete lesion, AIS C and D describe an incomplete lesion with some residual sensory functions where AIS C describes low voluntary muscle function and in AIS D at least half of the key muscles can produce movement against gravity (Kirshblum et al., 2011). The ISCNSCI belongs to ICF domain “body function”.

The Graded and Redefined Assessment of Strength, Sensibility and Prehension (GRASSP) is an assessment to quantify motor and sensory function as well as task performance of the upper extremities in tetraplegic persons (Kalsi-Ryan et al., 2012b, Kalsi-Ryan et al., 2012a). Basically, the GRASSP assesses sensation, strength, qualitative and quantitative grasping through a series of five examinations and therefore the GRASSP can also be assigned to different ICF domains, namely “body functions and structures” as well as “activity” (capacity). The five sub-tests of the GRASSP consist of an assessment of dorsal and palmar sensation of the hand (0-24 points on an ordinal scale, two sub-tests), assessed with Semmes Weinstein Monofilaments, an strength assessment of ten key arm and hand muscles (6-point ordinal scale, maximum 50 points), an assessment of the ability of applying three different grasps (4-

point ordinal scale, maximum 12 points), and assessment of 6 functional tasks such as opening a jar or picking up and turning a key (6 point ordinal scale, maximum 30 points). Note that GRASSP assesses the left and the right hand/arm individually and the previously mentioned scores are only for one extremity.

One of the only clinical assessments which measures to some extent performance in addition to capacity in individuals with a SCI is the Spinal Cord Independence Measure (SCIM (Catz et al., 1997)). The SCIM belongs to the ICF domain “activities” and is an interview with 19 items, which are divided into self-care (6 items, rated on ordinal scales, maximum 20 points), respiration and sphincter management (4 items, rated on ordinals scales, maximum 40 points), and mobility (9 items, rated on ordinal scales, maximum 40 points).

1.5 Limitations of clinical assessments

Although, the previously mentioned assessments are frequently used in the daily clinical routine as well as in research, some of those assessments, at least to some extent, cannot capture the intendant measurand (e.g., due to confounds). Furthermore, there are a number of major drawbacks of such assessments. Despite the fact that most of the previously mentioned assessments show an adequate to excellent test-retest reliability (Platz et al., 2005, Chen et al., 2009, Uswatte et al., 2005, Kalsi-Ryan et al., 2012a) as well as an adequate to excellent interrater reliability (Gowland et al., 1993, Itzkovich et al., 2007a, Kalsi-Ryan et al., 2012a, Mathiowetz et al., 1985a, Savic et al., 2007), the outcomes are presented on ordinal or even nominal scales, which can be a limiting factor in research, especially for statistical analyses. The use of ordinal scales leads, in almost all clinical assessments, to poor sensitivity and to ceiling effects. Apart from the fact that almost all assessment tools are only snapshots (i.e. may not be representative of function/impairment in everyday life), most of them do not differentiate true recovery from compensation (Kitago et al., 2012). Assessments targeting the ICF domain "performance" are usually clinical questionnaires such as FIM or SCIM and although they are easy to administer, they are rather subjective as they represent the perception of the patient or the therapist. Other important metrics such as, e.g. grasping force, are only assessed in a static case, without any functional context.

Even though, these assessments, with their drawbacks, may be acceptable for clinical use, they can only be applied to a limited extent in research. In order to track functional recovery, level of impairment and degree of compensation during rehabilitation sessions, activities of daily living (ADL), and in laboratory settings, objective and sensitive assessment tools are needed. In addition to good clinimetric properties, such as good reliability and good validity, these assessments should on the one side be able to detect even small changes in the level of impairment (sensitivity) and should therefore measure movement trajectories, interaction forces, muscle and joint coordination during dynamic tasks and on the other hand be able to track and quantify physical activity over extended periods of time during rehabilitative training as well as outside of the therapy. The measurement of physical activity outside of therapy is very important, because it might be a confounding factor when performing a training study. With such assessment tools, researchers could not only gain new insights into how different rehabilitative trainings

methods (differing in intensity, duration and task specificity) affect impairment, compensation and/or overall functional recovery, but also how the physical activity of the patient outside the therapy sessions might influence the overall functional recovery. Furthermore, such assessment tools can help to understand the mechanisms of recovery and can be used to establish prediction models of recovery.

1.6 Robotics and wearable sensors as promising assessment tools

1.6.1 Assessments with robotic technology

Over the last decades, the technological improvements in actuation, sensing, and computational power led to an increasing number of developments in the field of rehabilitation engineering (Kwakkel et al., 2007, Prange et al., 2006). Robotic tools are especially well suited for assessments of sensorimotor function and impairment (Bosecker et al., 2009, Wolpert and Flanagan, 2010) as they can render a variety of force fields in well-controlled and reproducible conditions (assisting, resisting, perturbing, stretching (Hertenstein and Weiss, 2011, Lambercy et al., 2015)). Furthermore, robotic systems can provide objective measures of movement trajectories, movement smoothness, range of motion, joint coordination, interaction forces, movement accuracy, and movement efficiency (de los Reyes-Guzmán et al., 2014), which can be used to evaluate the level of sensorimotor impairment.

The most common application of robotic manipulanda in neurorehabilitation is as therapy tool. Different robotic systems have been used in upper-limb rehabilitation to train proximal upper-limb function (Hogan et al., 1995, Klamroth-Marganska et al., 2014) or to train hand function (Lambercy et al., 2007, Dovat et al., 2008, Metzger et al., 2014a, Lum et al., 2012, Zariffa et al., 2012). These systems can, simultaneously to the therapy, collect kinematic and kinetic data which can be used to monitor the functional improvement and level of impairment of a patient (Lambercy et al., 2012, Lambercy et al., 2016) or to adapt the therapy to the patient's capability and needs, e.g., through assessment-driven therapy (Metzger et al., 2014b).

Furthermore, robotic systems have been used extensively in strict laboratory settings to assess passive and active joint properties (Milner and Cloutier, 1993, Milner and Cloutier, 1998, Perreault et al., 2004), or to gain new insights into motor learning, motor adaptation and compensation processes (Milot et al., 2010, Burdet et al., 2001, Shadmehr and Mussa-Ivaldi, 1994, Melendez-Calderon et al., 2011). Moreover, assessments with robotic systems such as for example the MIT Manus have been used to obtain insights into sensorimotor impairment and recovery after neurological injuries (Takahashi and

Reinkensmeyer, 2003, Krebs et al., 1999, Dewald and Schmit, 2003, Euving et al., 2016, Meskers et al., 2009).

A big advantage of robotic assessments is the possibility for synchronization with electroencephalography (EEG (Vlaar et al., 2016)) or with electromyography (EMG (Kamper et al., 2014, Budhota et al., 2016)), or to combine it with imaging techniques such as magnetic resonance imaging (MRI (Gassert et al., 2006, Vigaru et al., 2016)) in order to investigate brain mechanisms or to assess muscle activation patterns during dynamic movements in healthy subjects as well as in different neurological conditions, respectively. In addition to the usual assessment properties, i.e. sensitivity, objectivity, and validity, robotic assessment systems, which are designed for use in the daily clinical routine also need to be useful clinically. This means that such an assessment tool should be simple to apply, should not be time consuming, and should be relatively inexpensive. Furthermore, these assessment tools should provide useful outcome measures to clinicians and should be provided together with normative data, in order to estimate the level of impairment of a patient. There have already been robotic assessment tools developed, which potentially could be used in the daily clinical routine. The outcome measures of such robotic assessment tools involve the evaluation of proprioceptive functions of the hand (Lambercy et al., 2011, Rinderknecht et al., 2014), the assessment of motor synergies of the arm (Dipietro et al., 2007) or on the assessment of motor function in strictly predefined tasks (Fluet et al., 2011, Feys et al., 2009, Bardorfer et al., 2001, Keller et al., 2015).

Robotic assessments have been shown to be an important tool for understanding the motor adaptation processes and the change in movement patterns after neurological injuries and diseases. A 1 degree-of-freedom (DOF) wrist device called ReFlex was developed at the Rehabilitation Engineering Lab (Chapuis et al., 2010). The ReFlex was specifically designed to investigate the role of kinesthesia in motor learning and to investigate passive joint properties. The wrist joint was chosen because it is mostly a 1-DOF joint (flexion and extension), has a large range of motion and can generate high torques during dynamic interactions. Furthermore, wrist and finger muscles are accessible for surface EMG, which can be used to analyze muscle activation patterns during dynamic movements. With its hybrid actuation approach with a motor in parallel with a brake, the ReFlex is able to generate dynamic and isometric

task environments and furthermore allows fast switching between the two different task environments. In addition, the ReFlex is equipped with a high-resolution optical encoder for position sensing and a 6 DOF force/torque sensor. The design of the ReFlex makes it well suited for investigating human motor control in the able-bodied population as well as in populations with neurological conditions, and will serve as a robotic assessment tool for the laboratory/clinical setting in the context of this thesis.

1.6.2 Long-term monitoring using wearable sensors

The improvement in sensing technologies such as miniaturization, energy efficacy, new sensing technologies as well as advances in machine learning techniques opened new opportunities for clinical practice and research (Dobkin and Dorsch, 2011). Wearable sensors are currently the only objective assessment tools that can monitor upper-limb movement in real-world environments, as they can collect data over extended periods of time in a non-obstructive way. Although, wearable sensors can be used as a measure of capacity, the most promising application for this technology is in the assessment of the ICF domains “performance” and “participation”. The field of wearable sensors is rapidly growing and has already shown its potential for clinical applications and research (Bonato, 2005). Wearable sensors showed to be a promising tool, especially for the assessment of arm activity in daily life (Westerterp, 2009, Gebruers et al., 2010). Multiple research groups have developed and validated a large number of algorithms allowing the analysis of upper-limb movements in a wide range of neurological conditions. In stroke, wearable sensors such as accelerometers or inertial measurement units (IMU) have been used for example to quantify the amount of arm activity in general (van der Pas et al., 2011, Uswatte et al., 2000) or to compare the ratio of upper limb movement between the paretic and the non-paretic arm (Bailey et al., 2014, Uswatte et al., 2006). In PD, accelerometers were mainly used to assess tremor severity (Imbach et al., 2014). In CP, IMUs were used to analyze capacity in specific tasks (Strohrmann et al., 2013), and in MS, accelerometers were, among others, used to quantify the amount of upper-limb movement during seven consecutive days (Motl et al., 2009). Wearable sensor based assessments have already been used as primary outcomes in cross-sectional as well as in longitudinal studies (assessments at multiple time points), such as to monitor the use of the upper-limb in patients with neurological conditions (Bailey et al., 2015, Lemmens et al., 2014, Thrane et al., 2011, Taub et al., 2013).

In the field of SCI, many new assessment methods to quantify physical activity based on data of wearable sensors have been developed and validated in the last 10 years. The developed outcome measures focused on specific movements such as wheeling (Coulter et al., 2011, Sonenblum et al., 2012a, Postma et al., 2005, Hiremath and Ding, 2011, Ojeda and Ding, 2014, Dowling et al., 2016), on energy expenditure estimation (Hiremath et al., 2012, Garcia-Masso et al., 2013, Nightingale et al., 2015, Hiremath et al., 2016), on activity classification (Hiremath et al., 2013, Hiremath et al., 2015), and on the division of physical activities into different levels of intensities, based on activity count data (Warms et al., 2008). Despite the fact that some of these methodologies showed very promising results, almost all algorithms were tested and evaluated in highly controlled laboratory settings, and therefore cannot be easily transferred to real-world applications. Furthermore, some of the outcome measures are difficult to interpret, due partly to poor evaluation, lack of reference data, unknown relationships to other clinical assessments, and very narrow inclusion and exclusion criteria. This makes it difficult to derive general models for a very heterogeneous population. In addition, the developed methodologies overestimate the true contribution of the patient to physical activity as important information is missing, e.g. when measuring physical activity in terms of mobility in wheelchair users and self-propulsion is not distinguished from attendant propulsion. The lack of applicable methodologies for wearable sensor-based assessments might be one possible explanation for why there are only few observational or interventional studies, which used data from wearable sensors as a primary outcome. Nonetheless, some of the previously mentioned methodologies were, after development and validation, used as primary outcomes in observational studies. For example Sonenblum and coworkers used their developed algorithm (Sonenblum et al., 2012a) to observe how 28 manual wheelchair users moved in their natural environment over 7-14 consecutive days (Sonenblum et al., 2012b). Methodologies specifically designed for the SCI population have also been used in longitudinal studies observing the change in physical activity during rehabilitation in patients with SCI (van den Berg-Emons et al., 2008, Nooijen et al., 2012, Postma et al., 2005). In conclusion it can be stated that although some methodologies to quantify physical activity have been developed for the SCI population, only a few of them have found their way into observational or clinical studies. In order to use wearable sensors as a primary outcome

in studies with SCI individuals, more objective, sensitive and quantitative algorithms are needed, which should also be applicable in real world situations.

As a part of his PhD thesis, Kaspar Leuenberger developed a new wearable sensor (ReSense) which was specifically designed for long-term activity monitoring in patients with neurological conditions (Leuenberger and Gassert, 2011, Leuenberger, 2015). The ReSense module is a 10 degree-of-freedom IMU, which consists of 3D accelerometer, a 3D gyroscope, a 3D magnetometer, and a barometric pressure sensor. In addition, the sensor is compact, water resistant and has an intelligent power management system, which allows it to record motion data over 48 hours. Furthermore, ReSense modules can be temporally synchronized, which allows the investigation of more complex movements and activities using multi sensor setups. The ReSense has already been used to develop and validate algorithms in other neurological conditions such as stroke (Leuenberger et al., 2014, Leuenberger et al., 2016), PD (Imbach et al., 2014), neuropsychological disorders (Leuenberger et al., 2015) as well as in neurologically intact subjects (Moncada-Torres et al., 2014). The ReSense is – due to its sensing capacity, the possibility of synchronizing different modules, and the long recording duration – well suited for the development of new algorithms in the SCI population and also for the use in long-term observational or intervention studies and will serve as technology for long-term assessments outside the laboratory/clinical setting.

1.7 Aims of the thesis

Novel robotics and wearable sensing technologies create opportunities to develop objective and sensitive assessments beyond what is possible with current clinical assessments. Robots, with their ability to precisely measure movement trajectories and interaction forces, as well as render virtual dynamics in well-controlled and reproducible conditions, are an optimal tool to assess sensorimotor learning and control and therefore also for assessments of motor as well as somatosensory impairment. Furthermore, recent developments in sensing technologies such as miniaturization and energy efficiency allow the use of wearable sensors for long-term measurements outside the laboratory/clinical setting.

The aim of this PhD thesis is to develop objective kinematic and kinetic assessments of upper-limb function for individuals with a neurological injury such as stroke or SCI, both in the laboratory/clinical setting as well as outside, in order to gain a more complete picture of the functional impairments and abilities of patients. This thesis will address the assessments of capacity in sensorimotor function in order to gain new insights into neuronal control of finger and wrist muscles, which is essential for the design of rehabilitative therapy approaches. Furthermore, this thesis will also address the development of objective performance assessment methods for monitoring upper-limb activity, which can be used to characterize changes in activity level during the course of rehabilitation.

The first part of the thesis will focus on quantifying sensorimotor impairments of the upper extremities. It will consist of the development of a kinematic/kinetic assessment tool based on a wrist robot to provide deeper insights into (healthy/altered) multi-joint coordination (wrist + digits), force production, and muscle activation patterns. The second focus of this thesis lies in long-term monitoring of physical activity in individuals with neurological injuries in natural environmental conditions in the clinic and at home, i.e. outside the examination room/lab. For this purpose, an inertial measurement unit (IMU)-based assessment tool was developed. This tool should provide information about overall upper-extremity activity and energy expenditure, as well as specific physical activities such as upper limb activity in the context of wheelchair propulsion (mobility) and activities of daily living.

The novel assessments resulting from this thesis promise deeper understanding of the mechanisms underlying sensorimotor impairments and their reduction through therapeutic interventions.

Furthermore, the long-term assessment tool promises novel insights into how physical activity outside of therapy sessions affects functional recovery.

1.8 Thesis Outline

The thesis is organized into two parts covering the ICF domains capacity and performance. The first part focuses on the development and validation of a robotic assessment tool for the assessments of capacity and to investigate sensorimotor impairment in laboratory settings. Within this thesis, the robotic assessment tool was used to run a motor control study with stroke and a neurologically intact group. Chapter 2 presents a study published in the International Journal of Industrial Ergonomics. This study investigated how the design of physical interfaces between human and the robot can influence different assessment outcomes. Chapters 3 (healthy) and 4 (stroke) investigate the interdependence between wrist and digit control and how muscle activation patterns as well force production at the level of the fingers are influenced by wrist posture and by wrist stabilization conditions. Additionally, data from healthy and stroke subjects are compared in order to gain new insights into how wrist and digit control are altered following stroke. The second part of the thesis focuses on the objective assessment of performance in uncontrolled environments within and outside of the clinical setting. It consists in the development of IMU based assessment tools for long-term monitoring of physical activity in individuals with a SCI. Chapter 5 presents an algorithm able to quantify wheeling kinematics and propulsion type, which was published in Medical Engineering and Physics. Chapter 6 includes an IMU-based algorithm for estimating energy expenditure (EE) in wheelchair bound SCI individuals. Finally, the last chapter highlights the contributions of this thesis to extend current knowledge, and provides an outlook on how these assessments could be further improved and used in neuroscience research and clinical settings.

2 Effect of Handle Design on Movement Dynamics and Muscle Co-activation in a Wrist Flexion Task[1]

Werner L. Popp, Olivier Lambercy, Christian Müller, Roger Gassert

International Journal of Industrial Ergonomics (2016)

I would like to thank Dominique Chapuis, Remco Benthem de Grave, Lorenzo Tanadini, and Yeongmi Kim, who helped me with different aspects of this study.

[1] Reprinted from International Journal of Industrial Ergonomics, 56, Werner L. Popp, Olivier Lambercy, Christian Müller, Roger Gassert, Effect of handle design on movement dynamics and muscle co-activation in a wrist flexion task, 170-180, Copyright (2016), with permission from Elsevier.

2.1 Abstract

Arm and wrist manipulanda are commonly used as input devices in teleoperation and gaming applications, establish a physical interface to patients in several rehabilitation robots, and are applied as advanced research tools in biomechanics and neuroscience. Despite the fact that the physical interface, i.e. the handle through which the wrist/hand is attached to the manipulator, may influence interaction and movement behavior, the effects of handle design on these parameters has received little attention. Yet, a poor handle design might lead to overexertion and altered movement dynamics, or result in misinterpretation of results in research studies. In this study, twelve healthy subjects performed repetitions of a wrist flexion task against a dynamic load generated by a 1-DOF robotic wrist manipulandum. Three different handle designs were qualitatively and quantitatively evaluated based on wrist movement kinematics and dynamics, patterns of finger and wrist muscle activity, and ergonomics criteria such as perceived comfort and fatigue. The three proposed designs were further compared to a conventional joystick-like handle. Task performance as well as kinematic and kinetic parameters were found to be unaffected by handle design. Nevertheless, differences were found in perceived task difficulty, comfort and levels of muscle activation of wrist and finger muscles, with significantly higher muscle activation when using a joystick-like design, where the handle is completely enclosed by the hand. Comfort was rated high for the flat handle, adapted to the natural curvature of the hand with the fingers extended. These results may inform for the design of handles serving as physical interface in teleoperation applications, robot-assisted rehabilitation and biomechanics/neuroscience research.

2.2 Introduction

Physical human-machine interaction is a field of growing importance, with applications in teleoperation, gaming, robot-assisted rehabilitation and sensorimotor control research. With the ability to precisely track movement trajectories and render virtual dynamics in well-controlled and reproducible conditions, robotic devices are well-suited for the investigation of the mechanisms underlying human sensorimotor learning and control, or (neuro)mechanical joint properties (Wolpert and Flanagan, 2010) and find application as therapeutic tools in neurorehabilitation. In research, single-degree-of-freedom (DOF) manipulanda have been widely used to evaluate passive and active joint properties, typically at the level of the wrist, by applying external, well-controlled perturbations to the joint (Milner and Cloutier, 1998, Milner and Cloutier, 1993). More complex planar robotic manipulanda have allowed new insights into learning and adaptation processes of the central nervous system during reaching movements in stable or unstable force fields generated by the robot (Shadmehr and Mussa-Ivaldi, 1994, Burdet et al., 2001). Although there have been approaches to quantify hand-handle interaction forces (Kalra et al., 2015), other aspects such as handle ergonomics are also important as it has been shown that handle design can strongly influence performance as well as movement dynamics and kinematics during manipulation tasks (Dong et al., 2007, Herring et al., 2011, Horsfall et al., 2005, Kong et al., 2008, Santos-Carreras et al., 2012). Motivated by the ergonomics of hand-held machine tools, several studies have looked into optimizing cylindrically shaped handles, and found that the handle diameter influences forearm muscle activity, force generation capabilities, as well as perceived comfort during power grip tasks (Ayoub and Presti, 1971, Grant et al., 1992, Kong and Lowe, 2005, Gonzalez et al., 2015). However, in the case of isolated wrist tasks, there is less information on how handles should be designed and how the finger placement and guidance imposed by the handle might influence subjects' performance as well as affect comfort and fatigue. Yet, the wrist joint is ideally suited for motor learning experiments as, through an appropriate fixation, it can be reduced to a mostly 1-DOF joint with a large range of motion (up to 95°/98° [male/female] flexion), capable of generating high torques (around 8.6 Nm for males and 5.2Nm for females in isokinetic contraction, (Morse et al., 2006)) during dynamic interactions.

Most of the existing wrist robots used in motor learning research or in neurorehabilitation were designed with joystick-like handles (Masia et al., 2009, Suminski et al., 2007, Kadivar et al., 2012), in which the subject holds a cylinder-shaped handle using a power grasp, and the hand can enclose the entire handle surface. Pilot data previously collected by our group during dynamic wrist flexion tasks with a joystick-like handle mounted on a robotic wrist manipulandum (ReFlex, (Chapuis et al., 2010)) illustrated that such a handle may lead to high co-contraction levels between wrist flexor and extensor and between finger flexor and extensor muscle groups, which might affect the observation of adaptation mechanisms during motor learning experiments, and increase muscle fatigue or muscular pain during successive task repetitions. This might be an undesired side effect, especially in tasks involving intensive interaction with a robotic manipulandum, such as during robot-assisted rehabilitation.

An ergonomic interface between a robotic manipulandum and the wrist should in general consider several biomechanical and physiological factors. For example for the investigation of wrist joint control, it is desirable that movements are controlled mainly by wrist muscles and the contribution of extrinsic finger muscles is minimized. Mechanically unstable loading – e.g., caused by awkward postures due to ergonomically inadequate devices – may restrain or alter the formation of optimized patterns of muscle activity that occur during motor adaptation (Osu et al., 2002, Hermsdörfer et al., 1999), leading to increased co-activation or co-contraction (i.e. co-activation of an agonist-antagonist muscle pair) of the forearm muscles (Milner and Cloutier, 1993). High rates of co-contraction and co-activation affect joint impedance (Hogan, 1984a) and may result in higher rates of fatigue, possible overexertion and development of muscle pain (Tomatis et al., 2009, Zennaro et al., 2003). As subjects are typically required to perform many movement repetitions during motor learning tasks involving novel dynamics or in rehabilitation applications, the development of muscle fatigue or muscular pain should be avoided. It is thus important to reduce excessive muscle activation through an ergonomic design.

In this study, we present the qualitative and quantitative evaluation of three handle designs, evaluated on a 1-DOF robotic wrist manipulandum during repeated dynamic wrist flexion movements against a load generated by the robotic manipulandum. Handles are compared using ergonomics criteria such as comfort, fatigue and pain evaluated through questionnaires, as well as an analysis of muscle activity

patterns in wrist and hand muscle groups measured with surface electromyography (EMG). We further compare patterns of muscle activity for a joystick-like handle used in previous measurements with the manipulandum. In addition, wrist dynamics and performance in a target reaching wrist flexion task are analyzed. We hypothesized that handle design and finger position on the handle would influence the way subjects perform fast wrist flexion movements, generate wrist flexion torque, and modulate wrist impedance.

2.3 Materials and Methods

2.3.1 Subjects

Twelve healthy subjects (age 27.8 ± 10.7 years, 7 males) were recruited for this study. Participants came to the Rehabilitation Engineering Laboratory at ETH Zurich for a one-hour session with the robotic manipulandum (ReFlex, (Chapuis et al., 2010)). As inclusion criteria, subjects had to be over 18 years old and right handed. Exclusion criteria were any neurological disorders, functional deficits of the wrist/hand as well as any history of wrist injury, or presence of any dermatological diseases.

Prior to the experiment, each participant was informed about the details of the protocol and gave informed written consent. The study was approved by the ETH Zurich Ethics Commission (EK 2010-N-18).

2.3.2 Apparatus

A 1-DOF robotic manipulandum designed for the investigation of the wrist joint (ReFlex, Figure 2-1) was used to evaluate the different handle designs. It can precisely control, assess and perturb wrist movement in flexion and extension under dynamic or isometric experimental conditions (Chapuis et al., 2010). Thanks to its hybrid actuation system composed of a brushed DC torque motor (RE65, Maxon Motor, Sachseln, Switzerland) and a magnetic particle brake (S90MPA-B34D50H38, Stock Drive products/Sterling Instruments, New Hyde Park, NY, U.S.A.) connected in parallel over a timing belt transmission, the manipulandum can safely render a wide dynamic range of mechanical impedance and torque. Angular position of the handle is measured with a high-resolution optical encoder fixed directly to the motor shaft (R158, 1’000’000 counts/rev, Gurley Precision Instruments, Troy, NY, U.S.A) to allow for a high velocity resolution (0.36 deg/s) at high sampling rate (1kHz). Redundant position sensing is performed at the level of the brake using a rotary potentiometer (GL 60, Contelec AG, Biel, Switzerland) for safety purposes. A 6-DOF force/torque sensor (Mini45, ATI Industrial Automation, Apex, NC, U.S.A.) is mounted between the handle support and the motor shaft to monitor the wrist torque applied by the subject and compensate for the apparent dynamics of the manipulandum. During dynamic wrist flexion and extension, force and torque data are monitored to assure that the task is

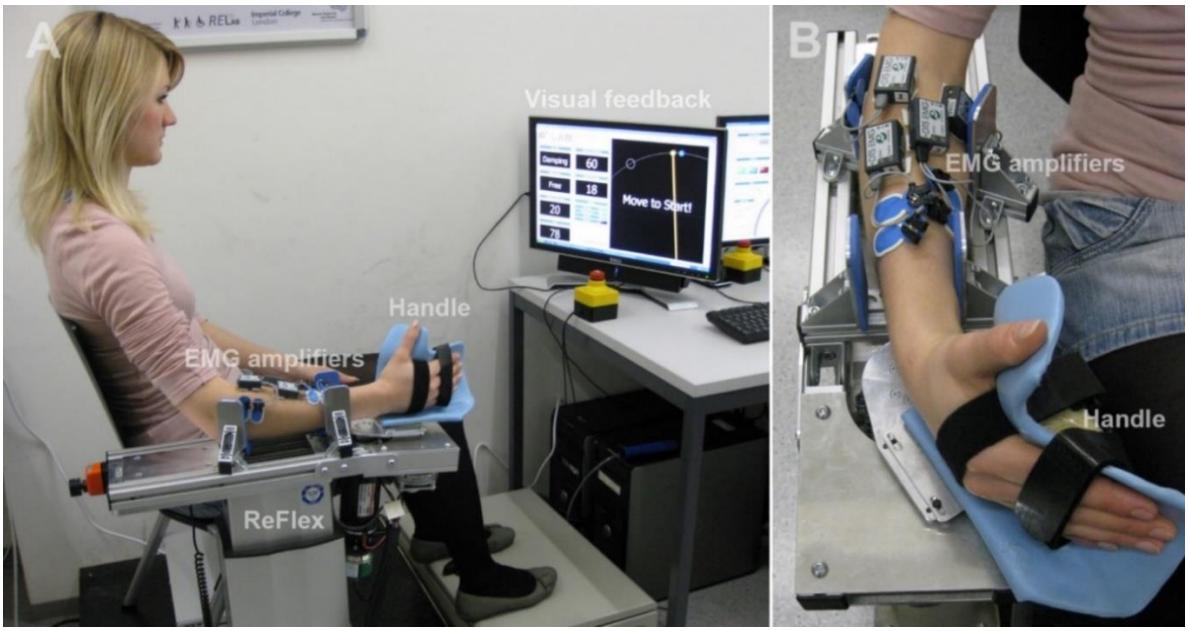

Figure 2-1: Haptic wrist interface ReFlex. Experimental setup during a measurement session including the visual feedback presented to the subject (A). Front view of the adjustable arm support with a curved handle (B).

performed correctly, with minimal compensatory force and torque in directions transverse to the movement under investigation. The manipulandum is controlled using 2 personal computers, i.e. a standard host PC running Windows 7 with LabVIEW 2011 (National Instruments, Austin, TX, U.S.A.) for the user interface and visual display, and a target PC running LabVIEW RealTime 11.0 (National Instruments, Austin, TX, U.S.A.) for robot control. The real-time control system runs at a sampling frequency of 1 kHz.

2.3.3 Handles

Handles are mounted to the robotic manipulandum through a rectangular aluminum base plate (70x80 mm^2) that can be shifted longitudinally to adapt to the user's arm length and to assure that the axis of rotation of the wrist is aligned with that of the motor shaft. The handles were formed from a sheet of thermoplastic material (Synergy Plain Blue Sheet, Sammons Preston, Bolingbrook, IL, U.S.A.) adapted to the shape of a middle size hand (hand length 193mm, palm length 114mm, hand breadth 88mm, hand thickness 32mm (Mohammad, 2005)), which is attached to the aluminum base plate on the palm side of the hand using rigid foam (50% Pedilen® rigid foam 300, 50% Hardener for Pedilen rigid foams, Otto Bock Suisse AG, Luzern, Switzerland). The design of the three handles used in this study (described

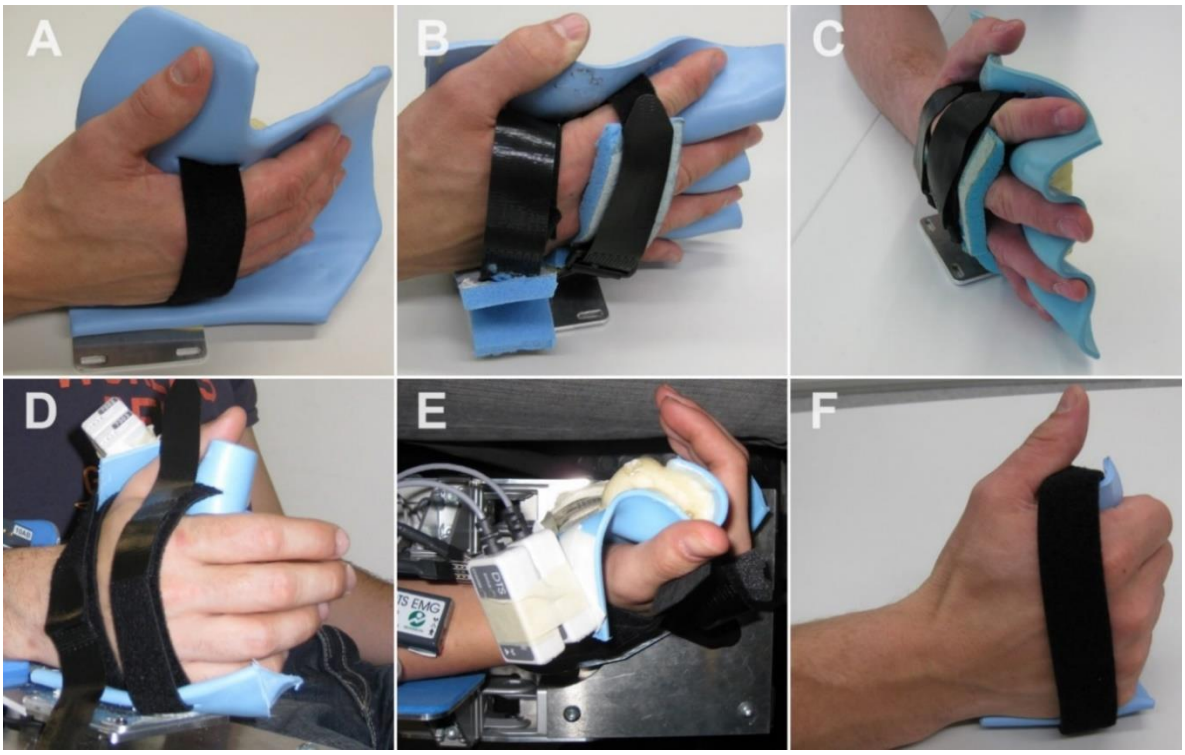

Figure 2-2: The different handles used during the experiment. The curved handle adapted to the natural curvature of the hand (A), the grooved handle with the fingers II to V in abducted position (B,C), the palm handle in which subjects were not allowed to flex the fingers around the handle (D,E) and the joystick-like handle used in previous experiment (F), in which finger flexion was not prevented.

below) was motivated by ergonomics and biomechanical considerations as well as based on a review of existing robotic devices used in physical human-robot interaction studies (Masia et al., 2009, Suminski et al., 2007, Kadivar et al., 2012, Dukelow et al., 2010, Milot et al., 2010, Cappello et al., 2015). In addition to the three investigated handles, a fourth handle used in previous measurements served as reference for the EMG analysis.

Curved handle

With the curved handle the hand is placed in a natural position, with the fingers II to V in adduction (Dukelow et al., 2010, Milot et al., 2010)(Figure 2-2, A). The thermoplastic sheet reaches 0.5cm over the fingertips on one side, and ends 1 cm before the wrist joint on the other (for the middle size hand described above). The metacarpophalangeal joints are held in a 10° flexed position. The thumb is supported by a plate and is placed in a 45° abducted position. Furthermore, the handle is curved at the bottom to support the hand. A Velcro® strap runs over the metacarpophalangeal joints of fingers II-V.

Grooved handle

The grooved handle is designed to minimize the torque produced by the fingers during wrist tasks. The handle is adapted to a splayed hand in order to immobilize the fingers during wrist movements (Chapuis et al., 2010), and to follow the natural curvature of the palm, reaching from the intermediate phalange of the middle finger up to 1 cm before the wrist joint (Figure 2-2, B, C). The thermoplastic sheet is adapted to the inside of the hand and has 4 escaping grooves which maintain the 4 fingers (i.e. index finger to little finger) in a position of 10° flexion and 20° abduction. The thumb is also guided within a groove in a 25° abducted position. To assure that the hand is firmly fixed to the handle, 2 padded Velcro® straps are placed over the dorsal side of the hand.

Palm handle

The palm handle is similar to a joystick-like handle where subjects can partly flex the fingers around a cylinder of 35mm diameter (Masia et al., 2009, Suminski et al., 2007, Kadivar et al., 2012) (Figure 2-2, D, E). To minimize co-contraction in finger muscles and prevent subjects from tightly grasping the handle during wrist tasks, two piezoresistive force sensors (Flexi Force ®-Model # A201 (0-110N), Tekscan Inc., South Boston, MA, U.S.A.) are fixed on the backside of the handle to monitor the finger force applied by the subject. In case a finger force above 2N is detected, a signal is given, requiring the subject to release the grip on the handle. This step was motivated by pilot data, previously collected with a standard joystick-like handle (Figure 2-2, F), where high levels of co-contraction for antagonistic muscle pairs at the level of the wrist and the fingers were observed in most subjects. Again, the

thermoplastic sheet is cut 1 cm before the wrist joint in order to assure that the handle does not interfere with the flexion of the wrist. The thumb is positioned in 35° abduction, and the handle is curved at the bottom to support the hand. Again two Velcro® straps placed over the dorsal aspect of the hand are used to fix the hand to the handle.

2.3.4 Wrist flexion task

To evaluate the three handles in the context of a representative and well-defined dynamic wrist task, a point-to-point target-reaching paradigm was implemented (Cameron et al., 2010). This task was selected as it is a commonly employed motor learning task that is challenging and demanding, in which, due to the high number of repetitions, comfort and fatigue might play a non-negligible role. Subjects were asked to perform a succession of fast and precise target reaching movements, from a starting position of 0 ± 0.5° wrist flexion to an end position of 30° wrist flexion. Start and end positions were represented by two circles displayed on a monitor placed in front of the subject (Figure 2-1, A). Visual feedback of the measured angular position of the wrist was further represented by a moving ball coupled through a lever to a virtual center of rotation. A window of ± 2° was given for the successful reaching of the target position. In addition, the movement time was constrained to a short window of 400 ± 50ms to assure a mostly feed forward control. Subjects had to initiate the movement within a given time window of 550ms, indicated by an acoustic countdown. During the wrist flexion movement, a resistive, velocity-dependent force was generated by the motor (equation 2.1),

$$\tau_n(t) = D * \dot{\varphi}(t) \qquad (2.1)$$

with τ_n the torque applied by the motor and $\dot{\varphi}$ the angular velocity of the wrist. The damping coefficient of D=0.011Nms/deg was empirically chosen in order to achieve a noticeable effect on the task dynamics. After each trial, corresponding to one target reaching movement, a qualitative feedback of the performance was displayed on the monitor. This feedback was based on the end-point error and reaching duration (target missed, too slow, too fast, early start, late start, good job). Both precision and time constraints had to be met in order for a trial to be considered successful. After the completion of the trial, subjects were asked to return the wrist to the initial angle, without any resistance from the robot, in order to initiate the next trial.

2.3.5 Protocol

A session was composed of 3 experimental blocks consisting of 100 trials to evaluate each of the handles. To avoid ordering effects, an individual sequence was pseudo-randomly determined for each subject prior to the experiment. Subjects were then informed about the experimental procedure and the use of the robotic device and its safety systems. Ag/AgCl surface EMG electrodes (Blue Sensor N, Ambu®, Ballerup, Denmark) were placed on wrist and finger muscles M. Flexor Carpi Radialis (FCR), M. Extensor Carpi Radialis (ECR), M. Flexor Digitorum Superficialis (FDS) and M. Extensor Digitorum Communis (EDC). Electrodes were positioned on the belly of each muscle and were individually checked for good placement before starting the measurement. The electrodes were connected to wireless amplifiers (Telemyo DTS System, Noraxon, Scottsdale, AZ, U.S.A.) streaming data to a separate desktop computer synchronized with the real-time target computer of the ReFlex through a TTL trigger pulse. The EMG data were sampled at 1.5 kHz. After placing the electrodes, three reference measurements were made to determine the maximal voluntary contraction (MVC) of each muscle through isometric contractions against a rigid and grounded object. The highest activation level over all measurements for each muscle was taken as MVC. The subject's arm was then installed in the device. Proper alignment between the wrist joint axis and the motor shaft was verified through visual inspection. Four padded supports located at the level of the elbow and distal part of the forearm were used to maintain the arm in proper position (Figure 2-1, A). The height of the robot was adjusted so that the elbow was in 35° flexion, the upper body was vertical and the shoulder was in 30° abduction at rest position. Once installed, a detailed explanation of the visual feedback was given, with the possibility for subjects to perform several test trials before starting the first experimental block. Between the blocks, a break of 5 minutes was given, during which the next handle was installed and aligned with the subject's hand. At the end of each block, subjects filled in a questionnaire, in which they were asked to rate handle comfort (0 = "uncomfortable", 10 = "comfortable"), task difficulty (0 = "very easy", 10 = "very difficult") and wrist fatigue (0 = "no fatigue", 10 = "severe fatigue") on 11-point numeric rating scales adapted from McDowell and Newell (McDowell, 2006). After completing the 3 blocks, subjects were asked to name their favorite handle (only one selection was possible), and indicate whether they felt any pain or discomfort (0 = "no pain", 10 = "severe pain", and if yes with which handle) throughout the

entire session on a similar numeric rating scale (Williamson and Hoggart, 2005). Overall, a measurement session lasted about two hours.

2.3.6 Outcome measures and statistical analysis

Position and force/torque data were sampled at a frequency of 1 kHz. The velocity estimate and the wrist flexion torque signals were filtered using a 2nd order Butterworth lowpass filter with a cutoff frequency at 20 Hz. This cutoff frequency was chosen as the bandwidth of human movements is typically below 10 Hz (Welk, 2002). In addition to position, velocity estimate and torque data, trial success/failure information was stored. For each trial, the part corresponding to the wrist movement was identified using position (starting position) and velocity thresholds (2 deg/s), then normalized over movement duration for averaging. The analysis of average trajectories for the successful trials of each experimental block was performed with MATLAB R2011a (The MathWorks, Natick, MA, U.S.A.), calculating a cross-correlation coefficient (R) between the average trajectory and a minimum jerk trajectory computed from the initial angle to the target angle (Wren et al., 2006). A minimum jerk trajectory was selected as reference trajectory as it is representative of fast and smooth target reaching movements in humans (Burdet and Milner, 1998, Hogan, 1984b).

EMG signals were post processed using commercial software (Myo Research XP 1.08.16, Noraxon, Scottsdale, AZ, U.S.A.). The signals were rectified and the root mean square (RMS) over a 50 ms (75 data points) sliding window was calculated. EMG signals were normalized with respect to the MVC, and signals from each trial were normalized over time. Based on these signals, a co-activation index (CI) was calculated between relevant muscle pairs (FCR-ECR, FCR-FDS, ECR-EDC, FDS-EDC), using the following method (adapted from (Ervilha et al., 2012)):

$$CI = \frac{1}{n}\sum_{t=1}^{n}\frac{2\cdot min(EMG_{1,t},EMG_{2,t})}{EMG_{1,t}+EMG_{2,t}} \qquad (2.2)$$

where $EMG_{1,t}$ and $EMG_{2,t}$ are the rectified muscle activity amplitude for the two muscles being compared at the time point t. The CI values were calculated for three different sections of the movement: i) the entire trial, ii) at the beginning of the movement (10-30% of the movement) where subjects accelerated the wrist against the resistive, velocity-dependent force field and iii) at the end (70-90%)

where the subjects had to stabilize the end point position. Additionally, the maximal and the average normalized muscle activity were calculated for the four muscles FCR, ECR, FDS and EDC over each the three different sections of the movement.

Statistical analysis was performed with SPSS Statistics 20 (IBM Corporation, Armonk, NY, USA). Repeated measures ANOVAs and post-hoc tests with Bonferroni correction were used, as data was normally distributed (first assessed using Kolmogorov-Smirnov tests). For the comparison between CI values of the three tested handles and the joystick-like handle used in previous measurements, using the same wrist task but within a different study (5 subjects), an unpaired t-test was used. For all tests the significance level was set to α=0.05.

2.4 Results

2.4.1 Task performance and wrist dynamics

The percentage of successfully accomplished trials (i.e. reaching the target position within the given time and accuracy constraints) over all subjects are presented in Figure 2-3 (A). The percentage of successful trials was not influenced by the choice of the handle ($F(2,22)=0.321$; $p=0.728$). Average movement trajectories, corresponding angular velocity and wrist torque profiles calculated from the successful trials are shown in Figure 2-3 (B-D) for the three handles used in this study. High correlations with a minimum jerk reference trajectory were found for each handle (curved handle: $R=0.998$, $p<0.01$; grooved handle: $R=0.997$, $p<0.01$; palm handle: $R=0.997$, $p<0.01$). Note that success rates remained relatively low for each handle (between 11-64% for a single block), illustrating the difficulty to achieve the dynamic wrist target-reaching task within the imposed time and accuracy constraints.

2.4.2 Patterns of muscle activity

Surface EMG signals obtained from the 4 forearm muscles (i.e. FCR, ECR, FDS and EDC), for all successful trials of a representative subject are shown in Figure 2-4 (A). These trials were performed with the palm handle and show the activation pattern of flexor muscles during the first phase of the movement (FCR, FDS), as well as a time-dependent activation shift of the extensor muscles in the later phase of the movement (ECR, EDC). The corresponding heat maps for the relatively low co-activated muscle pair FCR-ECR and for the highly co-activated muscle pair FCR-FDS are presented in Figure 2-4 (B) and Figure 2-4 (C), respectively.

Averaged co-activation indices calculated for muscle pairs formed between FCR, ECR, FDS and EDC are presented in Figure 2-5 for each handle. Only the two antagonistic muscle pairs (co-contraction) FCR-ECR and FDS-EDC and the two synergistic muscle pairs (co-activation) FCR-FDS and ECR-EDC were investigated, as the muscle pairs FCR-EDC and ECR-FDS are not relevant from an anatomical standpoint. Only nine subjects could be included in this analysis due to the presence of corrupted EMG-signals in part of the experiment for the other three subjects.

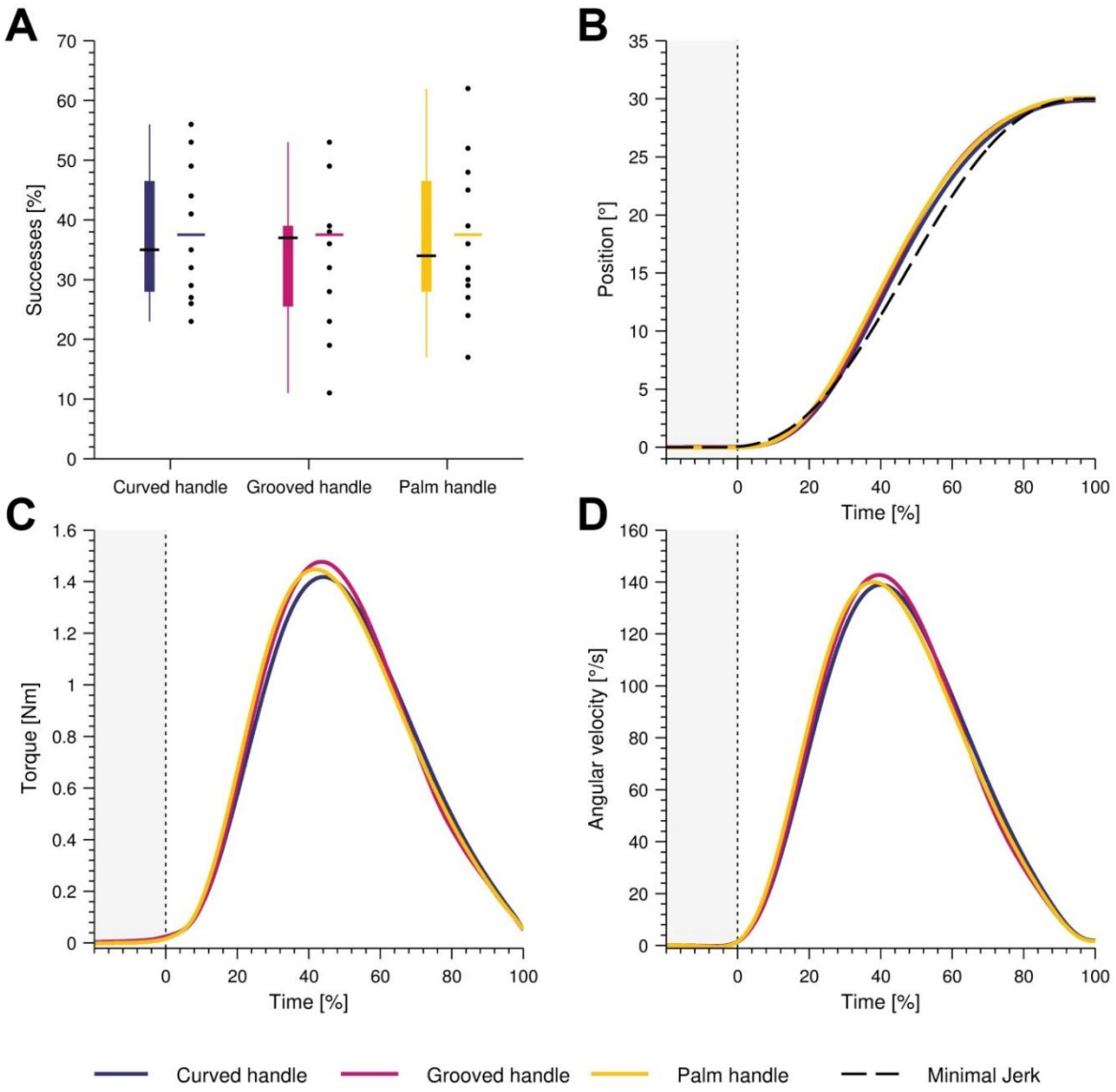

Figure 2-3: The boxplot represents the percentage of successful trials with the median presented as black line, the single data points presented as black points and the mean presented as colored line (A). The repeated measures ANOVA showed no significant difference between the investigated handles. In addition the averaged movement trajectories during successful trials of all subjects are presented (B). The minimum jerk trajectory computed between initial and target angular position serves as reference for a fast and smooth target reaching task. The corresponding torque (C) and velocity (D) profiles are additionally presented at the bottom part.

The overview of the repeated measure ANOVAs for the CI values are presented in Table 2-1. The statistical analysis of CI-values for the muscle pair FCR-ECR showed only a significant within-subject effect when analyzing the entire trial ($p<0.05$). The post-hoc analysis showed only a significantly higher CI value for the grooved handle compared to the palm handle. A significant within-subject effect was also found for the muscle pair FCR-FDS for the entire trial ($p<0.05$) as well as from the sub-part of 10-30% of the movement ($p<0.05$).

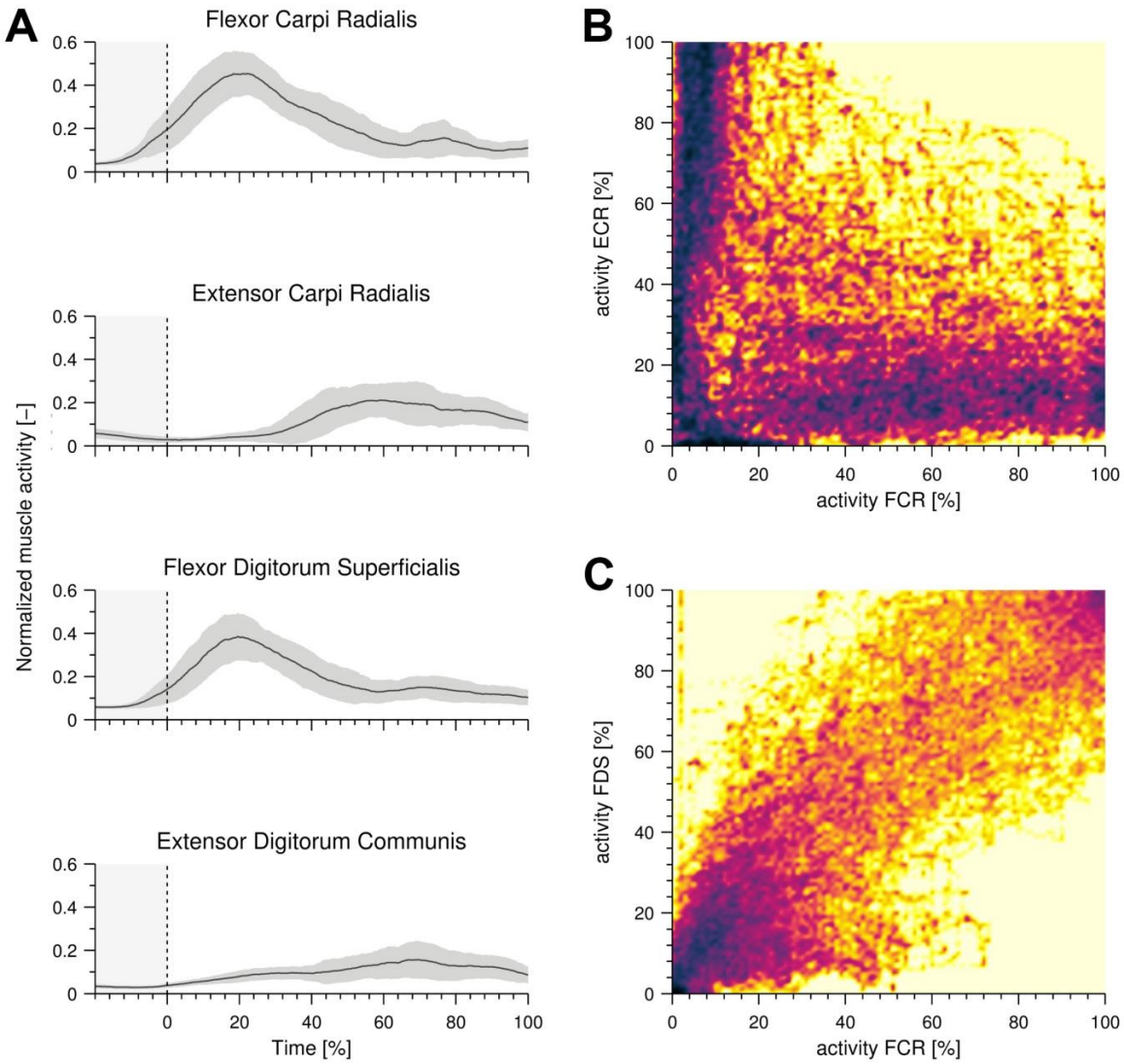

Figure 2-4: Mean EMG activation pattern (only successful trials) of one representative subject. Means of the four muscles Flexor Carpi Radialis (FCR), Extensor Carpi Radialis (ECR), Flexor Digitorum Superficialis (FDS) and Extensor Digitoum Communis (EDC) are shown in black and the standard deviation areas in grey (A). The dashed lines at 0% illustrate the start of the trials. Illustration of the co-activation showing the temporally shifted activation of both antagonistic wrist muscles (B) and the simultaneous activation of both flexors FCR and FDS contributing to wrist flexion (C). Dark areas are representative for a high number of data points whereas bright areas stand for low number of data points.

Despite the significant effects found in the within-subject tests the pairwise comparison did only survive the Bonferroni correction for the latter where the curved handle had a significantly higher CI value compared to the palm handle ($p<0.05$). The statistical analysis of the CI-values comparing the three investigated handles and the joystick-like handle is presented in the lower part of Table 2-1.

The statistical analysis of the mean and maximal EMG values of the four muscles showed no significant difference between the three investigated handles for any of the analyzed trial parts. The mean and the maximal values are presented in Figure 2-6 and the corresponding F-values and p-values are presented

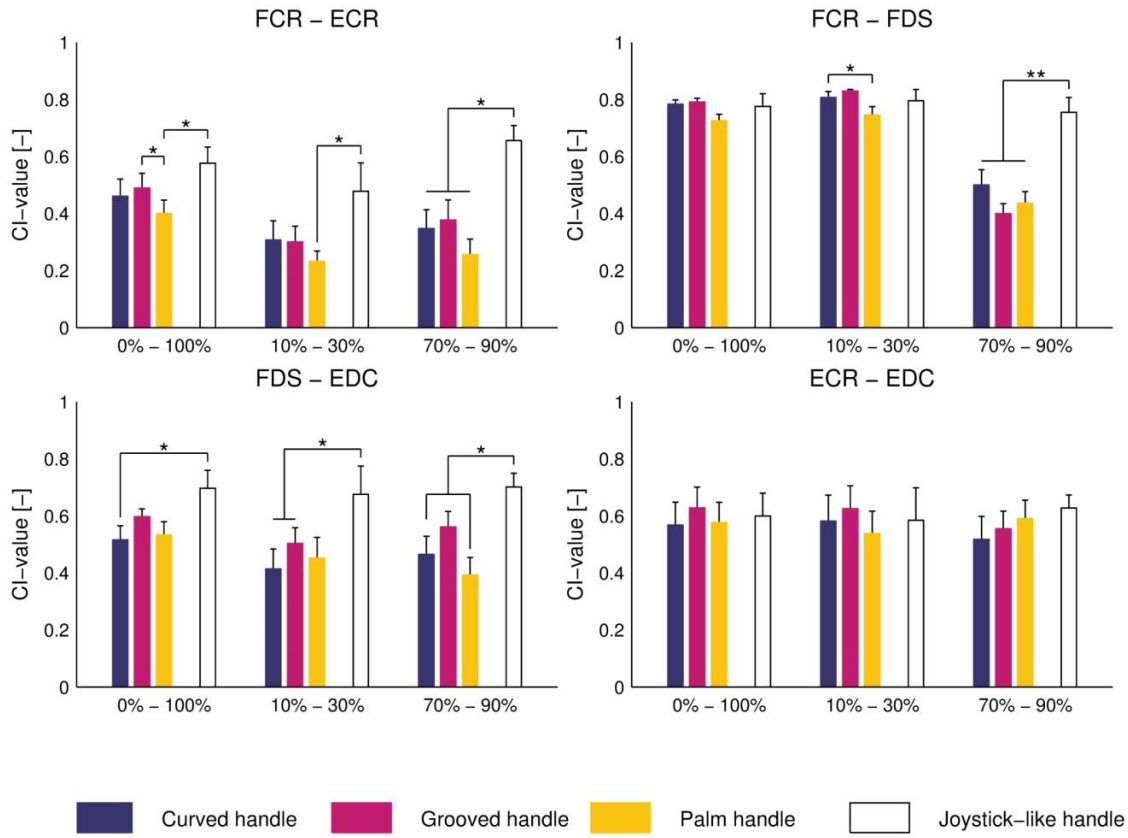

Figure 2-5: Mean co-activation index (CI-values, n=9, mean ± SE) for the investigated handles between four muscle pairs composed of Flexor Carpi Radialis (FCR), Extensor Carpi Radialis (ECR), Flexor Digitorum Superficialis (FDS), Extensor Digitorum Communis (EDC) during the complete trial (0-100%) the beginning of the trial (10-30%) and at the end of the trial (70-90%). CI values obtained in a preliminary study performed with five subjects using a joystick-like handle (white bar on the right for each muscle pair) are reported for comparison. *p<0.05, **p<0.01.

in Table 2-2. The statistical analyses of the mean and maximal EMG values between the joystick-like handle and the three investigated handle are presented at the bottom of Table 2-2.

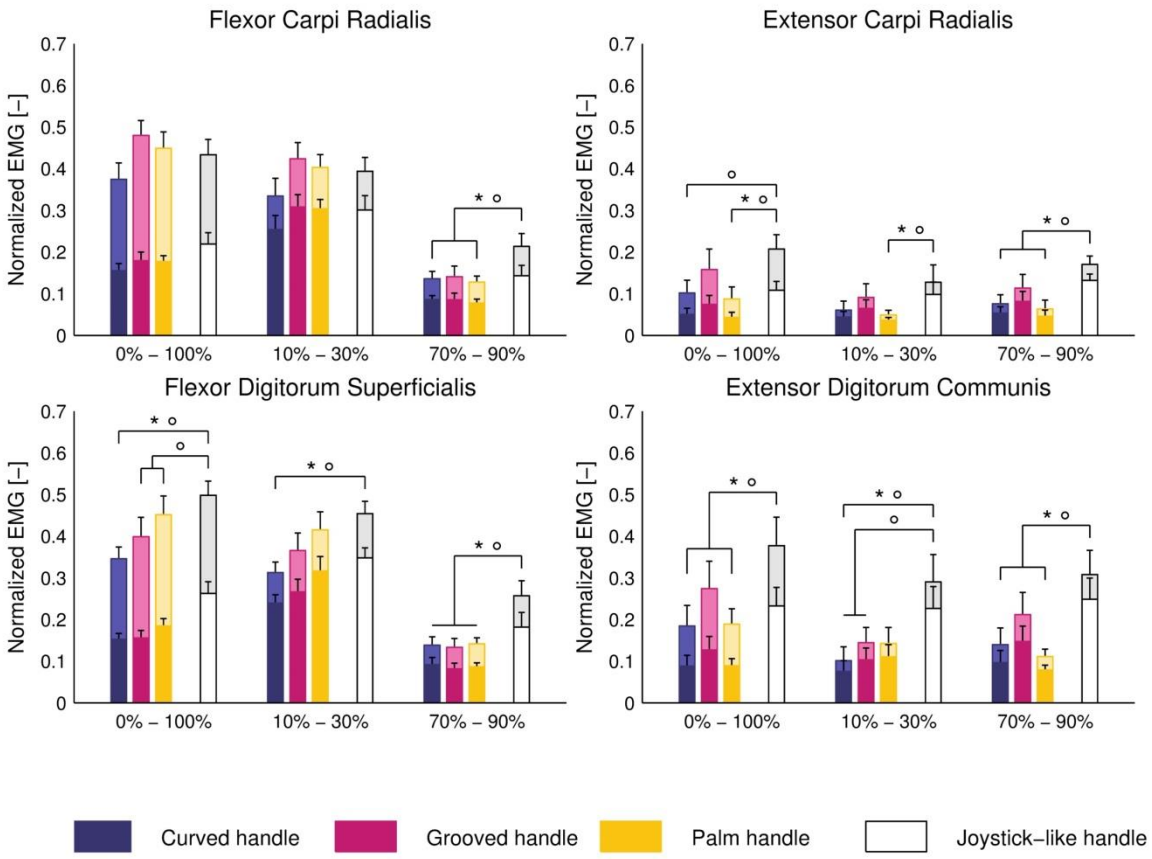

Figure 2-6: Mean (dark) and maximum (bright) EMG values for the four muscles Flexor Carpi Radialis (FCR), Extensor Carpi Radialis (ECR), Flexor Digitorum Superficialis (FDS) and Extensor Digitorum Communis (EDC) presented as mean ± SE. EMG values obtained in a preliminary study performed with five subjects using a joystick-like handle are reported for comparison. (*: p<0.05 (maximum); °: p<0.05 (mean))

2.4.3 Ergonomics

Results of the questionnaires for the twelve participants are summarized in Figure 2-7. All subjects rated the three handles to induce no pain (0 on a 0-10 scale) with repeated use, with the exception of two subjects, who stated that they felt slight pain (2 on a 0–10 scale) during the experiment with the grooved handle. In response to the question of which handle the participants rated as best for the evaluated wrist flexion task, the grooved handle was chosen 5 times, the curved handle 4 times and the palm handle 3 times. In terms of fatigue and pain the analysis of the different handles showed no significant differences (fatigue: $F(2,22)=0.809$, $p=0.458$, pain, with Greenhouse-Geisser adjustment for sphericity: $F(1,11)=2.200$, $p=0.166$).

Comfort, on the other hand, was influenced by the type of the handle ($F(2,22)=3.496$, $p<0.05$). The post-hoc analysis showed that subjects rated the palm handle significantly higher than the grooved handle ($p<0.05$). The other two pairs showed no statistical difference (grooved-curved: $p=0.087$, curved-palm:

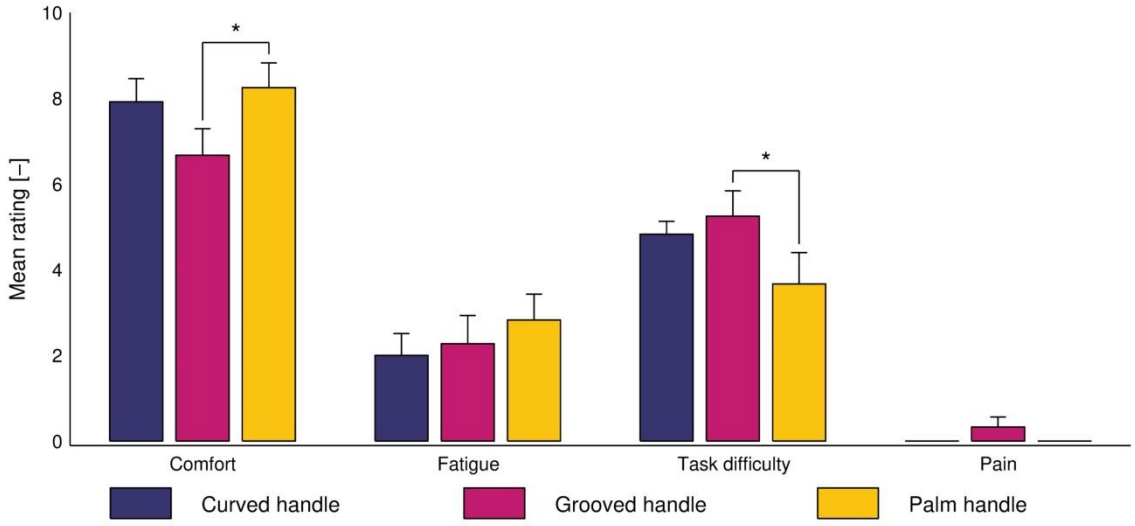

Figure 2-7: Mean ± standard deviation of the questionnaire data. For each criterion, the linear scales reach from 0-10 (Comfort: 0 = "uncomfortable", 10 = "comfortable"; Fatigue: 0 = "no fatigue", 10 = "severe fatigue"; Task difficulty: 0 = "very easy", 10 = "very difficult"; Pain: 0 = "no pain", 10 = "severe pain"). * p<0.05

p=0.601). Similarly, the perceived task difficulty was significantly influenced by the handle type ($F(2,22)=3.476$, $p<0.05$). The pairwise analysis again showed a significantly higher perceived task difficulty for the grooved handle compared to the palm ($p<0.05$). The other two combinations again showed no significant difference (grooved-curved: p=0.269, curved-palm: p=0.137).

Table 2-1: F-values and p-values for the repeated measure ANOVA analyzing the co-activation index (CI) values for different muscle pairs including the muscles Flexor Carpi Radialis (FCR), Extensor Carpi Radialis (ECR), Flexor Digiotrum Superficialis (FDS) and Extensor Digitorum Communis (EDC). Post-hoc analysis is reported when within-subject effect was significant. Bottom part of the table shows the results of the t-test comparing the three handles (curved, grooved, palm) to the joystick-like handle used in a previous study.

Muscle pair		**FCR - ECR**	**FCR - FDS**	**ECR - EDC**	**FDS - EDC**
			CI Values 0 -100%: F-value (p-value)		
Within-subjects effect F(2,16)		**3.968 (p=0.040)**	**5.717 (p=0.013)**	0.412 (p=0.669)	1.117 (p=0.352)
Post-hoc					
Curved - Grooved		1.000	1.000	-	-
Curved - Palm		0.412	0.103	-	-
Grooved - Palm		**0.048**	0.108	-	-
			CI Values 10 -30%: F-value (p-value)		
Within-subjects effect F(2,16)		1.209 (p=0.324)	**5.748(p=0.013)**	0.892 (p=0.429)	1.648 (p=0.223)
Post-hoc					
Curved - Grooved		-	1.000	-	-
Curved - Palm		-	**0.036**	-	-
Grooved - Palm		-	0.106	-	-
			CI Values 70 -90%: F-value (p-value)		
Within-subjects effect F(2,16)		3.305 (p=0.063)	1.533 (p=0.246)	0.557 (p=0.583)	2.962 (p=0.080)
			Comparison of CI values for the joystick-like handle: p-values		
Curved handle	entire trial	0.203	0.831	0.792	**0.032**
	10-30% of trial	0.138	0.763	0.982	**0.036**
	70-90% of trial	**0.006**	**0.006**	0.331	**0.018**
Grooved handle	entire trial	0.270	0.661	0.789	0.085
	10-30% of trial	0.089	0.236	0.756	0.096
	70-90% of trial	**0.014**	**<0.001**	0.410	0.091
Palm handle	entire trial	**0.028**	0.237	0.833	**0.042**
	10-30% of trial	**0.009**	0.296	0.715	0.070
	70-90% of trial	**<0.001**	**<0.001**	0.681	**0.004**

Table 2-2: F-values and p-values for the repeated measure ANOVA analyzing the maximal and mean normalized EMG values for the different muscles Flexor Carpi Radialis (FCR), Extensor Carpi Radialis (ECR), Flexor Digiotrum Superficialis (FDS) and Extensor Digitorum Communis (EDC). Greenhouse-Geisser (GH) adjustment is reported at the bottom if it was applied due to violation of sphericity. Bottom part of the table shows the results of the t-test comparing the three handles (curved, grooved, palm) to the joystick-like handle used in a previous study.

Muscle		**FCR**	**ECR**	**FDS**	**EDC**
		Normalized EMG 0 -100% F-value (p-value)			
Within-subjects effect F(2,16)					
maximum value		2.516 (p=0.112)	2.776 (p=0.129)[1]	1.792 (p=0.198)	2.418 (p=0.121)
mean value		1.451 (p=0.263)	3.474 (p=0.090)[4]	1.124 (p=0.349)	2.121 (p=0.152)
		Normalized EMG 10 -30% % F-value (p-value)			
Within-subjects effect F(2,16)					
maximum value		2.594 (p=0.106)	2.080 (p=0.157)	1.853 (p=0.189)	2.647 (p=0.102)
mean value		2.213 (p=0.142)	2.027 (p=0.164)	2.011 (p=0.166)	3.044 (p=0.076)
		Normalized EMG 70 -90% % F-value (p-value)			
Within-subjects effect F(2,16)					
maximum value		0.264 (p=0.654)[2]	2.993 (p=0.115)[3]	0.062 (p=0.940)	2.923 (p=0.083)
mean value		0.314 (p=0.629)[5]	2.957 (p=0.119)[6]	0.209 (p=0.814)	2.833 (p=0.088)
		Comparison to joystick-like handle: p-values			
Curved	*maximum 0-100%*	0.309	0.039	**0.004**	**0.028**
	mean 0-100%	**0.041**	**0.031**	**<0.001**	**0.007**
	maximum 10-30%	0.332	0.107	**0.003**	**0.008**
	mean 10-30%	0.351	0.061	**0.004**	**0.008**
	maximum 70-90%	**0.025**	**0.010**	**0.004**	**0.022**
	mean value 70-90%	**0.016**	**0.004**	**0.014**	**0.010**
Grooved	*maximum 0-100%*	0.388	0.481	0.146	0.301
	mean 0-100%	0.231	0.293	**0.004**	0.057
	maximum 10-30%	0.590	0.484	0.151	**0.039**
	mean 10-30%	0.881	0.334	0.076	**0.029**
	maximum 70-90%	0.086	0.227	**0.005**	0.244
	mean value 70-90%	0.051	0.145	**0.004**	0.103
Palm	*maximum 0-100%*	0.787	**0.018**	0.468	**0.013**
	mean 0-100%	0.117	**0.010**	**0.021**	**0.002**
	maximum 10-30%	0.848	**0.024**	0.520	**0.042**
	mean 10-30%	0.950	**0.013**	0.518	**0.042**
	maximum 70-90%	**0.009**	**0.005**	**0.002**	**<0.001**
	mean 70-90%	**0.007**	**0.002**	**0.003**	**<0.001**

[1] GH: F(1.118, 8.948), [2] GH: F(1.163, 9.303), [3] GH: F(1.130, 9.039), [4] GH: F(1.175, 9.403), [5] GH: F(1.2, 9.598)
[6] GH: F(1.102, 8.817)

2.5 Discussion

This paper presented the evaluation of three handle designs (i.e. curved handle, grooved handle and palm handle) to be used as interface between the hand and a robotic manipulandum during physical human-robot interaction. A study with 12 healthy subjects was performed with the objective of comparing the three handles in terms of movement dynamics and subjective ergonomic criteria such as fatigue, comfort and pain during repeated wrist flexion tasks. Additionally, patterns of muscle activity during this typical motor learning task were further evaluated for the three handles and compared to a widely used joystick-like design (Masia et al., 2009, Suminski et al., 2007, Kadivar et al., 2012).

2.5.1 Handle design does not influence performance in a wrist flexion task

The results of the present study suggest that the handle design did not influence subjects' performance in a dynamic wrist flexion task. All handles showed similar success rates for accomplished trials. An analysis of angular trajectories showed that, for all handles, successful reaching movements corresponded well to a minimum jerk profile, which is characteristic of natural feed-forward target reaching movements (Hogan, 1984b). Wrist torque profiles were also found to be similar across all handles. Thus, despite different finger positions on the handles, subjects could perform wrist tasks equally well with all handles. Several studies have shown that handle design, e.g. the diameter of a cylindrical handle or lid, or the wrist posture, affected by the handle design, influences variables such as maximal force and torque production at the level of the fingers and the wrist (Seo et al., 2007, Crawford et al., 2002, Plewa et al., 2016, Yoshii et al., 2015, Young et al., 2009). However, in the presented study the required wrist torque never exceeded 1.8 Nm, which is less than 40% of maximum voluntary wrist torque. Our results indicate that for this torque range the handle design has only limited to no impact on dynamic performance when the wrist is primarily involved in the task. Additionally, the similar subject performance with the three investigated handles might be explained by the fact that subjects could still learn to perform the dynamic task, despite a sub-optimal or uncomfortable interface.

2.5.2 Handle design influences muscle co-activation

Patterns of muscle activity during wrist flexion tasks were found to be similar across handles. Clear synergistic activation between wrist and finger flexors (FCR-FDS), and between wrist and finger extensors (ECR-EDC) were observed. This coupling can easily be explained by the wrist anatomy, as FCR and FDS both contribute to wrist flexion and ECR and EDC both contribute to wrist extension (Gonzalez et al., 1997). FCR and FDS generated the torque against the velocity-dependent force field and accelerated the hand in the first phase of the task. ECR and EDC were maximally activated at the end of the movement to slow down the hand and stabilize the end-point position. In general, the comparison between the antagonistic wrist muscle pair FCR-ECR and the antagonistic finger muscle pair FDS-EDC showed a time-dependent shift in activation of the respective agonist and antagonist muscles, resulting in low CI values. With the grooved handle, a significantly higher co-contraction of the wrist muscles (FCR, ECR) was observed compared to the palm handle. This might be caused by the specific shape of the grooved handle (i.e. with the fingers are maintained in an abducted position) that required subjects to perform the task with more activation of the ECR muscle. A significant difference in co-activation index was also found between curved handle and palm handle at the beginning of the movement for the muscle pair FCR-FDS. The higher co-activation index might be caused by the fact that the FCR and EDC muscles were similarly highly activated when using the curved handle even if FCR and EDC were by trend more highly activated when using the palm handle. It should be noted that a higher CI-value can result from a higher activation of the antagonistic muscle or from a lower activation value of the most active muscle. Interestingly, the agonist-antagonist co-activation was significantly lower for all three handles at the end of the trial compared to prior data collected with a joystick-like handle during the same dynamic wrist flexion task with the robot. With the joystick-like handle, subjects had the tendency to increase hand and wrist stiffness by tightly grasping the handle from the beginning of the movement. This was underlined by the mean and maximal EMG values recorded where all muscles were typically more active in each period of the movement when the joystick-like handle was used. While this may offer more stability during the movement, this non-task-related increase in wrist stiffness could alter endpoint impedance during motor tasks, and might lead to increased fatigue over time. With handles offering curved interaction surfaces, such as the curved

handle, the fingers are in a more extended position, such that the ability to generate finger force against the handle is decreased (Kong and Lowe, 2005). This limits finger muscle activity during the movement and allows to better isolate the contribution of wrist muscles to the task.

The complete absence of a physical support for the fingers when using the palm handle resulted in higher activity of the FDS muscle compared to the curved and the grooved handle. One would expect that, when freely moveable, fingers need to be stabilized. The stabilization of fingers could occur through increased joint stiffness, which should also result in a higher antagonistic activation of the EDC muscle. Interestingly, a higher EDC activation during the use of the palm handle was not seen. This would suggest that, with the palm handle, fingers are not stabilized by increased joint stiffness but rather through establishing contact of the proximal phalanges with the handle. Thus, despite the statistically significant differences in some of the reported EMG outcomes, the handle design seems to influence the muscle activity patterns only marginally.

2.5.3 Subjective feedback from questionnaires

Comfort was rated relatively high (>6.6/10) for all three handles. The results showed that the grooved handle was significantly less comfortable than the palm handle, and two subjects further reported minor pain while using the grooved handle. This might be due to the fact that for participants with small hands, it was difficult to fit the little finger into the designated groove. This underlines that grooved handles or, in general, handles that guided fingers into predefined positions should be customized to each individual subject, which might be a drawback. The level of fatigue reported by subjects was low, with no statistically significant difference between handles. Note that a quantitative fatigue analysis based on the EMG data (Balasubramanian et al., 2011, Jørgensen et al., 1988) was not implementable here, as muscles were not continuously activated during single trials.

2.5.4 Limitations

The outcomes of this study are limited by the relatively low number of subjects. Furthermore, the reported fatigue and comfort may have been influenced by the relatively long duration of each block (15 minutes) and the repetitions of blocks on a single day. The experiment was limited to a single dynamic target-reaching task in wrist flexion, and the results might therefore not translate to other tasks.

2.6 Conclusions and future work

The results of this study point at a very important component in physical human-robot interaction, which often receives only limited consideration. While robotic manipulanda are being developed for a variety of applications, it is crucial to evaluate how the design of the physical interface between the robot and the human can influence ergonomics and sensorimotor behavior. Our results from a wrist flexion task suggest that joystick-like handles lead to increased co-contraction at the level of the wrist and the fingers, especially for the two extensors ECR and EDC. While such handles might be ideal for planar manipulanda, where higher wrist stiffness might be beneficial to increase stability during arm movements, they should be avoided in devices dedicated to the study of wrist tasks. Robotic manipulanda interacting with the wrist joint for repeated flexion tasks should rather consider using a handle that is fixed on the palmar side of the hand with a rigid surface adapted to the anatomy of the hand. The use of a handle where the fingers can be freely moved may result in increased involuntary activation of the FDS muscle. This should be especially considered when investigating activation patterns of muscles running over multiple joints. For the wrist task presented in this study, both the proposed curved handle and palm handle were found to be suitable and will thus be used in future motor learning experiments. In general, all three handles lead to similar kinematic and kinetic parameters as well as task performance. However, a handle in which fingers are constrained, like the grooved handle presented in this study, is not advisable, as it might cause light pain if not adjusted to the anthropometry of the individual subjects' hand. Further, the palm handle was associated with increased FDS activity, thus it should not be used in studies where this is relevant, e.g. to investigate wrist impedance. In conclusion, we recommend using the curved handle for such tasks, as it is the most versatile and universal option.

3 The effect of wrist posture and wrist stabilization on precision grip strength and muscle activation patterns in neurologically intact individuals[2]

[2] This chapter is a manuscript in preparation. Authors will be Werner L. Popp, Lea Richner, Olivier Lambercy, Alex Barry, Camila Shirota, Roger Gassert and Derek Kamper.

3.1 Introduction

In our daily lives, we greatly rely on our hands to interact with the environment, such as when grasping and manipulating objects. The hand and the digits are actuated by muscles located in the hand itself (intrinsic) and in the forearm (extrinsic). The biological advantage of having a remote location of some muscles is that it reduces mass and inertia of the hand and especially the digits, increases strength and allows for a greater range of motion of the finger joints, resulting in improved fine-motor skills. These multiarticular muscles do, however, evoke a cost in terms of control, and might also have a substantial impact on the force generation at the level of the fingers. Furthermore, the involvement of extrinsic and intrinsic hand muscles during grasping might require a significant coordination effort.

Experimental studies have shown that force production at the level of the fingers (e.g. during power or precision grip) can be modulated by different factors. For instance, grip and pinch strength are influenced by pinch aperture and pinch type (Dempsey and Ayoub, 1996, Imrhan and Rahman, 1995, Shivers et al., 2002), as well as by the posture of the shoulder (Parvatikar and Mukkannavar, 2009), elbow (Halpern and Fernandez, 1996, Mathiowetz et al., 1985c), wrist (Li, 2002, Hazelton et al., 1975, LaStayo and Hartzel, 1999), and finger joints (Lee and Rim, 1991).

The long digit flexors and extensors can exert considerable moments at the wrist, especially in combination with the wrist flexors (i.e., fexor carpi ulnaris (FCU) and flexor carpi radialis (FCR)) and the wrist extensors (i.e., extensor carpi radialis brevis and longus (ECRB/L) and extensor carpi ulnaris (ECU)), respectively, as shown by Gonzalez and coworkers (Gonzalez et al., 1997). Similarly, wrist posture has a substantial effect on muscle fiber length of the extrinsic finger muscles, and thus the maximum strength of these muscles. Several studies, with widely varying results, have investigated the influence of wrist angle on force production of the finger in power grip tasks. Maximum power grip force was found at 35° of wrist extension and 7° of ulnar deviation (O'Driscoll et al., 1992). In the same study, the authors concluded that small deviations (e.g. 15° extension and 0° ulnar-radial deviation) from the optimal wrist posture can lead to a decrease of more than 25% in muscle strength. In contrast, another study showed that power grip strength was maximal when the wrist was at 15° of extension and between 0° and 15° of ulnar deviation (Pryce, 1980). In a third study, maximum grip strength was observed at

20° of wrist extension and 5° of ulnar deviation (Li, 2002). Another study looking at three different wrist flexion-extension positions found significantly higher power grip strength in extension (30°) as compared to flexion and to the neutral position (Di Domizio et al., 2008). In contrast to the power grasp, the effect of wrist position on precision grip has not been widely studied, even though precision grip is important for many activities of daily living. Imrhan (1991) investigated the influence of five different wrist positions (neutral, radial and ulnar deviation, flexion and extension) on pinch strength produced with four different pinch grips. He showed that any deviation from the neutral position (0° flexion and 0° ulnar deviation) degraded pinch strength. In summary, while these studies found different optimal wrist angles for force production at the level of the fingers, all unanimously conclude that wrist angle in general influences the force generation capacity of the fingers. This can mainly be explained by the fact that the lever arm of the tendons and the length of the muscles change depending on the wrist position (Imrhan, 1991). Wrist position therefore has a substantial impact on maximum finger strength due to different biomechanical mechanisms affecting finger muscles such as FDS or EDC. Nevertheless, it remains unclear how wrist posture influences the neural control of finger muscles.

In rehabilitation settings, splints are often used to support the wrist and allow functional grasping. However, while some studies showed that wrist splints are associated with reduced grip strength, the influence of such a splint on motor control remains uninvestigated. Bhardwaj and coworkers (Bhardwaj et al., 2011) for example investigated the influence of a splint on maximum power grip force. The results showed that the splint reduced the maximum grasping force by 19%-25% in comparison to maximum grasping force without a splint. Furthermore, the maximum grip force was found when the splint held the wrist in 45° of extension. Another study also showed a significant decrease in grip strength (6%-43%) when the wrist was restrained in a certain position by an orthosis (Lee and Sechachalam, 2016). This study also found a maximum grip force with orthosis at 45° wrist extension for the non-dominant hand, whereas the maximum grip force for the dominant hand was found at 15° extension. In contrast to the previous findings, Di Domizio and coworkers reported an increase in maximum power grip force when a wrist splint was used (Di Domizio et al., 2008). In summary, a number of studies investigated the influence of wrist posture and/or wrist splints on grip strength, with widely varying results. Furthermore, the effect of wrist angle or external stabilization (e.g., through a splint) on grip strength

and simultaneous wrist and finger motor control remains poorly investigated. In addition, due to the specific muscle activation required to generate a precision grip, the effects may differ considerably from those observed for power grasp.

The aim of the study was therefore to investigate how simultaneous wrist and finger control is affected by wrist posture (flexion-extension). This was investigated by means of a 2-finger precision grip task in which subjects had to generate maximum grip force. For this experiment, we used a robotic wrist manipulandum constraining the wrist in all degrees of freedom except for flexion-extension while providing well-controlled and reproducible conditions. Maximum grip force was investigated under two experimental conditions, one in which the wrist was maintained in a position by the robotic wrist manipulandum (i.e. similar to a splint, but mechanically grounded) and one in which subjects had to stabilize the wrist in flexion-extension themselves. Grip force was measured by a miniature load cell held between the index finger and thumb, while flexion/extension torque against the robotic manipulandum was measured via a force/torque sensor located directly beneath the handle of the manipulandum. Surface electromyography (EMG) was recorded from intrinsic and extrinsic muscles in order to investigate the effect of wrist posture and wrist stabilization on muscle activation patterns and cortical drive. We expected that maximum pinch grip force would be at around 30° of extension when ulnar deviation was imposed at 10° by the manipulandum. Additionally, we hypothesized that maximum grip force would be reduced when subjects have to stabilize their own wrist compared to when it is externally stabilized, and that muscle activity patterns would be influenced by the wrist posture as well as by the experimental condition.

3.2 Methods

3.2.1 Subjects

15 neurologically intact subjects (age 26.9 ± 3.1 years, 9 males) were recruited for this study. Inclusion criteria required that subjects were 18 years or older and right-handed. Exclusion criteria were any history of neurological, orthopedic or rheumatologic disorder affecting wrist or hand functions. Each participant was informed about the experimental protocol and gave written consent prior to the experiment. The measurements took place at the Rehabilitation Engineering Laboratory at ETH Zurich. The study was approved by the ETH Zurich Ethics Commission (EK 2014-N-58).

3.2.2 Apparatus

A robotic one degree-of-freedom (DOF) wrist manipulandum (ReFlex, (Chapuis et al., 2010)) was used for this study (Figure 3-1 left and center). It consists of a DC motor (RE65, Maxon Motor, Sachseln, Switzerland) and a magnetic particle brake (S90MPA-B34D50H38, Stock Drive products/Sterling Instruments, New Hyde Park, NY, U.S.A.) which are coupled through a timing belt. A high-resolution optical encoder (R158, 1.000.000 counts/rev, Gurley Precision Instruments, Troy, NY, U.S.A.) is fixed to the motor shaft, and a 6 DOF force/torque sensor (Mini45, ATI 126 Industrial Automation, Apex, NC, U.S.A.) is mounted between the motor shaft and the handle support. Thanks to its hybrid actuation architecture, the robot is capable of rendering a wide range of impedances, from high transparency (no resistance to motion) to completely locking the position of the output handle. The robotic wrist manipulandum is controlled through a target PC, running a real-time operating system at a sampling frequency of 1kHz (LabVIEW Real Time 2013, National Instruments, Austin, TX, U.S.A.) and a standard host PC running LabVIEW 2013 (National Instruments, Austin, TX, U.S.A.) for the user interface and visual feedback. Pinch grip force was recorded using a miniature load cell (LLB210, Futek, Irvine, CA, USA; Figure 3-1 right) with a measurement range of 0-111N, which was sufficient for the present study as peak pinch force for healthy individuals is typically below 100N (Nilsen et al., 2012).

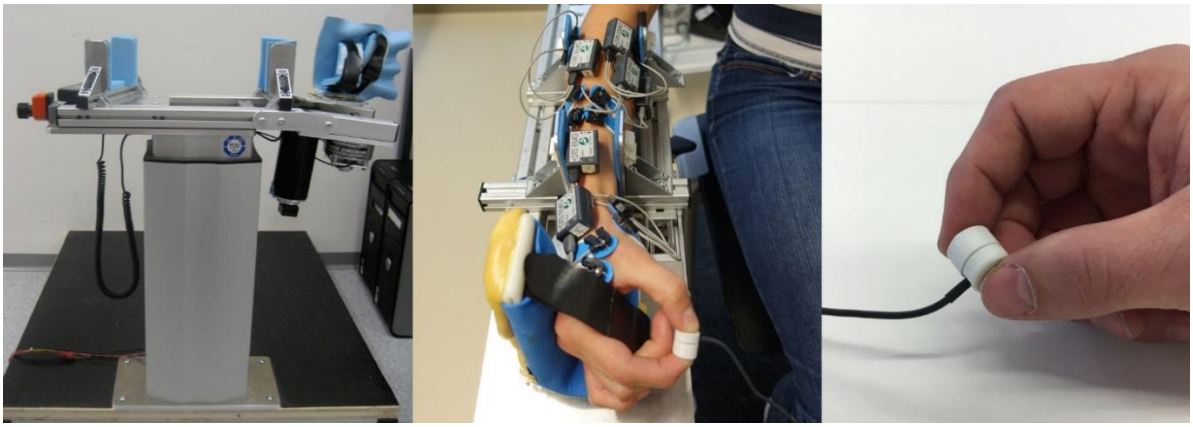

Figure 3-1: Experimental setup. Left: Side view of the robotic wrist manipulandum (ReFlex, Chapuis et al., 2010). Center: Wrist manipulandum with EMG electrodes and miniature load cell. Right: Miniature load cell during a precision grip.

For a comfortable pinch position, plastic finger pads with a diameter of 14mm were mounted on each side of the load cell such that the distance between the tips of the index finger and the thumb was 14.5mm (Figure 3-1 right). The small surface was chosen in order to prevent subjects from using their middle finger (tripod grip) during the experiment. Miniature load button data were acquired through the real-time operating system of the robotic wrist manipulandum.

EMG recordings were taken from flexor carpi radialis (FCR), extensor carpi ulnaris (ECU), flexor digitorum superficialis (FDS), extensor digitorum communis (EDU), thenar eminence (TE), and first dorsal interosseous (FDI). Muscle activity was recorded using wireless amplifiers (Telemyo DTS, Noraxon, Scottsdale, AZ, U.S.A.) with surface EMG electrodes (Blue Sensor N, Ambu, Ballerup, Denmark) which were placed above the muscle bellies (Figure 3-1 center). The EMG system was synchronized with the robotic wrist manipulandum through a TTL trigger pulse. EMG data were sampled at 1.5kHz and the EMG system had an integrated 1st order high-pass filter with a cutoff frequency of 10Hz.

3.2.3 Experimental protocol

Participants came to the lab for a single session lasting around 90 minutes. Prior to the experiment, participants were informed about the experimental procedure and the functioning of the robotic manipulandum. Then, EMG electrodes were placed on the participants' arms and EMG signals were individually checked for proper placement. Before starting the experimental session, the maximal voluntary contraction (MVC) of each recorded muscle was assessed three times for 5s to normalize

EMG signals. The highest activation level of each muscle over all MVC measurements was taken as MVC. Subsequently, subjects were seated comfortably next to the robotic manipulandum, and height and position of the device were adjusted. The hand was then strapped to the handle after aligning the wrist joint with the motor axis. A detailed explanation of the visual feedback was then provided to the subject.

A trial consisted of a 3-second window in which subjects generated maximal grip force using a two-finger precision grip (index finger and thumb opposition) at a given wrist posture. Eleven wrist postures, ranging from -50° (extension) to 50° (flexion) in increments of 10°, and two different wrist stabilization conditions were investigated. Wrist posture was either maintained by the manipulandum which was locked in place (externally stabilized), or the participant had to maintain the wrist within a specific target range (± 2 degrees) whilst the manipulandum was free to move (self-stabilized). A visual display alerted the participant to position deviations. An auditory cue instructed participants to generate maximal grip force. Each wrist posture/stabilization condition combination was repeated three times, resulting in a total of 66 trials (11 postures * 2 stabilization conditions * 3 repetitions). Trials were collected in 6 blocks with alternating stabilization conditions. Each block consisted of the 11 different postures presented in random order. To avoid fatigue during the experiment, subjects waited for 30s between consecutive trials, and five minutes between blocks. Trials in the self-stabilized conditions were automatically aborted and repeated when subjects left the target range (deviation of ±2° detected by the robot).

3.2.4 Outcome measures

Grip force, wrist torque (flexion-extension) and wrist position data were filtered using a 2^{nd} order Butterworth low-pass filter with a cutoff frequency of 20Hz, used in the forward and backward directions. For each trial, peak pinch force was extracted over the three-second window, and wrist torque and position were taken at the time point of peak pinch force.

For aligning the EMG signals with the robot signals, the EMG signal was downsample to 1kHz. Afterwards, EMG signals were band-passed filtered between 10–450Hz with a 4^{th} order Butterworth filter. In order to extract the envelope of the EMG signal, the root mean squared (RMS) value was

calculated using a 100ms sliding window. Signals were then normalized to the corresponding MVC measurement. Average and maximal normalized muscle activation for each trial were calculated for a 300ms window that ended when peak pinch force was reached, as EMG precedes muscle force. The average muscle activations were used to calculate the co-activation index (CI) for all possible muscle pair combinations using the following method (adapted from (Popp et al., 2016b)):

$$CI = \frac{2 \cdot min(EMG_1, EMG_2)}{EMG_1 + EMG_2} \qquad (3.1)$$

where EMG_1 and EMG_2 are the average normalized muscle activities for the two muscles being compared. CI values can range from 0 to 1, where at 0 only one or no muscle is activated, and at 1 both muscles have the same activation level. Co-activation indices were only calculated for the two synergistic (FCR-FDS, ECU-EDC) and the two antagonistic muscle pairs (FCR-ECU, FDS-EDC).

In order to analyze the similarity between muscle activation patterns across wrist angles, stabilization conditions, and subjects, we used the cosine similarity approach proposed by Poston and coworkers (Poston et al., 2010, Danna-Dos Santos et al., 2010). The average activation of each muscle (over the same 300ms window) was used to create a 6-dimensional vector, referred to as muscle activation pattern (MAP), where each element represents the mean activity of the corresponding muscles. In order to compare MAP similarity across subjects and experimental conditions, the cosine similarity was computed using:

$$similarity = \cos\alpha = \frac{A \cdot B}{\|A\|\|B\|} \qquad (3.2)$$

where A and B represent the two MAP vectors being compared and α represents the angle between the two vectors. As the processed EMG signals can only be equal or greater than 0, the similarity can only lie between 0 (= dissimilar) and 1 (=similar).

In order to analyze the cortical contribution to muscle co-activation, the EMG-EMG coherence between all possible muscle pair combinations was computed. The coherence analysis is based on the approach presented by Kamper and coworkers (Kamper et al., 2014, Halliday et al., 1995). For this analysis, raw EMG signals were filtered using a 4th order Butterworth bandpass filter between 20Hz and 55Hz. The

three trials (each of 300ms) per wrist posture and condition combinations were concatenated. The EMG-EMG coherence was calculated by computing the magnitude squared coherence $C_{xy}(f)$ for a given frequency f by using the cross-spectrum $S_{xy}(f)$ of the two EMG signals and the auto-spectrum of each EMG signal ($S_{xx}(f)$ and $S_{yy}(f)$):

$$C_{xy}(f) = \frac{|S_{xy}(f)|^2}{S_{xx}(f) \cdot S_{yy}(f)} \qquad (3.3)$$

The coherence for the concatenated EMG signals (900ms) was computed for segments with a length of 256 samples and a 50% overlap. The frequency resolution was 3.91Hz. The analysis focused on the 24Hz to 40Hz band as there is evidence that EMG signals within this band are mediated by common supraspinal inputs (Norton and Gorassini, 2006). The integral of coherence lying above the 95% confidence interval within the 24Hz - 40Hz cortical band was computed. The 95% confidence interval was computed by using an approach described by Rosenberg et al. (Rosenberg et al., 1989):

$$Z = 1 - \alpha^{1/(L-1)} \qquad (3.4)$$

where L represents the total number of segments used to calculate the coherence, and α is set to 0.05. By using this approach, a higher coherence integral value is related to an increased common supraspinal drive to the investigated muscle pair.

3.2.5 Statistical analysis

All statistical analyses were performed in MATLAB 2014a (MathWorks, Natick, MA, USA), with significance level α=0.05 for all tests. Descriptive statistics are reported as mean ± SD unless stated otherwise. In order to identify if maximal pinch force, average muscle activity or CI values were influenced by either experimental condition or wrist posture, repeated measures ANOVAs were used (F statistics reported as F). In case the assumption of sphericity was violated, a Greenhouse-Geisser correction was used (F statistics reported as F_{GH}). If data did not meet the criteria for a repeated measures ANOVA, data was square root transformed (F statistics reported as F_{sqrt}). In order to reveal relationships between data sets, Pearson correlation coefficients were computed, as all data were normally distributed (Shapiro-Wilk test). Finally, to identify significant differences in coherence between the different

muscle pairs, Friedman tests with Dunn-Bonferroni post-hoc tests were used as data was not normally distributed. In order to identify significant changes in coherence between both wrist stabilization conditions, paired t-tests or Wilcoxon signed-rank tests were used for normally or non-normally distributed data, respectively.

3.3 Results

The average maximal pinch force for the different wrist postures and the different wrist stabilization conditions are presented in Figure 3-2 (left). The maximal pinch force was influenced by the wrist posture ($F(10,140)=19.555$, $p<0.001$) as well as by the experimental condition ($F(1,14)=61.575$, $p<0.001$). A significant decrease in pinch force was found in wrist flexion (30°–50°). Maximal pinch force was significantly higher in the externally stabilized condition compared to the self-stabilized condition. Furthermore, a strong negative correlation in the externally stabilized condition was found between the wrist posture and the wrist torque ($R = -0.9835$, $p<0.001$, Figure 3-2 right). The linear regression for the previously mentioned correlation predicts a wrist torque of 0Nm at a wrist angle of -22.25°.

An overview of the averaged normalized muscle activity for the different investigated muscles (intrinsic and extrinsic) can be found in Figure 3-3 and the associated statistical analysis in Table 3-1. The average activity of all extrinsic hand muscles was significantly higher in the externally stabilized condition, whereas the intrinsic muscles were not influenced by the wrist stabilization conditions. Furthermore, the wrist posture had no significant influence on the activation level of any of the investigated muscles.

The CI values for the muscle pairs FCR-ECU, FCR-FDS, FDS-EDC, and ECU-EDC are represented in Figure 3-4. The CI value for the muscle pair FCR-ECU was significantly influenced by the wrist posture ($F(3.796,53.140)=3.728$, $p = 0.011$) but not by the wrist stabilization condition ($F(1,14)=0.072$, $p = 0.792$). The CI values for the other three muscle pairs were neither statistically influenced by the wrist posture (FDS-EDC: $F(2.576,35.934)=2.722$, $p = 0.067$; FCR-FDS: $F(3.959,55.421)=1.649$, $p = 0.176$, ECU-EDC: $F(2.645,37.025)=2.488$, $p = 0.082$) nor by the experimental condition (FDS-EDC: $F(1,14)=0.265$, $p = 0.615$; FCR-FDS: $F(1,14)=2.398$, $p = 0.144$; ECU-EDC: $F(1,14)=1.858$, $p = 0.194$).

A strong negative correlation was found between maximal pinch force and absolute wrist torque ($R = -0.899$, $p < 0.001$) as well as between absolute wrist torque and CI value of the FCR-ECU muscle pair ($R = -0.933$, $p < 0.001$) under the externally stabilized condition (Figure 3-5). Additionally, a strong positive correlation was found between pinch force and CI value of the FCR-ECU muscle pair for the

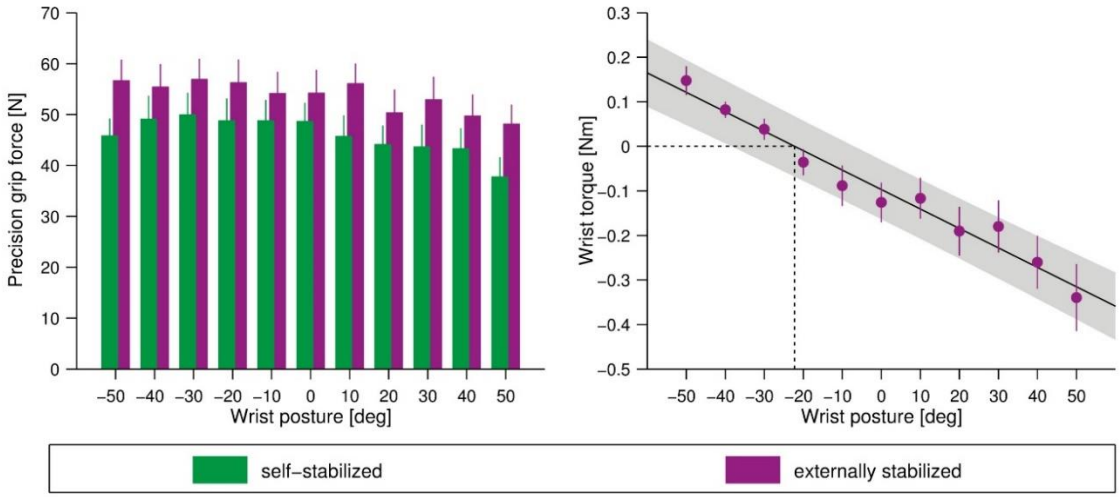

Figure 3-2: Average maximal pinch force (N=15) for the self-stabilized and the externally stabilized conditions are presented on the left side. The right plot presents the relationship between wrist posture (positive: flexion, negative: extension) and wrist torque in the externally stabilized condition. The dashed line indicates the estimate where no wrist torque would be produced (-22.25 deg). The black line represents the regression line and the shaded region represents the 95% confidence interval.

externally stabilized condition ($R = 0.882$, $p < 0.001$) and a moderate positive correlation for the self-stabilized condition ($R = 0.676$, $p < 0.001$).

Figure 3-6 shows the MAP averaged across all wrist angles for the two experimental conditions. Note that all subjects showed very similar MAPs between self-stabilized and externally stabilized condition, with cosine similarity values above 0.951. In order to show how the MAPs change with wrist flexion angle, the cosine similarity was normalized for each wrist posture MAP against the 30° extension MAP, which is represented on the left side of Figure 3-7. The reference angle of 30° extension was chosen, as subjects were able to produce maximum grip force in this position. Note that with increasing distance, the similarity of the muscle activation patterns decreases. Nevertheless, with all values >0.92, the similarity between muscle activation patterns remained high.

The cosine similarity of the MAPs varied substantially between subjects (Figure 3-7, middle and right). Intersubject cosine similarity values ranged between 0.270 and 0.980 with an average value of 0.784 for the self-stabilized condition and between 0.519 and 0.972 with an average value of 0.813 for the externally stabilized condition.

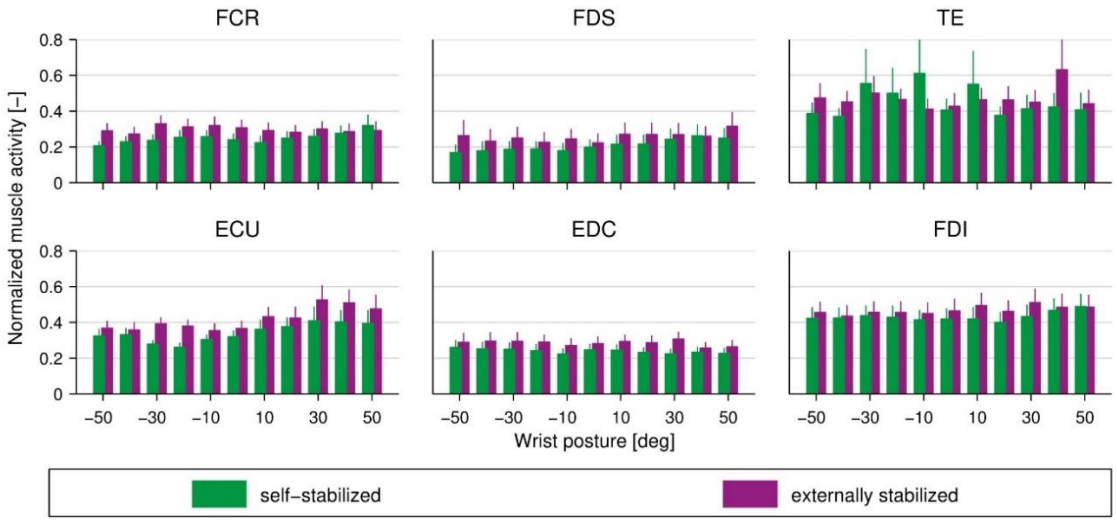

Figure 3-3: Mean ± SE normalized muscle activity across subjects for the self-stabilized and the externally stabilized condition is presented for the muscles flexor carpi radialis (FCR), extensor carpi ulnaris (ECU), flexor digitorum superficialis (FDS), extensor digitorum communis (EDC), thenar eminence (TE) and first dorsal interosseous (FDI). The corresponding statistics can be found in Table 3-1. Note that the activation of the extrinsic muscles was influenced by the wrist stabilization condition, but not by the wrist flexion angle. The intrinsic muscles were not influenced by any of the investigated factors.

The results of the EMG coherence analysis are presented in Figure 3-8. The statistical analysis showed significant differences in EMG coherence levels between the investigated muscle pairs for the self-stabilized condition (Chi-squared(14)=78.127, $p < 0.001$, $n = 11$) as well as for the externally stabilized condition (Chi-squared(14)=73.609, $p < 0.001$, $n = 11$). The results of the post-hoc analyses are also presented in Figure 3-8. The comparison of the coherence for each muscle pair under the self-stabilized and the externally stabilized condition showed no significant differences, with all p-values lying above 0.083, except for the muscle pair ECU-TE ($p = 0.036$) where the coherence in the self-stabilized condition was significantly higher than in the externally stabilized condition.

Table 3-1: Statistics for the level of muscle activation presented in Figure 3-3.

Muscle	Factor	F	p-value
FCR	Condition	F_{sqrt} (1,14) = 13.490	0.003
	Angle	$F_{GH,sqrt}$ (1.885,26.394) = 1.288	0.291
ECU	Condition	F_{sqrt} (1,14) = 14.753	0.002
	Angle	$F_{GH,sqrt}$ (1.666,23.329) = 2.553	0.107
FDS	Condition	F_{sqrt} (1,14) = 12.813	0.003
	Angle	$F_{GH,sqrt}$ (1.920,26.887) = 3.378	0.051
EDC	Condition	F_{sqrt} (1,14) = 8.235	0.012
	Angle	$F_{GH,sqrt}$ (4.157,58.192) = 0.824	0.519
TE	Condition	F_{sqrt} (1,14) = 1.446	0.249
	Angle	$F_{GH,sqrt}$ (2.708,37.911) = 0.736	0.524
FDI	Condition	F (1,14) = 3.875	0.069
	Angle	F_{GH} (4.515,63.203) = 1.615	0.175

3.4 Discussion

The aim of this study was to investigate how simultaneous control of wrist and fingers is affected by wrist posture as well as wrist stabilization in two conditions. Additionally, the influence of these variables on maximum precision grip strength was studied.

3.4.1 Maximal precision grip strength is achieved around 30 degrees of extension

The wrist flexion-extension angle had a significant influence on the maximum precision grip strength in both wrist stabilization conditions. Maximum grip strength was generated at 30° of extension in both conditions, but only the values obtained at extreme flexion (30° or more) were statistically significantly different from the maximum force at 30° of extension. These results are in line with other studies reporting a maximal power grip strength at 15° (Pryce, 1980), 20° (Li, 2002), and 35° (O'Driscoll et al., 1992) of wrist extension in self-stabilized conditions, and also with studies reporting a maximal power grip strength around 15°-30° of wrist extension when the wrist position was constrained with a splint (Lee and Sechachalam, 2016, Bhardwaj et al., 2011). Di Domizio and coworkers (Di Domizio et al., 2008) also showed a significant influence of wrist flexion-extension angle on grip strength. This group showed that maximum grip strength with and without splint was significantly reduced at 30° wrist flexion compared to the two other investigated positions (neutral and 30° extension).

When looking at the externally stabilized experimental condition, we found a very strong linear relationship between wrist flexion angle and the torque generated at the level of the wrist. In addition, a strong negative correlation was also found between the maximum pinch force and the absolute wrist torque. According to our linear fit (Figure 3-2), no torque is generated at the level of the wrist at around 22° of wrist extension. The larger the angular deviation (flexion-extension) from this optimal position, the more the wrist torque increases. This finding could be explained by the fact that the extrinsic finger muscles have a minimal moment arm relative to the wrist at this optimal position where the maximum pinch force is produced. Any deviation from this optimal position results in an increased moment arm. As a consequence, the maximum pinch strength is reduced.

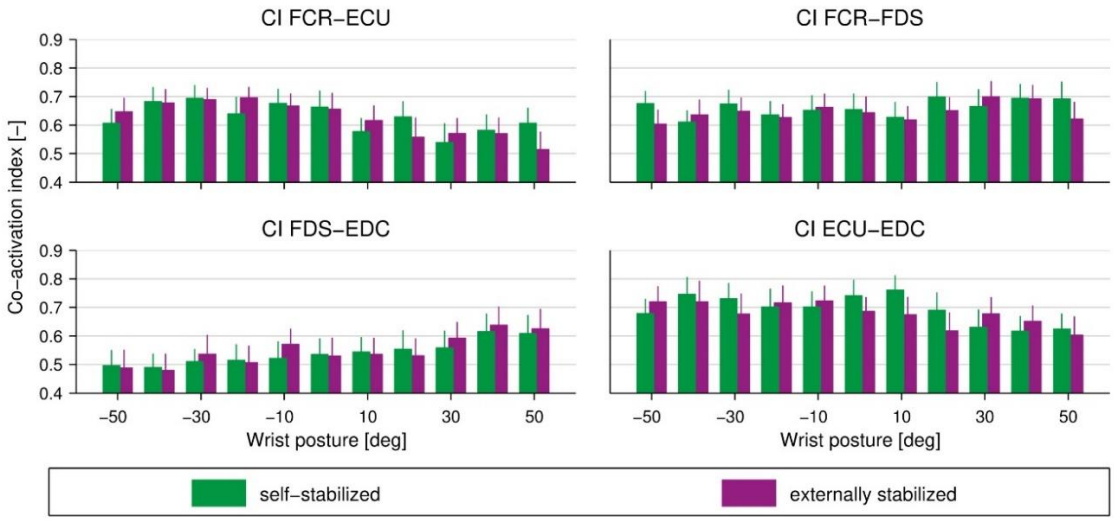

Figure 3-4: Mean ± SE co-activation index (CI) for the self-stabilized and the externally stabilized conditions for the muscles pairs FCR-ECU, FCR-FDS, FDS-EDC, ECU-EDC. Note that all investigated CI values showed no significant influence of wrist stabilization conditions and wrist postures, except for the CI value of the FCR-ECU muscle pair where a significant influence of the wrist posture was found.

3.4.2 Wrist stabilization leads to increased grip strength

Our results showed that subjects benefited from the wrist stabilization by the robot, producing higher precision grip forces than in the self-stabilized condition. The maximum grip strength decreased 14.5% on average from the externally stabilized to the self-stabilized condition. This is in contrast to what has been found in previous studies investigating the influence of wrist splints on force generation at the level of the finger (power grip). Although one study showed a tendency similar to ours, the increased power grip strength was not significant when using a splint (Di Domizio et al., 2008). However, an increase of 43% and 25% in power grip strength was found when the wrist was not restrained compared to splinted condition (Lee and Sechachalam, 2016, Bhardwaj et al., 2011). There are two main reasons why our study might have shown different results. First, in this study we investigated the influence of external wrist stabilization on precision grip while the other two studies investigated the influence on power grip. Long and coworkers (Long et al., 1970) have reported that precision grip requires different muscle activation patterns than the power grip. Therefore, contrasting results between power grip and precision grip can be expected, due to changes in tendon lever arms and muscle length. Second, in the previously mentioned studies the unconstrained maximum grip force (i.e., without splint) was measured in the preferred/optimal position, while the constrained maximum grip force was limited to five wrist flexion-

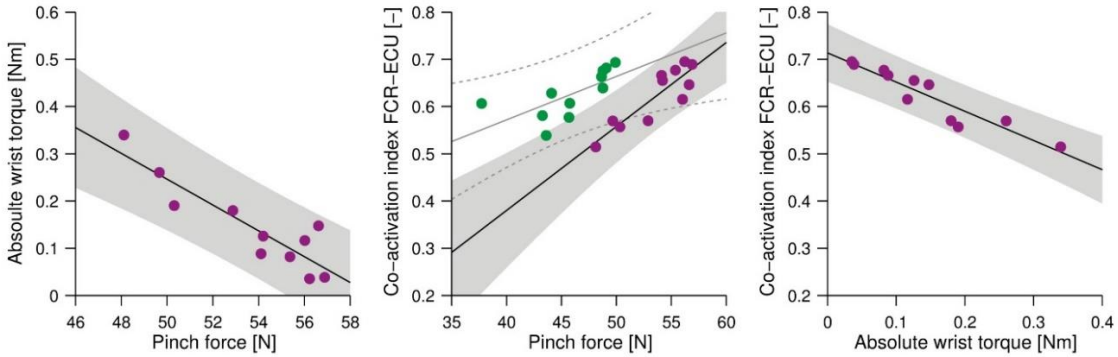

Figure 3-5: A strong correlation between pinch force and absolute wrist torque under external stabilization was found (left). In the middle, a strong correlation between pinch force and co-activation index of the FCR-ECU muscle pair under the externally stabilized condition is (purple) presented (moderate correlation under self-stabilized condition, green). On the right side, a strong correlation between absolute wrist torque and co-activation index for the FCR-ECU muscle pair is presented. The black lines represent the regression line for the externally stabilized condition (self-stabilized: grey line) and shaded region represents the corresponding 95% confidence interval (self-stabilized: grey dotted line).

extension angles that did not include the optimal position. Furthermore, in our study the wrist was mechanically grounded by the robotic manipulandum imposing a specific posture to the wrist, elbow, and shoulder, allowing only wrist flexion-extension. Additionally, the ulnar deviation of the wrist was maintained for both stabilization conditions at 10°. This allowed for a high reliability in the experiment, thereby enabling the comparison of the two different stabilization conditions. This might not have been the case in previous experiments, because subjects could have accessed all degrees of freedom in the unrestrained condition and the constraints of the splint could have been limited only to the flexion-extension and ulnar-radial deviation of the wrist. Even though ulnar deviation has a significant influence on grip strength, previous studies did not control this DOF throughout assessment conditions.

3.4.3 Maximum pinch strength is slightly lower than literature

The average maximum precision grip strength was 57.1N for the externally stabilized condition, and 48.8N for the self-stabilized condition. These values are slightly lower than in other studies. For the age range of our subjects, we should have seen a maximum precision pinch force (optimal wrist posture and self-stabilized) between 59.3N and 68.9N (Mathiowetz et al., 1985b, Nilsen et al., 2012). The discrepancy between our values and the values reported in the other studies can be due to the restraint at 10° of ulnar deviation, which might not be optimal for maximal precision pinch strength (similar to

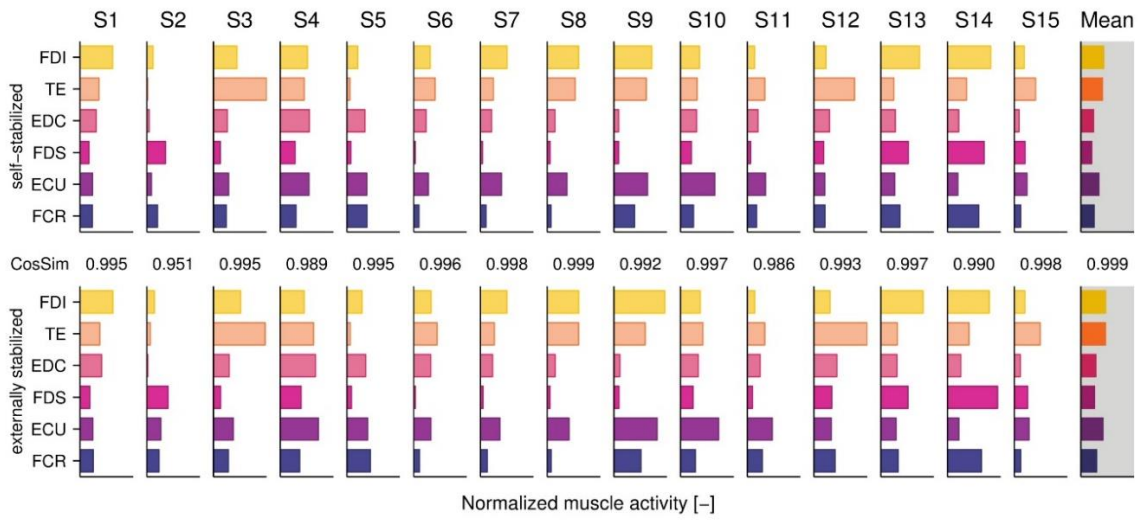

Figure 3-6: Muscle activation patterns (MAPs) for each subject in the self-stabilized (top) and the externally stabilized (bottom) conditions. The cosine similarity (CosSim) is presented between the plots; a value of 0 represents no similarity and a value 1 prefect agreement. Note that in general all muscle activation patterns are highly consistent within subjects.

what has been found for power grip (O'Driscoll et al., 1992)). Further, in our study wrist flexion-extension was limited to postures in 10° intervals and the optimal wrist flexion-extension angle might have been between postures. Finally, pinch width was not identical in the three studies using a 2-finger pinch grip, which can strongly influence the force production at the level of the fingers (Dempsey and Ayoub, 1996, Imrhan and Rahman, 1995, Shivers et al., 2002).

3.4.4 Level of muscle activation only depends on the wrist stabilization condition

The levels of muscle activity of the extrinsic muscles (FCR, ECU, FDS, and EDC) were significantly influenced by the wrist stabilization conditions, whereas the intrinsic muscles were not. Muscle activation was significantly higher for all four extrinsic muscles in the externally stabilized position. These findings are in line with increased muscle activity in FCR and FDS when a wrist splint was used during maximal power grip (Di Domizio et al., 2008); ECU and EDC showed a similar tendency although the effect was not significant. Other studies investigating the influence of a wrist splint on muscle activation patterns showed varying results. Some studies showed a significant increase in muscle activity of the flexors but not of the extensors (Johansson et al., 2004) while other studies only found increased extensor activity (Bulthaup et al., 1999). The different results can be xplained by the fact that

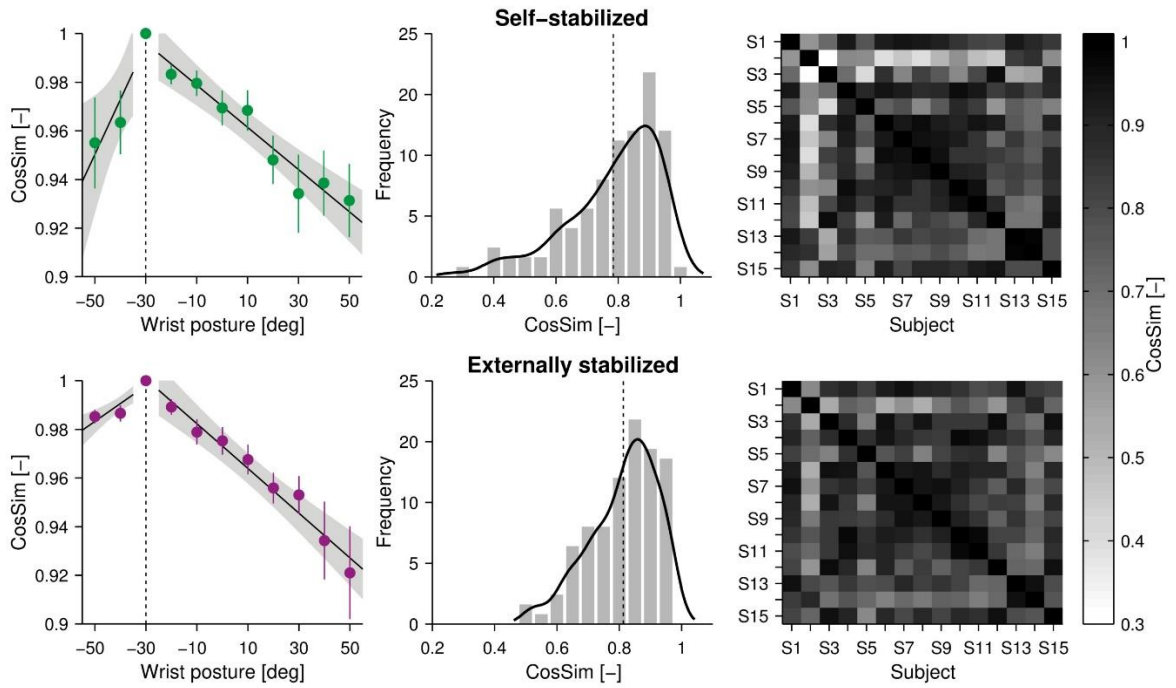

Figure 3-7: Left: cosine similarity (CosSim) of the muscle activation pattern for each wrist flexion angle normalized against the 30° extension position is presented. Right: CosSim values between subjects are presented and the overall distribution plot across subjects is presented in the middle. The dashed line represents the mean CosSim value across subjects. The muscle activation patterns are very inhomogeneous across subjects, with CosSim values ranging from almost 1 down to around 0.3.

different grip types (both cylinder grip with different diameters) were investigated and that the required force at the level of the fingers was not consistent. Within each wrist stabilization condition, we found that wrist angle had no statistical influence on the level of muscle activation of the six recorded muscles.

3.4.5 Only FCR-ECU co-activation is influenced by wrist flexion-extension angle

The analysis of muscular co-activation revealed that the only one muscle pair, namely FCR-ECU, was influenced by the wrist posture, and that the co-activation of the muscle pairs was not influenced by the wrist stabilization conditions. The maximal CI value for the FCR-ECU muscle pair was at 30° of extension in the self-stabilized condition and at 20° of extension in the externally stabilized condition. It should be noted that higher CI values can result from a higher activation of the antagonistic muscles or from a decreased activation of the most active muscle. In our case, the high CI value results from a decrease in ECU activity. FCR activity is quite stable over the whole range of investigated wrist angles, except for a slight (non-significant) increase in extreme wrist flexion in the self-stabilized condition.

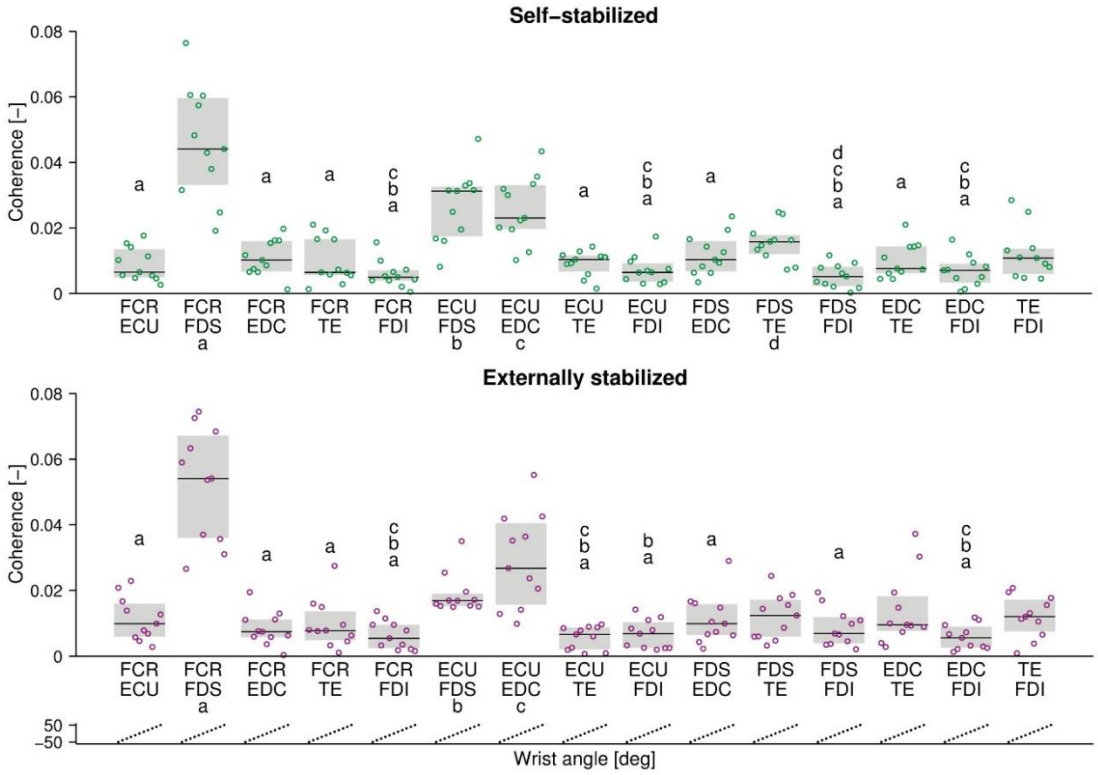

Figure 3-8: Coherence between all muscle pair combinations and wrist flexion angles are presented for the self-stabilized condition (top) and the externally stabilized condition (bottom). The black line represents the median, the shaded region represents the interquartile range, and the circles represent the single values per wrist posture averaged over all subjects. Note the "a" represents a significantly lower coherence value compared to the FCR-FDS muscle pair, "b" represents a significantly lower coherence value compared to the ECU-FDS muscle pair, "c" represents a significantly lower value compared to the ECU-EDC pair, and "d" represents a significantly lower coherence value compared to the FDS-TE pair. Note that there are no significant differences between wrist stabilization conditions, except for the muscle pair ECU-TE.

The higher ECU activity in flexion can be due to the increased activity required to stabilize the wrist in a fixed position, while increased ECU activity in extreme extension is required to maintain the wrist extended. Interestingly, a strong positive correlation was found between co-activation of the antagonistic muscle pair FCR-ECU and the maximum pinch force. We hypnotize that finger muscles minimally contribute to wrist stabilization at the optimal wrist position, where maximum pinch force can be produced. At the same time, the finger muscles might be at an optimal length for producing a maximum precision pinch and the tendon moment arm might also be favorable. The combination of these two factors probably causes our results of co-occurring maximum FCR-ECU co-activation and maximum pinch force.

3.4.6 Muscle activation patterns varied across subjects but not between conditions

The MAPs did not change as a function of the wrist stabilization condition. This was the case despite higher muscle activation of FCR, ECU, FDS, and EDC in the externally stabilized condition. This implies that the involved muscles change their activity in a similar way in dependence of the wrist stabilization condition, probably due to muscle synergies. Thus, the angles between MAP vectors remain constant. In contrast, an intra-individual change in MAPs was found as a function of wrist angle for both stabilization conditions. The farther the wrist angle is away from the optimal position (30° extension), the bigger the change in MAP. This can be explained by the change in the level of FCR, FDS, and ECU activation in extreme wrist flexion and extension positions as a result of changes in muscle fiber lengths.

Interestingly, the MAPs varied across subjects, revealed by an average cosine similarity value ranging between 0.3 and almost 1. The varying MAPs could be due to differences in the type of two-finger pinch grip employed (Ng et al., 2014); although lateral pinch was not allowed, pulp pinch or tip pinch were both used by participants in this study. The angles of the different index finger joints can vary up to 50° when comparing tip pinch to pulp pinch (Chao, 1989). Therefore, the contribution to force production of the involved index finger muscles can also change. For example in tip grip, force production at the index finger arises from the flexor digitorum profundus (FDP, not recorded in this study) as well as from the FDS (Maier and Hepp-Reymond, 1995, Chao, 1989). In contrast, the main force of the index finger in the pulp grip arises from the FDP and the FDS contributes less to the index finger force (Chao, 1989). This is reflected in FDS activity across subjects but is not sufficient to explain the observed variability in MAPs. One source of variability might be the existence of sub-types of pulp and tip grip, resulting in multiple potential solutions to produce a two-finger pinch grip.

3.4.7 Neurological correlates

In addition to the muscle activity analysis based on EMG data, which was explained in the previous paragraph, we further analyzed the EMG data in terms of neurological correlates by computing the EMG-EMG coherence. Thereby, an increased EMG-EMG coherence describes an increased common

corticospinal drive to the investigated muscle pairs (Norton and Gorassini, 2006). In our study we found increased common drive for the muscle pairs FCR-FDS, ECU-EDC, and FDS-ECU in both wrist stabilization conditions. FCR-FDS coherence might be explained by the synergistic contribution of both muscles to wrist flexion, and therefore an increased common corticospinal drive would be plausible. Similarly, ECU as well as EDC both contribute to extension at the level of the wrist, which might be a possible explanation for an increased common corticospinal drive. However, the existence of such common corticospinal drive has only been shown for other extrinsic muscles of the hand in a three-digit grasp (Poston et al., 2010), and not directly for FCR-FDS and ECU-EDC. Therefore, this interpretation remains speculative. The increased coherence of the FDS-ECU muscle pair might reflect a deeply-ingrained synergy which has the origin at a higher level of the central nervous system, as has been reported in monkeys (Holdefer and Miller, 2002). Interestingly, the increased coherence was also present in the externally stabilized condition although an activation of the wrist muscles was not required, which in turn might also support the existence of a potential FDS-ECU synergy.

3.4.8 Limitations

The results of this study are limited by the relatively low number of subjects, which might have had an influence on the statistical analysis. Additionally, fatigue might have affected MAPs, given the large number of maximum force trials (66), although we verified that the maximal pinch strength was not affected by the experimental duration. Variability might also have been introduced by the different two-finger pinch types (i.e. pulp grip and tip grip), which were not controlled but should be in future experiments. Lastly, the study was conducted with an imposed ulnar deviation of 10° and pinch width of 14.5mm and results might vary when ulnar deviation or pinch width are changed.

3.5 Conclusion

The optimal wrist posture for generating maximum pinch strength was around 20°-30° of wrist extension for a 10° ulnar deviation, independent of the wrist stabilization condition. Maximum precision pinch strength was consistently higher in the externally stabilized condition compared to the self-stabilized condition. This can be explained by the fact that in the externally stabilized condition the full muscle potential is available, while in the self-stabilized conditions muscles contributing to pinch force are also involved in maintaining the wrist at a specific position. Indeed, the activity level increased consistently and uniformly across all extrinsic muscles from the self-stabilized to the externally stabilized condition. This means that subjects used the same activation pattern in both conditions rather than generating new patterns. In the optimal position for generating maximum pinch strength, the level of co-contraction of the antagonistic muscle pair FCR-ECU was maximal due to low ECU activity. Additionally, net torque at the level of the wrist was minimal in this optimal position. The obtained MAPs and precision grip strength values may result from the interaction between biomechanical constraints and muscle synergies, which should be further investigated. Overall, the results of this experiment provide novel insights on wrist and finger interdependence during precision grip control in static conditions, furthering our understanding of the neural control of intrinsic and extrinsic hand muscles, which is critical for the design of targeted neurorehabilitation therapies and the development of wrist and hand rehabilitative or assistive devices.

4 The effect of wrist posture and wrist stabilization on precision grip strength and muscle activation patterns in stroke survivors[3]

[3] This chapter is a manuscript in preparation. Authors will be Werner L. Popp, Lea Richner, Olivier Lambercy, Mike D. Rinderknecht, Camila Shirota, Roger Gassert and Derek Kamper.

4.1 Introduction

Around 80% of stroke survivors suffer from persistent motor deficits (Cirstea and Levin, 2000) and around 50% have somatosensory deficits (Carey, 1995). These deficits affect an individual's ability to grasp and manipulate objects with the impaired hand, a common problem in approximately 40% of stroke survivors (Duncan et al., 2003). At the level of the fingers, it has been reported that grip strength is typically reduced after stroke (Sunderland et al., 1989, Boissy et al., 1999) and that the force production at the level of the finger tip of individual fingers (e.g., index finger) is also significantly reduced (Cruz et al., 2005). This weakness can, to a small part, be attributed to muscle atrophy after stroke (Kamper et al., 2006), as significantly lower muscle volumes have been found on the affected side of stroke survivors compared to the non-affected side (Metoki et al., 2003). The more important factor affecting finger weakness is of neurological origin. According to Kamper and coworkers (Kamper et al., 2006), excessive co-activation between finger flexors and extensors is one reason for the reduction in finger strength, while another might be a reduction in corticospinal activation of spinal segmental neurons. An additional factor affecting motor execution and therefore force production at the level of the fingers is spasticity (Raghavan, 2007), which includes exaggerated tendon reflexes and muscle hypertonia (Dietz and Sinkjaer, 2007). Whilst all these factors lead to impairment in hand and finger function, problems affecting higher-order processes, such as motor planning and learning (Raghavan, 2007), can also lead to impairment in hand and finger motor control. This is especially important for fine-motor skills, as for example for precision grip, which is used in many different activities of daily living like writing or manipulating small objects.

A study investigating grip force production and control in stroke survivors found altered grip force direction (Seo et al., 2010) resulting from altered muscle activation patterns in stroke. Furthermore, it is known that during grip tasks, force scaling can be impaired (McDonnell et al., 2006, Blennerhassett et al., 2008) and that force fluctuation during gripping tasks can occur (Blennerhassett et al., 2006). These findings have also been associated with altered muscle activation patterns, altered muscle synergies as well as with impaired grip control due to deficits in somatosensory function (Hermsdörfer et al., 2003, Blennerhassett et al., 2007).

While difficulty in producing an accurate precision grip or high force at the level of the fingers has been reported in stroke patients, it remains unclear how, for example, wrist posture, or the use of a wrist splint (typically used in stroke rehabilitation), affect the force production and the control of the fingers. In Chapter 3 we investigated how maximal precision pinch strength in neurologically intact subjects is influenced by wrist posture and wrist stabilization with the goal of furthering the understanding of multiarticular muscle control. We found that maximum precision grip strength is influenced by wrist posture as well as by external stabilization of the wrist. Furthermore, we saw an increased level of FCR-ECU co-activation at the wrist position where maximal pinch grip was produced (30° extension). Muscle activation patterns varied across subjects due to different precision pinch grips used. Finally, we found muscle synergies for the flexor muscles FCR-FDS as well as for the extensor muscles ECU-EDC, and for the muscle pair FDS-ECU.

These findings could have implications for the design of rehabilitative and assistive hand and wrist devices and therapy approaches for stroke patients. For example, based on these results, a wrist splint might be beneficial for the production of precision grip force. However, it first has to be shown that stroke survivors can increase finger strength or muscle coordination with a wrist splint. Furthermore, it is important to know how muscle activation patterns as well as muscle synergies change in precision grip following stroke. Therefore, we repeated the experiment presented in Chapter 3 with chronic stroke subjects having moderate hand impairment.

The study aimed at investigating maximum pinch grip force in function of the wrist flexion-extension angle and wrist stabilization (the wrist is either self-stabilized or stabilized externally, similar to a splint, by a robotic manipulandum). In addition to the kinematic and kinetic measurements with the robot, muscle activation patterns as well as the cortical drive to different muscle groups were assessed with EMG recordings from intrinsic and extrinsic hand muscles. We hypothesized that maximum pinch grip strength would be reduced in the stroke group compared to the neurologically intact group. Furthermore, we hypothesized that, similar to the neurologically intact group, the stroke group would be able to increase grip strength when the wrist was stabilized by the robot. Lastly, we expected that muscle activity patterns (MAPs) within and across subjects would be highly heterogeneous.

4.2 Methods

4.2.1 Subjects

Ten chronic stroke subjects were recruited for this study, of which seven were able to perform all tasks required in this study and thus included in the data analysis (age 59.0 ± 7.0 years, 3 males). Inclusion criteria required that subjects were between 21-80 years old, that they had a unilateral ischemic or hemorrhagic stroke at the chronic stage (mean time post stroke: 8.6 ± 2.2 years), and with moderate hand impairment. The Chedoke-McMaster Stroke Assessment Scale was used to evaluate the level of hand impairment (Gowland et al., 1993); a rating of 4 or 5 out of 7 was considered as moderate. Exclusion criteria were severe cardiovascular conditions that contraindicate strenuous exertion, apraxia, communication deficits impairing the ability to follow simple instructions, severe pain in the shoulder, severe contracture in the upper extremity as evidenced by bony changes or fixed deformity, and other musculoskeletal injuries and diseases not related to stroke. The experiment took place at the Rehabilitation Institute of Chicago (RIC) and was approved by the Institutional Review Board of Northwestern University (STU00200301). Each participant was informed about the experimental protocol and gave written consent prior to the experiment.

4.2.2 Apparatus

Similar to the study presented in chapter 3, a 1 DOF robotic wrist manipulandum (Kamper et al., 2003) was used for this study. The robotic manipulandum (referred to as RIC manipulandum) had a similar architecture to the ReFlex robot (Chapuis et al., 2010) used in the previous experiment with neurologically intact subjects. It consists of a servomotor (1.4HP, PMI Motion Technologies, Kollmorgen Corporation, Radford, VA, U.S.A), an incremental encoder (HA625-2500, DynaTECH, Elm Grove Village, IL, U.S.A.), and a torque transducer (TRT-200, Transducer Techniques, Temecula, CA, U.S.A.) mounted between the motor shaft and the handle support. Similar to the ReFlex, the RIC manipulandum can render a transparent training environment, and completely lock the handle at specified wrist flexion angles. The robot is controlled through a real-time operating system running at a sampling frequency of 1kHz (LabVIEW Real Time 2011, National Instruments, Austin, TX, U.S.A.)

and a host PC running LabVIEW 2011 (National Instruments, Austin, TX, U.S.A.) for the user interface and visual feedback. Note that the robot ran the same LabVIEW code as the ReFlex robot used in the study in Chapter 3.

A miniature load button (LLB210, Futek, Irvine, CA, USA) with a measurement range of 0-111N, the same as used in the study with neurologically intact subjects (Chapter 3), was used to record pinch grip force. The same plastic finger pads with a diameter of 14 mm were mounted on each side of the load cell in order to have the same pinch width of 14.5 mm. Data acquisition of the miniature load cell data was achieved with the real-time operating system of the robotic manipulandum, at a sampling rate of 1kHz.

Muscle activity was recorded from muscles flexor carpi radialis (FCR), extensor carpi ulnaris (ECU), flexor digitorum superficialis (FDS), extensor digitorum communis (EDC), thenar eminence (TE), first dorsal interosseous (FDI) using active surface EMG electrodes (Delsys Inc., Boston, MA, U.S.A.). Data acquisition was achieved through the real-time operating system of the robotic manipulandum at 1kHz.

4.2.3 Experimental protocol

In order to compare the data from the stroke subjects collected in this study to the data from the neurologically intact subjects (Chapter 3), the same protocol was followed. Only a brief summary of the protocol will be presented here. More information can be found in Chapter 3.

Participants came to the RIC for a single session lasting around 1.5 hours. First, EMG electrodes were placed on the participant's arm and then maximal voluntary contractions (MVCs) were measured. Participants were then asked to generate maximum pinch grip force at eleven different wrist angles, ranging from 50 degrees of extension to 50 degrees of flexion in steps of 10 degrees, and under two different stabilization conditions, namely self-stabilized (free wrist flexion-extension movement; other DOF locked) and externally stabilized (flexion/extension also stabilized by the robot). Each combination of wrist posture and wrist stabilization condition was repeated three times, resulting in a total of 66 trials. Trials were presented in pseudo-random order.

4.2.4 Outcome measures

Outcome measures were identical to the ones used in the study with the neurologically intact subjects (Chapter 3.2.4), in order to allow for comparison between the two data sets. In summary, the outcome measures were the maximum grip strength, the torque produced at the level of the wrist, the average and maximal normalized muscle activation for all six investigated muscles, the co-activation index (CI (Popp et al., 2016b)) values for the muscle pairs FCR-FDS, ECU-EDC, FCR-ECU, and FDS-EDC, the similarity between MAPs (cosine similarity (Poston et al., 2010, Danna-Dos Santos et al., 2010)), and the common corticospinal drive to all muscle pair combinations evaluated with the EMG-EMG coherence (from Kamper et al. (2014), based on Halliday et al. (1995)).

4.2.5 Statistical analysis

The same methodologies as described in Chapter 3.2.5 were used to analyze data of the stroke subjects. For the comparison between the neurologically intact and stroke subject data, the following statistical tests were applied: the Shapiro-Wilk test was used to test for normality, and t-tests or Manny-Whitney-U-tests were used to compare between the neurologically intact and stroke groups in the case of normal or non-normal data, respectively. The statistical analyses were conducted using MATLAB 2014a (MathWorks, Natick, MA, USA) with a significance level of $p=0.05$ for all tests.

4.3 Results

The maximal pinch grip force was significantly higher for the externally stabilized condition compared to the self-stabilized condition ($F(1,6)=7.065$, $p=0.038$). The wrist flexion-extension angle, however, had no statistical influence on the maximum pinch force (Figure 4-1; $F_{GH}(1.903,11.416)=0.812$, $p=0.462$). In the externally stabilized condition, a strong negative correlation was found between wrist posture and total wrist torque (Figure 4-1, right; $R = -0.9837$, $p<0.001$), with increasing wrist flexion torque with increasing extension angle and vice-versa. According to the linear regression, a wrist torque of 0Nm can be predicted at -3.10° (wrist extension).

The average normalized muscle activity across subjects for the different investigated muscles can be found in Figure 4-2 and the corresponding statistical values are summarized in Table 4-1. Note that only the muscles ECU and TE showed a significantly different activity level depending on the wrist stabilization conditions, and none of the muscles were statistically influenced by the wrist posture.

The CI values for the muscle pairs FCR-ECU, FCR-FDS, FDS-EDC, and ECU-EDC are presented in Figure 4-3. Neither the wrist posture (FCR-ECU: $F(1.887,11.324)=0.471$, $p = 0.625$; FCR-FDS: $F(1.638,9.825)=0.099$, $p = 0.871$; FDS-EDC: $F(1.580,9.478)=1.119$, $p = 0.351$; ECU-EDC: $F(2.134,12.801)=0.468$, $p = 0.648$) nor the stabilization condition (FCR-ECU: $F(1,6)=0.252$, $p = 0.634$; FCR-FDS: $F(1,6)=4.546$, $p = 0.077$; FDS-EDC: $F(1,6)=0.927$, $p = 0.373$; ECU-EDC: $F(1,6)=1.505$, $p = 0.266$) had a significant influence on any of the calculated CI values.

Average MAPs for the self-stabilized and the externally stabilized conditions are presented for all subjects individually (Figure 4-4). The differences in MAPs between the wrist stabilization conditions were negligible. This result is represented in a minimum cosine similarity value of 0.982 within subject. In order to show how the MAPs vary with wrist posture, the cosine similarity was computed for each wrist posture MAP against the 0° flexion-extension MAP, which is represented on the left side of Figure 4-5. An increasing deviation from the neutral position into flexion or extension resulted in decreased similarity of the MAPs.

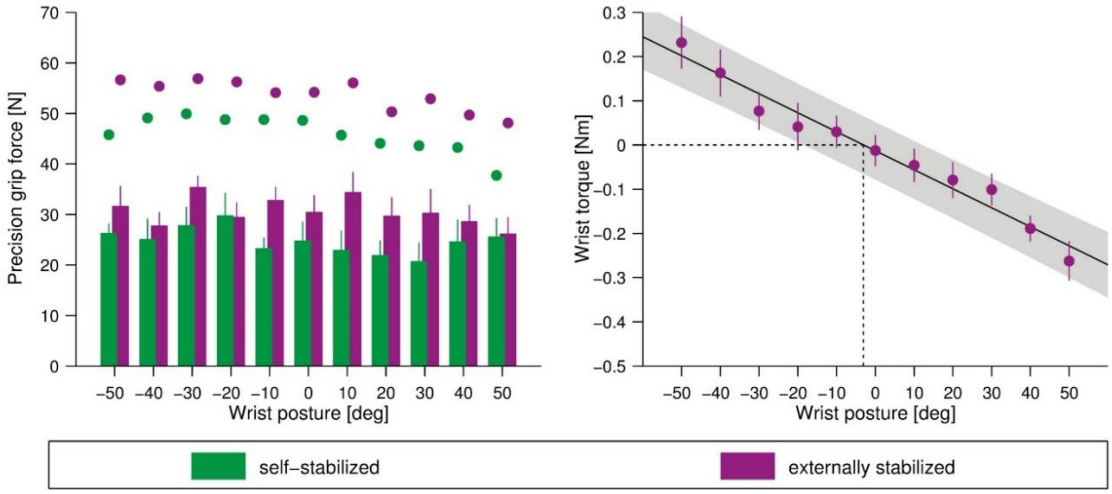

Figure 4-1: Left: Average maximal pinch force across subjects for the self-stabilized and the externally stabilized conditions. The dots represent the values obtained from the neurologically intact group (Chapter 3). Right: relationship between wrist posture (positive value: flexion, negative value: extension) and active wrist flexion torque in the externally stabilized condition. The dashed line indicates the estimated flexion angle where no wrist torque would be produced (-3.10°). The black line represents the regression line and the shaded region represents the 95% confidence interval.

Between subjects, the cosine similarity of the MAPs varied from 0.549 to 0.968 in the self-stabilized condition, and from 0.567 to 0.949 in the externally stabilized condition (Figure 4-5, right).

Significant differences in coherence values between different muscle pairs were found for both stabilization conditions (Figure 4-6; self-stabilized: $\chi^2(14)=26.200$, $p = 0.024$; externally stabilized: $\chi^2(14)=51.836$, $p < 0.001$). A statistically significant difference in coherence between the two stabilization conditions was only found for the muscle pair ECU-FDI ($p = 0.024$).

The correlation analysis revealed a moderate negative correlation between maximal pinch force and absolute wrist torque ($R = -0.548$, $p = 0.081$), and no correlation between the CI values of the FCR-ECU muscle pair and the absolute wrist torque ($R = 0.181$, $p = 0.593$). In addition, no correlation was found between CI values of the FCR-ECU muscle pair and maximum pinch force for the externally stabilized condition ($R = 0.124$, $p = 0.717$) nor for the self-stabilized condition ($R = 0.087$, $p = 0.800$).

The comparison between the neurologically intact and the stroke subjects (Figure 4-7) revealed a significant difference in maximum pinch grip force for both wrist stabilization conditions (both $p<0.001$). Apart from that, there were statistically significant differences in coherence values: FCR-FDS

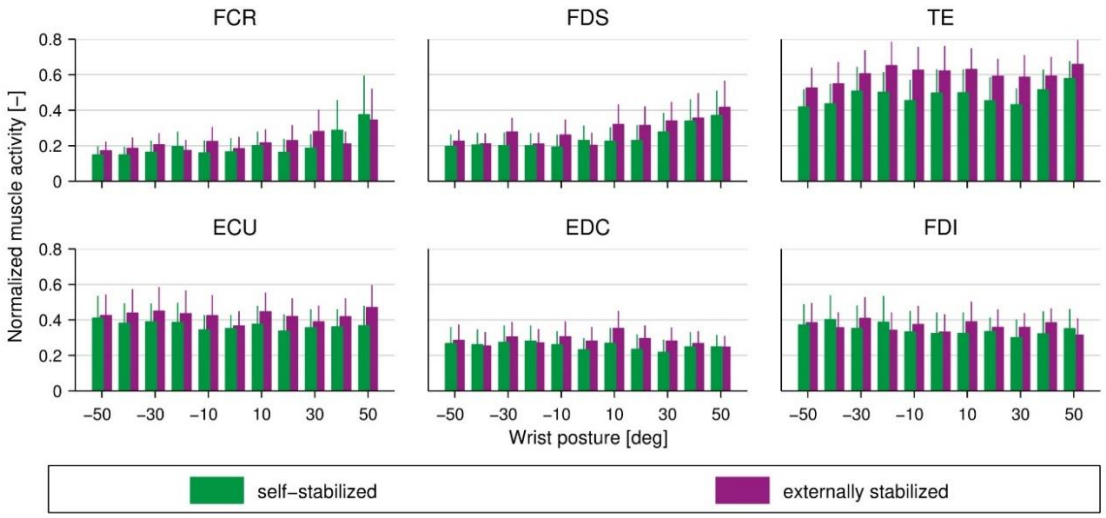

Figure 4-2: Mean ± SE normalized muscle activity across subjects for the self-stabilized and the externally stabilized condition for the muscles flexor carpi radialis (FCR), extensor carpi ulnaris (ECU), flexor digitorum superficialis (FDS), extensor digitorum communis (EDC), thenar eminence (TE), first dorsal interosseous (FDI). The corresponding statistics can be found in Table 4-1. Note that the muscles TE and ECU were influenced by the wrist stabilization condition but not by the wrist posture (Table 4-1).

(both conditions: $p<0.001$) as well as ECU-FDS (both conditions $p<0.001$) coherence were significantly higher in the neurologically intact group for both stabilization conditions. The FDS-EDC muscle pair showed a significantly higher coherence for the neurologically intact group only during the externally stabilized condition ($p=0.011$, self-stabilized: $p=0.114$). The coherence for the intrinsic muscle pair TE-FDI was significantly higher in the stroke group during both stabilization conditions (self-stabilized: $p=0.036$, externally stabilized: $p= 0.008$). All other muscle pairs were not significantly different between neurologically intact and stroke group in terms of coherence.

Table 4-1: Statistics for the muscle activation presented in Figure 4-2.

Muscle	Factor	F	p-value
FCR	Condition	F_{sqrt} (1,6) = 1.075	0.340
	Angle	$F_{GH,sqrt}$ (1.128,6.766) = 2.012	0.203
ECU	Condition	F_{sqrt} (1,6) = 15.733	0.007
	Angle	$F_{GH,sqrt}$ (2.392) = 0.397	0.714
FDS	Condition	F_{sqrt} (1,6) = 2.347	0.176
	Angle	$F_{GH,sqrt}$ (1.316,7.896) = 4.497	0.060
EDC	Condition	F_{sqrt} (1,6) = 2.315	0.179
	Angle	$F_{GH,sqrt}$ (3.016,18.099) = 0.895	0.463
TE	Condition	F (1,16) = 8.256	0.028
	Angle	F_{GH} (2.480,14.881) = 1.824	0.191
FDI	Condition	F_{sqrt} (1,6) = 2.032	0.204
	Angle	$F_{GH,sqrt}$ (2.501,15.006) = 0.683	0.683

4.4 Discussion

The aim of this study was to investigate how maximum precision grip strength is influenced by wrist posture and wrist stabilization in chronic stroke survivors. Furthermore, muscle activation patterns as well as muscle synergies during precision grip were compared between stroke survivors and neurologically intact controls.

4.4.1 Maximum grip force in general

The average maximum precision grip strength at the optimal wrist position for force production was 35.3N for the externally stabilized condition (at 30° of extension) and 29.7N for the self-stabilized condition (at 20° of extension). These values are in average 38.7% lower than what was observed for the neurologically intact group. One hypothesis for the reduction in maximum grip force might be the age difference between the two groups (neurologically intact: 26.9 ± 3.1 years, stroke: 59.0 ± 7.0 years). However, based on normative data (Mathiowetz et al., 1985b, Nilsen et al., 2012) we would expect a decrease in grip strength by around 15%, due to the age and gender difference in the two groups. Therefore, the difference in grip strength cannot be explained solely by the different demographics of the groups. That implies that stroke leads to a decrease in precision grip strength. This is in line with other studies reporting a general decrease in grip strength following stroke (Boissy et al., 1999, Sunderland et al., 1989). This finger weakness in stroke has been specifically associated with altered co-activation of finger muscles (Kamper et al., 2003) and in general with altered patterns of muscle activation (Cruz et al., 2005).

4.4.2 Wrist stabilization leads to increased grip strength

Similar to what was observed in the neurologically intact subjects, the stroke subjects were able to produce higher precision grip forces when the robot stabilized the wrist. The maximum grip strength decreased 19.6% on average from the externally stabilized to self-stabilized condition. This is in a similar range (14.5%) to what was found for the neurologically intact group. As a consequence, stroke survivors with moderate hand impairment and insufficient finger force to manipulate objects may benefit

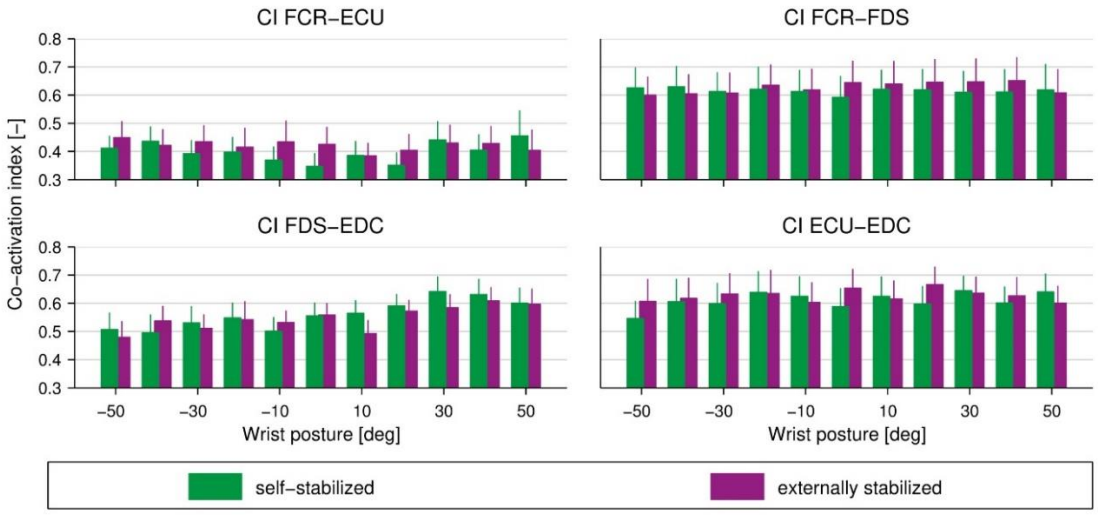

Figure 4-3: Mean ± SE co-activation index (CI) for the self-stabilized and the externally stabilized conditions for the muscles pairs FCR-ECU, FCR-FDS, FDS-EDC, ECU-EDC. Note that all investigated CI values showed no significant influence of wrist stabilization conditions and wrist postures.

from using a wrist splint. Nevertheless, for the design of a wrist splint or an assistive device, further investigation is needed in order to see if the findings on precision grip transfer to other grip types (e.g. power grip).

4.4.3 Wrist posture had no influence on grip strength

Our data showed that the wrist-flexion extension angle had no significant influence on the maximum grip strength. This stands in contrast to what we have reported for the neurologically intact group and also to what other research groups have reported for the health population (Pryce, 1980, Li, 2002, O'Driscoll et al., 1992, Bhardwaj et al., 2011, Lee and Sechachalam, 2016, Di Domizio et al., 2008). The fact that no influence of wrist posture on grip strength was found might be explained by the relatively low number of subjects included in the analysis. Typically, low-powered studies are susceptible for false negative results (Button et al., 2013). An indication that there could be an existence of an optimal wrist posture for generating maximum precision grip force can be found in the strong linear relationship between wrist angle and torque produced at the level of the wrist during the externally stabilized condition. According to the linear model, no torque is generated at around 3° of extension. This means that the location of minimal wrist torque shifted toward wrist flexion in comparison to what has been measured in the neurologically intact group (22° extension). There are different possible

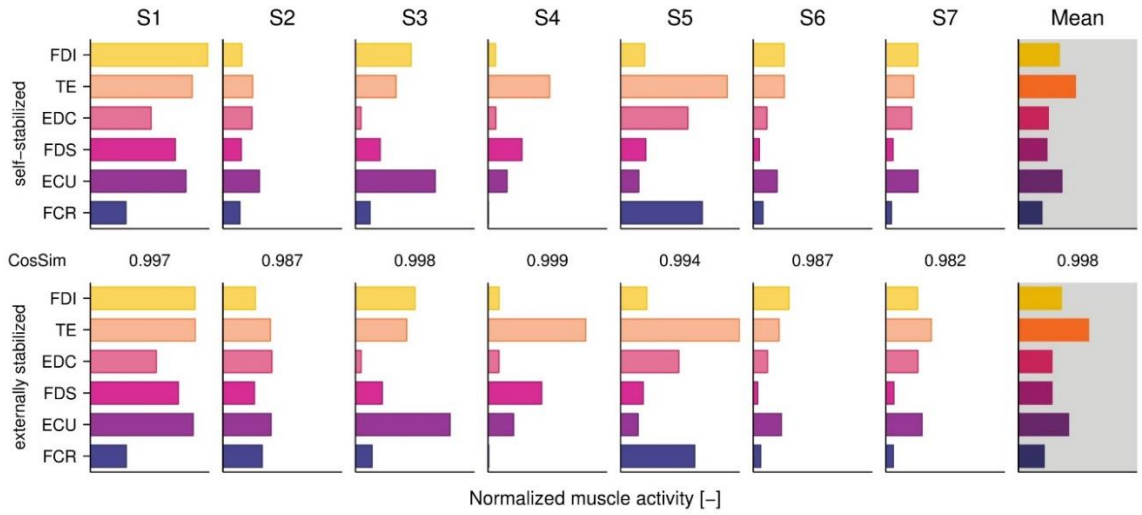

Figure 4-4: Muscle activation patterns for each subject in the self-stabilized (top) and the externally stabilized (bottom) conditions. The cosine similarity (CosSim) is presented between the plots; a value of 0 represents no similarity and a value of 1 perfect agreement. Note that, in general, all muscle activation patterns are very consistent within subjects, as shown by CosSim values of 0.982 and higher.

explanations for this. Besides the altered muscle activation patterns, a change in the mechanical properties of the muscle tissue (O'dwyer et al., 1996, Dietz et al., 1991) may also be a possible explanation for this shift towards wrist flexion.

4.4.4 Level of muscle activity of TE end ECU changed depending on the stabilization condition

In general, muscle activation levels were not significantly influenced by wrist posture or wrist stabilization condition, except for the TE and ECU muscles, which showed a significantly higher activation level in the externally stabilized condition compared to the self-stabilized condition. The increased ECU activity in the externally stabilized condition was also found in the neurologically intact subjects. In addition to the increased ECU activity, the neurologically intact subjects showed also an increased muscle activity level in all the other extrinsic muscles (FCR, FDS, and EDC). By tendency, a slight increase in extrinsic muscle activity can also be seen in the stroke subjects, although not significant. Surprisingly, the intrinsic muscle TE showed a significantly increased activation level in the externally stabilized condition. A possible explanation for this finding is that the stroke subjects relied more on intrinsic hand muscles for generating maximal pinch force, by slightly changing the posture.

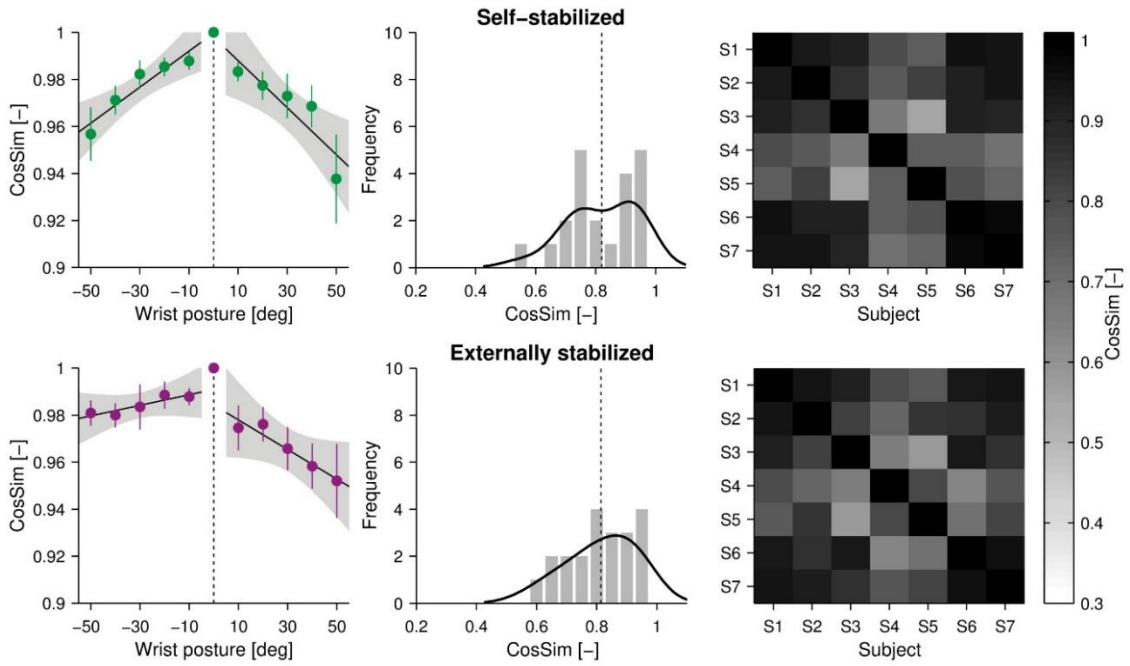

Figure 4-5: On the left side, the cosine similarity (CosSim) of the muscle activation pattern for each angle against the 0° flexion-extension position. On the right side, the CosSim values between subjects and the overall distribution plot across subjects is presented in the middle. The dashed line represents the mean CosSim value across subjects. The muscle activation patterns are very inhomogeneous across subjects, with CosSim values ranging from almost 1 down to around 0.55.

The increased activity in the externally stabilized condition might be directly related to increased force production at the thumb due to the increased counter force produced by the index finger, as FDS does not contribute to wrist stabilization.

4.4.5 Co-activation not influenced by wrist posture or stabilization condition

None of the investigated muscle pairs showed an altered co-activation level due to wrist posture or wrist stabilization condition. This is similar to the findings of the neurologically intact group with one exception: In the neurologically intact group, the co-activation of FCR-ECU was significantly influenced by the wrist posture with a peak at 30° of extension where also maximum grip strength was measured. In this group, a strong negative correlation between absolute wrist torque and level of co-activation between FCR and ECU was also found. This strong negative correlation was completely absent in the stroke group. An obvious interpretation of this finding is that in stroke other muscles groups have substantial impact on wrist stabilization and torque production at the level of the wrist.

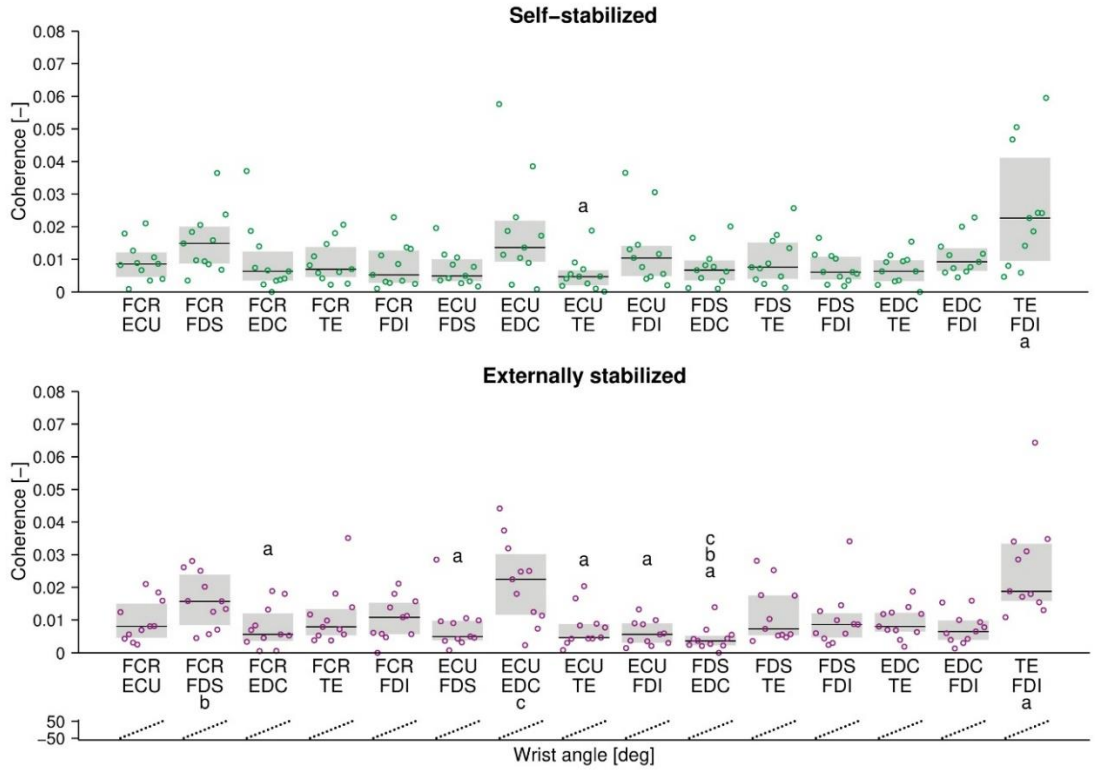

Figure 4-6: Coherence between all muscle pair combinations are presented for the self-stabilized condition (top) and the externally stabilized condition (bottom). The black line represents the median, the shaded region represents the interquartile range, and the circles represent the single values per wrist posture. Note that "a" indicates a significantly lower coherence value compared to the TE-FDI muscle pair, "b" a statistically lower coherence value compared to the FCR-FDS muscle pair, and "c" a statistically lower value compared to the ECU-EDC pair.

4.4.6 Muscle activation patterns varied across subjects but not between conditions

Identically to what we have shown for the neurologically intact group, the angle (cosine similarity) between MAPs did not change as a function of the wrist stabilization condition. However, while in neurologically intact subjects the extrinsic muscle activity increased from the self-stabilized to the externally stabilized, in stroke patients the levels did not change. Nevertheless, the reported intra-individual changes in MAPs depending on the wrist angle are similar in both groups. Any deviation from the optimal wrist flexion-extension angle for force production resulted in changes in MAPs. These changes in MAPs were more prominent in the extreme flexion and extension positions (+50° and -50°). Most likely, the observed changes in MAPs can be explained by the level of muscle activity of FCR, FDS and TE in the extreme wrist positions (flexion and extension).

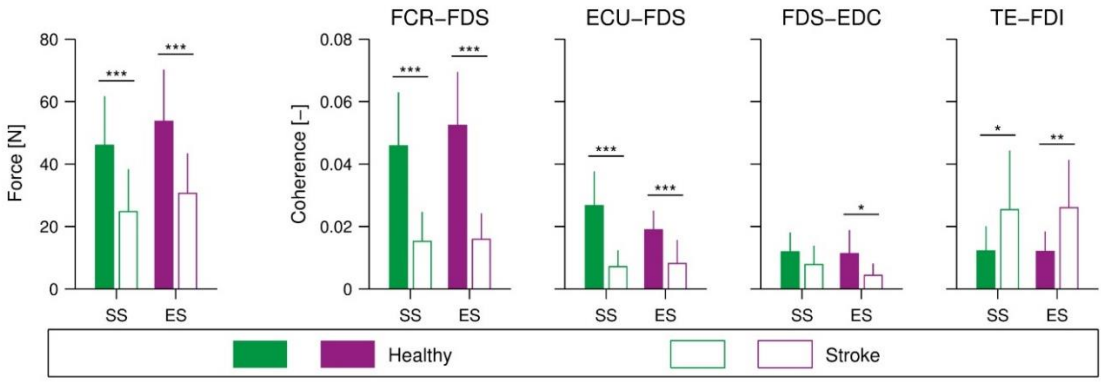

Figure 4-7: Average maximum pinch grip force for neurologically intact and stroke subjects and both wrist stabilization conditions are presented in the left plot. The right four plots present the coherence for muscle pairs FCR-FDS, ECU-FDS, FDS-EDC, and TE-FDI. "SS" stands for self-stabilized condition and "ES" for externally stabilized condition. Statistical significance is indicated with * p<0.05, ** p<0.01, and *** p<0.001.

As has been shown in the neurologically intact group, the MAPs varied considerably across stroke subjects. This can of course again be explained by the different type of two-finger pinch grip (Ng et al., 2014) used in this study, namely tip pinch and pulp-pinch, which can result among others in different activation levels of FDS and FDP (Maier and Hepp-Reymond, 1995, Chao, 1989). Moreover, inter-individual differences in muscle activation patterns between stroke subjects might also result from anomalous neural activation which can typically occur after stroke (Kamper et al., 2003).

4.4.7 Stroke subjects showed altered muscle synergies

Within the stroke group, a higher common corticospinal drive to the intrinsic muscle pair TE-FDI was found compared to other muscle pairs. Furthermore, the level of common corticospinal drive to TE-FDI was significantly larger than the values obtained from the neurologically intact group. There are two possible explanations for why this TE-FDI muscle synergy can only be seen in the stroke group. First, this TE-FDI synergy might by a purely pathological synergy. Although the specific TE-FDI synergy has not been reported for stroke survivors so far, the occurrence of altered muscle synergies has typically been associated with stroke (Twitchell, 1951, Roh et al., 2013). A second explanation might be that this muscle synergy is also present in neurologically intact people, but as they might rely more on extrinsic muscles for the generation of precision grip, the occurrence of this synergy was absent or undetectable in our study. However, as this TE-FDI synergy has not been reported neither for people with stroke nor for neurologically intact people, further investigations are needed to understand the mechanisms leading to the existence of this specific synergy in stroke survivors. The increased common corticospinal drive

to the synergistic muscle pairs FDS-FCR and ECU-EDC supports the findings of other studies which concluded that neurologically intact muscle synergies can be preserved following stroke (Roh et al., 2013, Cheung et al., 2012). At the same time, common corticospinal drive to the FDS-FCR muscle pair was significantly reduced in stroke subjects compared to the neurologically intact subjects. This decrease might be explained by a reduction in corticospinal activation following stroke (Kamper et al., 2006). The FDS-ECU synergy, which was present in the neurologically intact subjects, completely disappeared in the stroke group. This finding might also be related to decreased corticospinal activation, but at the same time could also be related to altered muscle synergies (Twitchell, 1951, Roh et al., 2013).

4.4.8 Limitations

A major limitation of this study is the small sample size, resulting in low statistical power for the detection of differences between groups or experimental conditions. Further, similar to the study with the neurologically intact subjects, fatigue might have affected MAPs, given the large number of maximum force trials. The fact that two different robotic manipulanda were used for the neurologically intact and the stroke group might also have had a slight influence on the results, although the differences between experimental setups were kept minimal.

4.5 Conclusion

Stroke subjects were able to benefit from external wrist stabilization for the production of precision grip strength. This can be explained by the fact that more muscle potential is available when the wrist does not have to be stabilized, i.e. finger muscles are not involved in wrist stabilization and can therefore be fully used for generating force at the fingertip. Therefore, stroke survivors with weaknesses at the level of the fingers may benefit from a wrist splint to increase functional use of the impaired limb. In contrast to the neurologically intact group, no optimal wrist posture for generating maximal pinch strength was found. In contrast, an optimal position for generating minimal wrist torque when generating a pinch force has been found in almost neutral position (3° extension). This is different to the value obtained from the neurologically intact group (22° extension), suggesting that a splint, used in stroke rehabilitation, should have an approximately neutral (0° of flexion) wrist angle. Differences in muscle synergies between neurologically intact and stroke subjects were found in this study. Although some muscle synergies, such as the FCR-FDS synergy, were preserved after stroke, the amount of common corticospinal drive was significantly decreased in the stroke group (with preserved co-activation levels). Furthermore, this study revealed a strong muscle synergy between the intrinsic muscles TE and FDI in the stroke survivors. This could be an indication that stroke survivors rely more on intrinsic hand muscles for the production of pinch grip force than neurologically intact people. In summary, this study provides novel insights into altered wrist and finger control in static conditions following stroke. The altered muscle activation patterns and the origin of different muscles synergies merit further investigation.

5 A novel algorithm for detecting active propulsion in wheelchair users following spinal cord injury[4]

Werner L. Popp, Michael Brogioli, Kaspar Leuenberger, Urs Albisser, Angela Frotzler, Armin Curt, Roger Gassert, Michelle L. Starkey

Medical Engineering and Physics (2016)

I would like to thank Lorenzo Tanadini, Larissa Angst, and Anne Brust who helped me with different aspects of this study.

[4] Final publication is available from http://dx.doi.org/10.1016/j.medengphy.2015.12.011.

5.1 Abstract

Physical activity in wheelchair-bound individuals can be assessed by monitoring their mobility as this is one of the most intense upper extremity activities they perform. Current accelerometer-based approaches for describing wheelchair mobility do not distinguish between self- and attendant-propulsion and hence may overestimate total physical activity. The aim of this study was to develop and validate an inertial measurement unit based algorithm to monitor wheel kinematics and the type of wheelchair propulsion (self- or attendant-) within a "real-world" situation. Different sensor set-ups were investigated, ranging from a high precision set-up including four sensor modules with a relatively short measurement duration of 24 hours, to a less precise set-up with only one module attached at the wheel exceeding one week of measurement because the gyroscope of the sensor was turned off. The "high-precision" algorithm distinguished self- and attendant-propulsion with accuracy greater than 93% whilst the long-term measurement set-up showed an accuracy of 82%. The estimation accuracy of kinematic parameters was greater than 97% for both set-ups. The possibility of having different sensor set-ups allows the use of the inertial measurement units as high precision tools for researchers as well as unobtrusive and simple tools for manual wheelchair users.

5.2 Introduction

Regular physical activity is associated with positive health benefits following spinal cord injury (Washburn and Hedrick, 1997), but only 13-16% of affected individuals report being physically active (Nash, 2005). Wheelchair propulsion is one of the most intense activities performed by wheelchair-bound individuals, and the measurement of wheelchair mobility has therefore been proposed as a means of estimating and tracking physical activity in these individuals. Such activity measurements could be powerful tools to monitor rehabilitation progress and motivate these individuals to maintain an active lifestyle. Wheelchair mobility can be quantified through direct observation, questionnaires, satellite navigation systems, specialized wheel modifications (e.g. SmartWheel, Three Rivers Holdings LLC) or through accelerometers mounted to the wheels. Direct observation is a valid approach but it is not practicable in long-term settings as it requires that the subject is followed with a video camera for the entire recording and involves intensive post processing to label the videos. Questionnaires require less effort but are rather subjective due to the individual (possibly biased) perception of subjects making it difficult to objectively quantify mobility. Furthermore, well-established questionnaires regarding wheelchair mobility used in clinical set-ups such as the SCIM III (Itzkovich et al., 2007b) do not reflect mobility in terms of physical activity but rather in terms of independence. A more objective way of describing mobility is to use a global positioning system (GPS) as described by Sindall et al. in a sport application (Sindall et al., 2013). However one major drawback is the dependence on the availability of GPS signals via satellites and therefore indoor applications that likely reflect the majority of daily activities are challenged.

Dedicated wheelchair activity measurement devices such as the SmartWheel are very powerful tools, allowing the collection of not only kinematic parameters, but also interaction forces with the wheelchair push-rims. The SmartWheel has already been used in several studies, for example to investigate start-up and steady state velocity in experienced wheelchair users (Lawrence et al., 1997), or to investigate push frequency and stroke length in manual wheelchair users with SCI (Cowan et al., 2008). Although the SmartWheel is a very promising and powerful tool to measure wheelchair mobility, it is a costly solution that requires a mechanical modification of the wheelchair that might affect the dynamic

behaviour (e.g. through increased weight and a shift in the centre of mass). Furthermore it may not be applicable to subjects that need wheelchairs adapted to specific morphological characteristics (e.g. wheels with larger diameters), or that employ multiple wheelchairs (athletes).

A more simple approach to track mobility in manual wheelchair users is through the use of inertial sensors. In order to describe mobility in terms of distance travelled, velocity or number of wheel revolutions the angular velocity cab be estimated through the use of accelerometers attached to the wheel (Coulter et al., 2011, Sonenblum et al., 2012a). This method has demonstrated a high accuracy of the estimated kinematic parameters such as distance travelled and has already been used for long-term monitoring (Sonenblum et al., 2012b). Whilst describing mobility and thus physical activity in terms of e.g. distance travelled is a good approach it has one major drawback, namely that it overestimates the mobility produced by the wheelchair user because it does not distinguish between the user moving the wheelchair himself ("self-propulsion") and being pushed by someone else ("attendant-propulsion"). The alternative is to use accelerometers attached to the upper extremity of the user to detect manual wheelchair propulsion. For example, during standardised mobility-related activities, Postma and co-workers were able to detect hand-rim wheelchair propulsion with a high accuracy, sensitivity and specificity (Postma et al., 2005). However, an estimation of wheelchair mobility based purely on activity measurements at the upper extremity might be misrepresented by upper limb activities unrelated to wheeling. Furthermore, complementary inertial sensors such as gyroscopes might provide a more accurate measure of wheel kinematics, as they directly measure angular velocity. In this direction, Hiremath and colleagues combined the two aforementioned approaches and showed that a multimodal system, consisting of a two-axis gyroscope fixed to the spoke of the wheel and multiple tri-axial accelerometers fixed to the upper extremity, were able to detect wheelchair activities (e.g. self-propulsion) with higher accuracy than with the individual components alone (e.g. only the accelerometers) (Hiremath et al., 2014). Although the system has been tested in a structured laboratory, semi-structured organizational and unstructured home environments (real-world), for the cross validation the three datasets were mixed together which limited the generalization (approximated to the real world) of the study's results.

The aim of this study was to develop and validate an algorithm to continuously monitor the type of wheelchair propulsion (self- or attendant-propulsion) and wheel kinematics using an enhanced inertial measurement unit (IMU)(Leuenberger and Gassert, 2011) within a "real-world" situation. Similar to the methodology used by Hiremath and co-workers (Hiremath et al., 2014), the algorithm fuses two approaches, i.e. using accelerometers attached to the human body to detected manual wheelchair propulsion (Postma et al., 2005) and accelerometers attached to the wheel to estimate kinematic parameters such as wheel revolutions, angular velocity or distance travelled (Coulter et al., 2011, Sonenblum et al., 2012a) and further allows the precise detection of wheeling phases and the distinction of self-propulsion from attendant-propulsion. The algorithm consists of two components, the first detects if the wheelchair was moved based on heuristic rules and the second component then determines whether the wheelchair was moved by the user itself based on a support vector machine (SVM) classifier. Six different sensor set-ups were investigated, ranging from a high precision measurement tool set-up involving multiple sensor modules and a relatively short measurement duration (around 1 day) where gyroscope data is included to a simple, less precise set-up with only one sensor module and an increased measurement duration exceeding one week (without gyroscope). In addition to kinematic parameters, the algorithm determines the percentage of wheelchair use which can be attributed to self-propulsion. The results obtained by this new approach provide a better insight into the effective mobility behaviour of wheelchair users, and the algorithm is especially suited for application both in acute in-patient rehabilitation through to discharge into the home environment (out-patient situation), and hence can provide information about mobility as patients progress from learning to use the wheelchair to eventually integrating the wheelchair into their activities of daily living.

5.3 Methods

5.3.1 Subjects

Seven paraplegic (age 61.85 ± 16.93 years, six male, one female, ASIA A, C and D) and 14 tetraplegic (age 38.71 ± 14.84 years, 12 male, two female, ASIA A-D) subjects in the chronic stage (at least 90 days post-injury) with traumatic SCI were recruited for this study. Inclusion criteria required that subjects were 18 years or older and were trained to use a manual wheelchair. Exclusion criteria were any neurological disorders, orthopaedic or rheumatological diseases affecting the upper limb (other than SCI) and pre-morbid or on-going major depression. Each participant provided written informed consent after having the experimental procedure explained to them. The measurements took place at the University Hospital Balgrist and the Swiss Paraplegic Center in Nottwil. The study was approved by the ethics committees of the cantons of Zurich (KEK-ZH 2013-0202) and Lucerne (EK 13018).

5.3.2 Measurement device

For this study an enhanced version of the ReSense module was used (Leuenberger and Gassert, 2011) (Figure 5-1 B). The new ReSense module is a miniature 10-degrees-of-freedom (DOF) IMU designed for long-term monitoring of human motor activities. It consists of a 3-axis accelerometer (ADXL345, Analog Devices), a 3-axis gyroscope (ITG-3050, InvenSense), a 3-axis magnetometer (MAG3110, Freescale) and a barometric pressure sensor (BMP 085, BOSCH). The electronics board is encased in a robust, water-resistant and biocompatible plastic housing. ReSense weighs 15g (including the battery and housing), measures 36x29x13mm^3 and can continuously record data for over 24h at a 50Hz sampling rate. An integrated power-management system can increase the operating time by a factor of 2-3. In addition, deactivation of the gyroscopes increases the operating time to 20 days. The collected data, which includes an absolute time stamp, is stored on an internal 2GB microSD card. An advantage of the ReSense is the possibility to synchronize the on-board clock across different modules with a host PC via a custom-built USB base station.

Figure 5-1: A: Attachment of the sensor modules to the subject. One module is attached at each wrist, and an additional module is attached at the chest. The fourth ReSense module is attached to the wheel of the wheelchair B: Module worn at the wrist with the AlphaStrap Blue and Velcro Straps fixation. C: Custom made fixation plate for the wheel module.

5.3.3 Data collection

Participants were equipped with four ReSense modules (Figure 5-1 A) for up to six hours. One module was worn on each wrist, attached with AlphaStrap Blue (North Coast) and Velcro Straps (Velcro). The chest module was attached with a custom-made chest strap (BalgristTec AG, Switzerland). The fourth sensor was fixed between the spokes of the wheelchair using a custom-designed fixation (Figure 5-1 C). The subjects, who were all in-patients, were asked to carry on with their daily clinical routine during the entire duration of the measurement. In order to validate the algorithm, a video camera (GoPro Hero HD 2, GoPro Inc.) was attached to the back of the wheelchair to film the right wheel only. The frame rate of the camera was set to 30fps and it was synchronized with the ReSense modules prior to the recording.

To assess the accuracy of estimating the kinematic parameters with the wheel sensor two additional healthy subjects (age: 28.5 ± 2.12 years, both male) completed three pre-defined indoor courses and three outdoor courses set at Balgrist University Hospital. The courses were each completed two times and the subjects propelled the wheelchair at a self-selected speed. In addition to the measurement set-up described above, four additional sensors were attached at different distances from the center of the

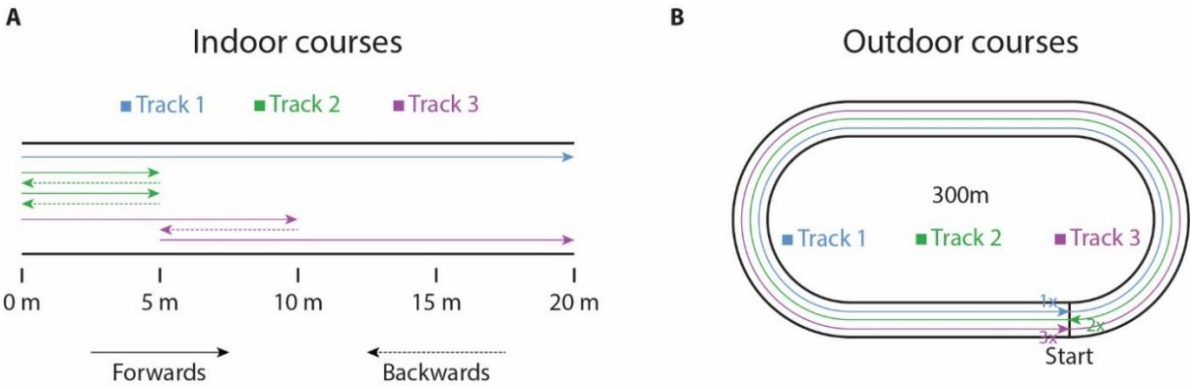

Figure 5-2: Illustration of the indoor and outdoor courses. A: Indoor courses consisting of three different tracks with forward and backward segments. B: Outdoor courses with a length of 300m, 600m and 900m. The 600m long track 2 was performed in the opposite direction. For illustration purposes, the tracks are offset.

right wheel (5, 10, 15, 20cm) in order to identify the influence of sensor position. The indoor courses were performed along a straight corridor, and consisted of forward and backward segments during which the subjects had to travel in total 20m (20m forward), 20m (2x 5m forward and 5m backward) and 30m (10m forward, 5m backward and 15m forward, Figure 5-2 A). The outdoor measurements were performed on a 300m athletic track and subjects completed one, two and three laps (Figure 5-2 B).

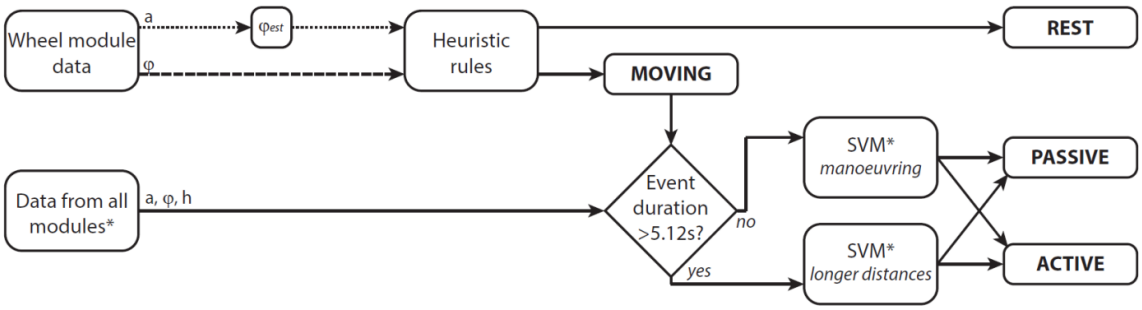

Figure 5-3: The flow chart of the presented algorithm. First a classifier using heuristic rules identifies if the wheelchair was moving or not based on the angular velocity of the wheel. The angular velocity of the wheel can, depending on the set-up, be taken directly from the gyroscope of the wheel (dotted line) or estimated though the acceleration signal of the wheel sensor (dashed line). Then the data which was previously labelled as moving is separated into manoeuvring and longer wheeling distances. Depending on the set-up, acceleration (a), angular velocity (ϕ) and altitude (h) is fed into the support vector machine classifiers which distinguish between active and passive wheelchair motion. (* indicates the dependency from the specific set-up)

5.3.4 Data analysis and classification

The complete data processing, training of the SVM classifier and statistical analysis was performed using MATLAB R2013a (The MathWorks Inc). All processing steps were conducted offline.

In total three different sensor set-up combinations were investigated and trained. Set-up I included raw data from all four ReSense modules and was designed to be a high precision configuration. For set-up II, only raw data from three of the sensor modules were included in the analysis (left and right wrist and wheel sensor module). This set-up configuration was chosen because some of the participants complained about discomfort with the chest sensor module. The last set-up (Set-up III) contained only raw data from the wheel sensor module. The inclusion of this set-up was motivated by the fact that three sensor modules attached to body may disturb the user during certain activities of daily living and hence we wondered how accurate the data would be if only the wheel module were used. For each of the set-ups data was analysed separately once with the gyroscope data included (a) and once without the gyroscope data (b). The omission of the gyroscope recordings increases the operating time of our sensor modules from 2–3 days up to 20 days, which would be beneficial for long-term monitoring.

The final algorithm is split up into two different parts (Figure 5-3). The first part detects if the wheelchair was in motion by applying heuristic rules to the pre-processed data from the wheel module and the second part divides the wheelchair propulsion in active and passive phases by applying, depending on the selected set-up, different SVM classifiers.

Labelling: The synchronized videos were labelled by two different raters with an inter-rater agreement of 0.99. A video editing tool (AVS Video Editor, Online Media Technologies Ltd.) was used for video labelling and the raters were asked to identify if the wheelchair was at rest, if it was moved passively ("attendant-propelled") or if it was moved actively ("self-propelled"). The only instructions the raters received were that wheelchair movement meant that the wheel should make at least a quarter turn. Furthermore, if the participant was not sitting in the wheelchair or if, due to the camera position, it was impossible to identify what the participant was doing, the activity was removed prior to the analysis.

Pre-processing: Data stored on the microSD cards of the ReSense modules were transferred to a PC via a custom made Basestation. The recordings from the modules were resampled at 50Hz using a cubic spline interpolation function. This step was necessary to ensure that all sensors had the same number of samples and that the data was temporally aligned.

Detection of wheelchair movement: For the detection of wheelchair movement, the angular velocity of the wheel was taken. For the set-ups I.a, II.a, III.a where the gyroscope data was included in the analysis, the angular velocity of the wheel was directly estimated through angular velocity of the wheel module (z-axis of the 3D gyroscope). The angular velocity was filtered using a 4^{th} order Butterworth high-pass filter with a cut-off frequency of 0.3Hz. For the set-ups without gyroscope data (I.b, II.b, III.b) the angular velocity of the wheel was estimated using previously described methods (Coulter et al., 2011, Sonenblum et al., 2012a) where the gravity acting on the accelerometer is used to calculate the absolute angle of the wheel and therefore the angular velocity. The approach from (Sonenblum et al., 2012a) suggests a second order Butterworth low-pass filter with a cut-off frequency of 3.1Hz to filter the acceleration signals in order to measure wheelchair speeds up to 3 m/s. For higher angular velocities the presented filter design did not work. For angular velocities of around 500°/s and higher (=9.4 km/h with a wheel diameter of 0.6m), which can easily be achieved by wheelchair athletes, the centrifugal acceleration dominated the measured acceleration signals. Therefore, we changed the filter design proposed by Sonenblum and co-workers (Sonenblum et al., 2012a) to a second order Butterworth band-pass filter with lower and higher cut-off frequencies of 0.5 and 3.1Hz, respectively, as soon as the wheelchair starts moving. For a detailed description of the procedure used to estimate the angular

velocity of the wheel, the reader is referred to the work of Sonenblum and colleagues (Sonenblum et al., 2012a).

To detect if the wheelchair was moving or not a threshold of 0.4°/s was applied to the angular velocity to identify possible movement windows. In order to classify such phases as a valid movement of the wheelchair the following rules were applied to each window separately:

- The angular velocity had to reach 10deg/s at least once.
- The wheel rotation had to be at least 80deg.
- The duration of a movement window had to be greater than or equal to 2s.

Finally, two consecutive windows were merged if they were separated by less than 2s. The events classified as "moving" were then used in the next step to distinguish between active and passive propulsion.

Pre-processing for the classifier: The different filters applied to the resampled signal are mostly based on previous work (Moncada-Torres et al., 2014). Firstly, the acceleration signal was filtered with a median-filter with a window size of 3 samples. Subsequently, the acceleration signal was passed through an infinite impulse response eight order elliptic low-pass filter with a cut-off frequency of 0.3Hz, a passband ripple of 0.02dB and a minimum stopband attenuation of 200dB in order to separate the static acceleration component due to gravity from the dynamic acceleration component resulting from body or wheel movement (Karantonis et al., 2006a). The dynamic acceleration was obtained by subtracting the static acceleration component from the original signal. Gyroscope signals were filtered with a high-pass filter with a cut-off frequency of 0.3Hz with the same filter design as described above. The altitude signal was filtered with a second order low-pass Butterworth filter with a cut-off frequency of 0.07Hz.

Segmentation: Data that were previously labelled as "moving" were divided into two sub-sets, one containing short lasting "moving" events (less than 5 seconds, defined as "manoeuvring") and one containing longer periods of wheelchair movements (5 seconds or more).

Each manoeuvring phase was taken as a single event and was assigned as such using the video recording. For the longer wheelchair motion dataset the first and the last five seconds of the movement were cut because the acceleration and deceleration of the wheelchair adversely affected the training of the SVM classifiers. The remaining data were divided into windows of 5.12 seconds with an overlap of 50%. Again, a single label from the video recording was assigned to each window.

Feature calculation: Features were calculated from the pre-processed acceleration signal containing the static component; the acceleration signal containing the dynamic motion; the gyroscope data; and the altitude signal. It is important to note that features were taken from single axis data and also from the magnitude of the different sensor modalities. The complete overview of the data analysed can be found in Table 5-1. Features computed from the angular velocity or the acceleration signal were based on previously used features in activity classification studies (Curone et al., 2010a, Ravi et al., 2005, Maurer et al., 2006, Bouten et al., 1997a, Karantonis et al., 2006a, Herren et al., 1999, Baek et al., 2004a, Bao and Intille, 2004b, Stikic et al., 2008b, Leuenberger et al., 2014). Features calculated from the altitude signal were based on the work of Moncada-Torres et al. (Moncada-Torres et al., 2014). Additionally, the inter-sensor correlations of the acceleration magnitude were taken as additional features. Depending on the analysed set-up the number of features changed: e.g. for the full set-up (I.a) all 755 features where used; for the full set-up without gyroscope data (I.b) 579 features were used; for the full set-up with three sensors (II.a) 565 features were used; and finally for the data that did not contain gyroscope information (II.b) 433 features were used. The number of features for the single wheel sensor set-up with and without gyroscope data was 155 (III.a) and 111 (III.b), respectively.

Table 5-1: Features calculated for each sensor with Acc.P. being the acceleration with the gravity component and Acc.A. the acceleration including the movement components.

Domain	Feature	Alt.	Acc. P.	Acc. A.	Gyro.
Time	Mean		X		X
	Standard Deviation	X	X	X	X
	Variance	X	X	X	X
	IQR	X	X	X	X
	RMS	X	X	X	X
	Interquartile Range	X	X	X	X
	Percentile (3, 10, 20, 97)		X	X	X
	Peak to Peak Amplitude	X		X	X
	Peak to RMS			X	X
	Counts		X	X	X
Frequency	Max Frequency Component			X	X
	Energy			X	

Feature selection: To reduce the set of features to a smaller subset the ReliefF algorithm (Kononenko, 1994) was used. For each of the set-ups investigated (I.a – III.b) the 15 most highly weighted features were selected for further investigations. For each of the set-ups the best feature combination was selected, in order to train the classifiers with a maximum of eight features.

Training SVM classifiers: In total 12 different SVM classifiers were trained. For each of the six different set-ups (I.a-III.b) two classifiers were trained: one for the manoeuvring and one for the longer wheelchair movements. For each of the SVM classifiers different kernel functions were evaluated and the one showing the best performance was chosen. The investigated kernel functions were linear kernel, quadratic kernel, Gaussian radial basis function kernel (scaling factor = 1) and a multilayer perceptron kernel (scale [1 -1]).

Testing SVM classifiers: The performance of the SVM classifier was analysed by using the leave-one-subject-out method. This means that the data of all participants except one was used to train the algorithm and the data from the remaining participant was used to evaluate the performance of the classifiers.

Classification example: To describe the overall algorithm, a single set-up will be presented in detail, i.e. set-up II.b which contains data from three ReSense modules without the gyroscope information. After pre-processing the angular velocity of the wheel is estimated using the acceleration signals. Next, using

heuristic rules applied to the wheel sensor data, the algorithm classifies the wheelchair state as “rest” or “moving”. The events categorized as “moving” are then separated into “manoeuvring” or “longer wheelchair movements” and further classified into active/passive propulsion using the corresponding SVM. In the case of the “longer wheelchair movements” the previously cropped segments at the beginning and the end are classified. Finally, for each of the classified movement events, duration, speed and distance travelled are calculated.

Performance analysis: The performance of the complete algorithm and the different sub-parts was analysed in terms of:

accuracy

$$accuracy = \frac{TP+TN}{TP+TM+FP+FN} \qquad (5.1)$$

sensitivity

$$sensitivity = \frac{TP}{TP+FN} \qquad (5.2)$$

and specificity

$$specificity = \frac{TN}{FP+TN} \qquad (5.3)$$

with TP as true positive rate, TN as true negative rate, FP as false positive rate and FN as false negative rate. Additionally the kinematic parameters were analysed in terms of absolute mean errors. The estimation of the angular velocity of the wheel from the accelerometer data was compared to the values obtained through the gyroscopes using a paired t-test.

5.4 Results

The average length of evaluated data was 219.12 ± 83.24min (range: 73.48min - 335.29min) per subject. The video showed that subjects were not moving the wheelchair for 87.54 ± 4.71% of the time (range 79.82% - 96.75%). On average a subject self-propelled the wheelchair 12.19 ± 4.47% of the time (range 3.02% - 20.18%), whereas 0.27 ± 0.37% of the time the wheelchair was attendant-propelled (range 0% - 1.38%). In total, 18 out of the 21 subjects had at least one phase where the wheelchair was attendant-propelled. Table 5-2 shows the performance of the classifier based on heuristic rules for the direct input of gyroscope data and for the modified approach based on Clouter et al. (Coulter et al., 2011) and Sonenblum et al. (Sonenblum et al., 2012a) where the angular velocity of the wheel was estimated through accelerometer data. Note that the accelerometer-based approach performed slightly worse in terms of specificity (1.11%). Table 5-3 shows the performance of the 12 trained classifiers in terms of overall accuracy, sensitivity and specificity as well as the number of features selected and the kernel function chosen for the evaluation. For training of the SVM classifiers to analyse the manoeuvring data a total of 376 time windows were generated. For the training of the SVM classifiers for analysis of the long motion periods a total of 4151 windows were included. Table 5-4 shows the performance of the complete algorithm with the classification of moving or rest and the following part with the SVM classifiers.

Finally, the results of the estimated distance travelled and the duration of movement for the additional measurements on the indoor and outdoor tracks are presented in Table 5-5. The statistical analysis showed no significant difference between the approach using the gyroscope data and the one using the accelerometer data for each of the estimated parameters.

5.5 Discussion

The aim of this study was to develop and validate an algorithm that could continuously monitor "real-world" wheelchair propulsion and distinguish attendant- or self-propulsion using an enhanced IMU. Here we present a valid method that, firstly estimates time-distance parameters of mobility, such as distance travelled and the speed and duration of movement, and secondly distinguishes passive (attendant-propelled) from active (self-propelled) wheelchair propulsion by using data collected from unobtrusive IMUs. Furthermore, we were able to show that even with a reduced numbers of IMU modules (one instead of four) and different set-ups (with or without the gyroscope) overall the accuracy remained high.

The full sensor set-up using four sensors with gyroscope data included in the analysis, performed best with an overall accuracy of more than 93%. Reducing the set-up to only one sensor module still showed a sufficiently high overall accuracy (82%) and can thus be used as a basic, unobtrusive tool for monitoring subjects' overall mobility. The set-ups where gyroscope data was not included performed slightly worse than the set-ups where the gyroscope data was included with a maximal difference of around 2%.

The wheelchair algorithm developed by Sonenblum and colleagues (Sonenblum et al., 2012a) focused on evaluating overall wheelchair use (Sonenblum et al., 2012b). However, overall mobility data alone are less sensitive for describing the true physical activity of the wheel chair user, as it does not distinguish between self- and attendant-propulsion (being propelled by another person) and consequently the assessment of overall physical activity is limited. For wheelchair users it can be quite difficult to estimate their overall wheelchair activity both during the early phases of rehabilitation and after discharge when they are living in their home environment as they have no obvious parameters for comparison of their activity (i.e. meaningful thresholds of low or high wheelchair activity). In particular, this is of high relevance when after an SCI wheelchair activity replaces all the previous bodily activities (walking, running, stair climbing etc.) and a novel way of measuring activity needs to be developed. Therefore, it is important to be able to distinguish between active (self-) propulsion of the wheelchair

Table 5-2: Sensitivity and specificity of the classification if the wheelchair was moving compared to the data from the video recording. The accelerometer-based approach is a modified version of the work presented from Coulter et al. 2011 and Sonenblum et al. 2012 (Coulter et al., 2011, Sonenblum et al., 2012a).

	Gyroscope	Accelerometer
Sensitivity	95.80 ± 1.91%	94.69 ± 3.01%
Specificity	99.58 ± 0.29%	99.25 ± 0.43%

from passive attendant-propulsion and to provide patients with feedback about active wheeling not only in parameters such as time-distance but also readouts that can be translated into dynamic values (acceleration, managing levels, ramps etc.).

For this purpose the SVM classifiers showed a good overall performance. Interestingly, the features selected were mostly single axis accelerometer data containing the static components (3rd and the 97th percentile). In other words, the features selected were mostly related to the orientation of the IMU as none of the features with high frequency content were selected. This is in contrast to the previously reported findings of Hiremath and co-workers (Hiremath et al., 2014) where the features identified by the classification algorithm were mostly frequency-based , e.g. entropy of the velocity. This divergence may be attributed to the different nature of the environment where we performed our experiment, a real-world environment where activities are performed spontaneously, compared to the one used by Hiremath and colleagues which was a mixture of laboratory and real-world settings, where subjects performed artificially defined activities. By way of illustration Hiremath and co-workers reported that in each case the same attendant was used and that because it was always the same individual this may have resulted in specific movement patterns that may have influenced the sensitivity of the developed algorithm. The pushing or propelling the wheelchair with a heterogenic speed or acceleration pattern may result in a more homogeneous frequency spectrum compared to a more natural and spontaneous propulsion, as observed in our set-up, which might shift the classifier feature selection toward placing a priority on frequency-based features. This example may explain the importance of validating such methodologies in a real-world environment in order to achieve a higher ecological validity.

Table 5-3: Overall accuracy and sensitivity for the trained support vector machine classifiers are presented in this table. Additionally the numbers of features used to train the classifier and the chosen kernel function are indicated (rbf = Gaussian radial basis function).

Set-up	Number of modules	data type analysed	Overall Accuracy	Sensitivity "passive"	Sensitivity "active"	Number of features	kernel function
I.a	4 modules	long mobility bouts	98.24%	90.38%	98.57%	4	rbf
		manoeuvering	90.77%	84.85%	98.11%	3	rbf
I.b	4 modules	long mobility bouts	98.24%	90.38%	98.57%	4	rbf
	without gyroscope	manoeuvering	88.74%	85.61%	97.93%	2	rbf
II.a	3 modules	long mobility bouts	96.34%	87.21%	98.28%	4	rbf
		manoeuvering	88.54%	85.88%	97.91%	3	rbf
II.b	3 modules	long mobility bouts	96.34%	87.21%	98.28%	4	rbf
	without gyroscope	manoeuvering	88.54%	85.88%	97.91%	3	rbf
III.a	1 module	long mobility bouts	87.68%	81.73%	85.08%	4	linear
		manoeuvering	88.36%	74.45%	84.35%	5	linear
III.b	1 module	long mobility bouts	87.68%	81.73%	85.08%	4	linear
	without gyroscope	manoeuvering	84.52%	73.94%	84.16%	4	linear

Most of the trained SVM classifiers did not include gyroscope data. From the six possible set-ups that included gyroscope data only two used gyroscope-related features in the final SVM classifier. To support this, it has been reported previously that gyroscopes do not include information that is valuable for the purpose of activity (Moncada-Torres et al., 2014). Also, it should be noted that the classification accuracy of propulsion is within the same range as previously published data (Postma et al., 2005).

The accuracy of our estimation of the distance travelled agreed with previously published studies (Coulter et al., 2011, Sonenblum et al., 2012a, Hiremath et al., 2013) both approaches to estimate the angular velocity of the wheel, i.e. the accelerometer-based approach and the gyroscope-based estimation of distance, have previously been shown to be valid. The adaptation of the algorithm presented by Sonenblum and co-workers (Sonenblum et al., 2012a) was necessary to match the requirements of a long-term monitoring device, i.e. for recordings longer than three days the gyroscope will need to be turned off to extend battery life. Additionally, although manual wheelchair users do not usually achieve a wheelchair speed of 9km/h in daily life, a future application might be to monitor highly active people, e.g., wheelchair athletes where speeds of 15km/h can be easily reached.

Table 5-4: The overall accuracy of the presented algorithm combining heuristic rules and a support vector machine classifier.

		Overall accuracy
I.a	4 modules	93.29%
I.b	4 modules without gyroscope	91.12%
II.a	3 modules	90.96%
II.b	3 modules without gyroscope	90.51%
III.a	1 module	83.77%
III.b	1 module without gyroscope	82.07%

Some study limitations should also be mentioned. Firstly, for training of the SVM classifiers we had much more data from active wheelchair propulsion compared to passive phases which might result in a classifier rating slightly in favour of the active propulsion. Additionally, for this study we also had to separate between events classified as manoeuvring and longer events where the wheelchair was moving. This made an already complex algorithm even more complex. We reported small deviations between how an operator labelled the videos and how the data was labelled by the classifier based on heuristic rules. This discrepancy may be due to the fact that it was sometimes difficult to recognize wheelchair motion from the video. Alternatively, the synchronization between the video and the sensor data may not have been optimal.

Table 5-5: Estimation of the distance using the modified accelerometer based approach or directly using the gyroscope data. Data was collected from 5 sensors placed at different distances from the center of rotation of the wheel. Each trial was repeated twice. Note that there are no significant differences between the two estimation methods for the estimation of the distance.

	Real Distance	**Gyroscope**		**Accelerometers**	
		Estimated distance		**Estimated distance**	
		Average Distance	*Accuracy range*	*Average Distance*	*Accuracy range*
Indoor track 1	20m	19.8±0.2	97.7-99.8%	20.1±0.0	99.2-99.6%
Indoor track 2	20m	19.9±0.3	98.5-99.1%	20.2±0.0	98.7-98.9%
Indoor track 3	30m	29.7±0.3	97.7-99.8%	30.2±0.0	99.2-99.4%
Outdoor track 1	300m	303.1±1.8	98.5-99.4%	302.9±0.7	99.3-99.5%
Outdoor track 2	600m	605.3±3.8	98.6-99.6%	604.1±1.5	99.3-99.6%
Outdoor track 3	900m	908.0±5.9	99.7-99.9%	907.9±4.2	99.5-99.8%

5.6 Conclusion

The methods presented in this study allow for an accurate identification of active and passive wheelchair propulsion, as well as a valid estimation of kinematic parameters of wheelchair movement such as distance travelled. The possibility to switch between different sensor set-ups allows the use of the ReSense as a high precision tool for research and as an unobtrusive and simple tool which could be implemented on future commercial activity trackers for manual wheelchair users. Future work will focus on using this algorithm to gain new insights into the "true" mobility behaviour of manual wheelchair users with a special focus on elderly persons, wheelchair athletes and those in the acute stage of recovery from a spinal cord injury. This tool has the potential to help clinicians assess and motivate manual wheelchair users, to adapt therapy when needed or to promote a more active lifestyle. In addition, the presented tool could help identify if abilities as measured by clinical assessments are transferred into performance in daily life, e.g., self-propulsion.

6 Estimation of energy expenditure in spinal cord injured individuals using inertial measurement units

Werner L. Popp, Lea Richner, Michael Brogioli, Britta Wilms, Christina M. Spengler, Armin Curt, Michelle L. Starkey, Roger Gassert

Manuscript submitted to Journal of Neurotrauma

I would like to thank Thi Dao Nguyen, Fanny Leimgruber, Sophie Schneider, Kaspar Leuenberger, Mike D. Rinderknecht, and Larissa Angst who helped me with different aspects of this study.

6.1 Abstract

A healthy lifestyle reduces the risk of cardio-vascular disease. As wheelchair-bound individuals with spinal cord injury (SCI) are challenged in their activities, promoting and coaching an active lifestyle is especially relevant. Although there are many commercial activity trackers available for the able-bodied population, including those providing feedback about energy expenditure (EE), activity trackers for the SCI population are largely lacking, or are limited to a small set of activities performed in controlled settings. The aims of the present study were to develop and validate an algorithm based on inertial measurement unit (IMU) data to continuously monitor EE in wheelchair-bound individuals with a SCI, and to establish reference activity values for a healthy lifestyle in this population. For this purpose, EE was measured in 30 subjects each wearing four IMUs during 12 different physical activities, randomly selected from a list of 24 activities of daily living. The proposed algorithm consists of three parts: resting EE estimation based on multi-linear regression, an activity classification using a k-nearest-neighbours algorithm, and EE estimation based on artificial neural networks (ANN). The mean absolute estimation error for the ANN-based algorithm was 14.4% compared to indirect calorimeter measurements. Based on reference values from the literature and the data collected within this study, we recommend wheeling 3 km per day for a healthy lifestyle in wheelchair-bound SCI individuals. Combining the proposed algorithm with a recommendation for physical activity provides a powerful tool for the promotion of an active lifestyle in the SCI population, thereby reducing the risk for secondary diseases.

6.2 Introduction

The life expectancy of individuals with a spinal cord injury (SCI) has increased significantly over the last decades (Wyndaele and Wyndaele, 2006). Nowadays, the leading causes of death are not a direct consequence of injury-related complications (sepsis, respiratory or renal complications) but rather related to cardiovascular disease (McColl et al., 1997, Samsa et al., 1993). Obesity, hypertension, hyperlipidemia, and diabetes have all been identified as risk factors for cardio-vascular disease, with a higher prevalence in the SCI population (Myers et al., 2007). Regular physical activity has been associated with a reduction of these risk factors in the able-bodied population, as well as in the SCI population (Buchholz et al., 2009, Warburton et al., 2006, Phillips et al., 1998). Unfortunately, the SCI population is challenged due to their limited choice of activities (Rauch et al., 2016, Anneken et al., 2010), and there is a great need to promote and coach physical activity (Washburn and Hedrick, 1997). One possible approach to promote a more active lifestyle is to provide feedback on daily physical activity and energy expenditure (EE).

Vanhees et al. showed that accelerometers and inertial measurement units (IMUs) can be used as objective assessment tools for physical activity and EE in the able-bodied population (Vanhees et al., 2005). Over the past 20 years, different approaches to estimate EE from IMU or accelerometer data have been proposed, ranging from simple linear regression models based on activity counts (Klippel and Heil, 2003, Swartz et al., 2000, Freedson et al., 1998), to complex non-linear regression models based on more advanced statistical features (Crouter and Bassett, 2008), as well as approaches using artificial neural networks (Staudenmayer et al., 2009, Freedson et al., 2011). To increase the accuracy of EE estimation, additional sensors such as heart rate monitors to compensate for weight-loading activities (Brage et al., 2004), or air pressure sensors to improve the estimation for activities involving altitude changes were added (Anastasopoulou et al., 2012). Despite the improvements in the field of EE estimation based on accelerometers and IMUs, commercially available devices show a wide range of estimation accuracy (root mean squared error of 14-28% in EE estimation (Dannecker et al., 2013)). However, considering that many individuals with SCI present different movement characteristics due to

the use of a wheelchair, the application of methods developed in able-bodied populations will likely result in a moderate to poor EE estimation in individuals with SCI.

Although accelerometer-based EE estimation models were developed for subjects with SCI using a manual wheelchair (Hiremath et al., 2012, Hiremath et al., 2013), combining accelerometer and demographic variables, these studies focused on a restricted set of activities and were only validated in a semi-structured environment. In a more recent study, linear regression models for the estimation of EE became available based on recordings of 20 different activities, with a mean absolute error (MAE) of around 25% (Hiremath et al., 2016). Using methods that are more sophisticated the quality of the EE estimation may be improved.

The main aim of this study therefore was to develop and validate an EE estimation model for wheelchair-bound SCI individuals based on non-obstructive IMU recordings in a natural setting. We included a comprehensive set of 24 different physical activities, covering a broad range of activities of daily living. Furthermore, the collected data formed a basis for a recommendation that could promote a healthy lifestyle in the wheelchair-bound SCI population.

6.3 Methods

6.3.1 Subjects

Thirty chronic SCI subjects (age 45.4 ± 11.4 years, 11 tetraplegics, 19 paraplegics) who rely on a wheelchair for daily ambulation were recruited. Inclusion criteria were an age over 18 years old and suffering from SCI for more than 6 months post injury. Subjects with all neurological levels of injury (NLI) according to the International Standard for Neurological Classification of Spinal Cord Injury (ISNCSCI), and ASIA Impairment Scale (AIS) grades (A, B, C and D) were included (Table 6-1). Exclusion criteria were any neurological diseases other than SCI, metabolic, orthopaedic or rheumatologic diseases as well as pre-morbid or ongoing psychiatric disorder. Prior to the experiment, each subject was informed about the experimental protocol and gave informed written content. The study was approved by the local ethics committee of the canton of Zurich (KEK-ZH Nr. 2013-0202).

6.3.2 Measurement devices

Activity monitor: An IMU (ReSense) developed by Leuenberger and Gassert was used for this study (Figure 6-1 B-C) (Leuenberger and Gassert, 2011). The sensor consists of a 3-axis accelerometer, a 3-axis gyroscope, a 3-axis magnetometer (not used in this study), as well as a barometric pressure sensor for altitude estimation. This low-power 10-degrees-of-freedom IMU can continuously record data for around 48 hours at a sampling rate of 50Hz. Thanks to its lightweight (15g) and robust housing, the ReSense module is particularly well suited for clinical applications. In addition, the on-board clock of multiple modules can be synchronized temporally via a custom-built USB base station.

Indirect calorimetry: EE was assessed using a portable metabolic cart (Oxycon mobile, Carefusion, Hoechberg, Germany; Figure 6-1 A, D, E). This system consists of a facemask, a turbine to assess flow as well as O2 and CO2 analysers. The data exchange unit as well as the sensor box were fixed on the participant's back via a harness. Data were recorded continuously breath-by-breath (i.e., one data point per breath) and synchronized offline with ReSense measurements. EE was derived from the O2 consumption and CO2 production using the proprietary software JLAB (Carefusion, Hoechberg, Germany).

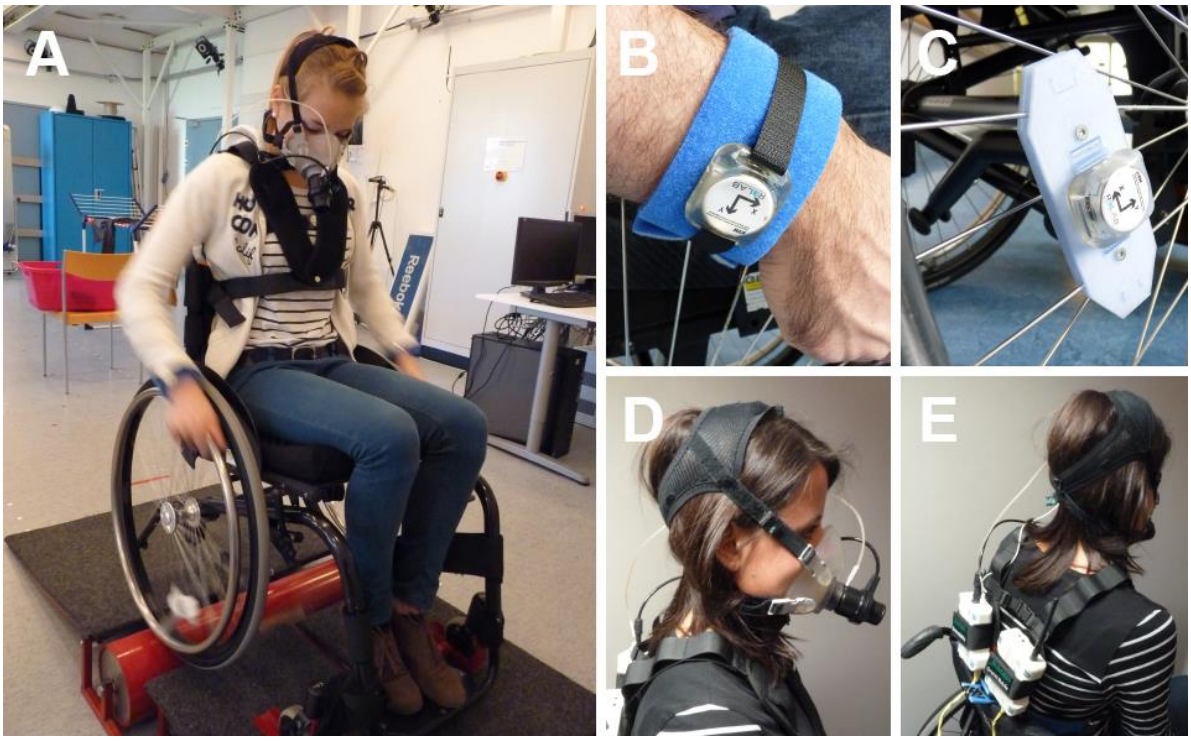

Figure 6-1: A: Examiner wearing the full experimental setup during the activity training on the wheelchair ergometer. One sensor module was attached at each wrist, one at the chest and one on the wheel of the wheelchair. B: Sensor worn at the wrist with the AlphaStrap Blue and Velcro Strap fixation. C: Wheel sensor with dedicated attachment. D: Oxycon mobile mouth piece. E: Back view of the Oxycon Mobile with sensor box and data exchange unit.

The system was calibrated according to the manufacturer's recommendation, 30min prior to and immediately after each session in order to ensure high accuracy. Additionally, heart rate (HR) and blood oxygen saturation were measured by infrared technology, using an ear clip that was connected to the same system.

Bioelectrical impedance analysis (BIA): BIA was used to determine fat mass (FM) and fat-free mass (FFM) of each subject. Based on FM and FFM, an additional reference value for the resting energy expenditure (REE) was calculated. For BIA measurements, a signal electrode as well as a measurement electrode were attached at each hand and foot and connected to the BIA device (AKERN BIA 101 system, SMT medical, Würzburg, Germany). FM and FMM were calculated using the proprietary software (BodyComposition, MEDI CAL HealthCare GmbH, Karlsruhe, Germany).

6.3.3 Clinical assessments

Prior to the experiment, three standard clinical assessments were conducted to gather information on the NLI, the severity of the lesion, and the independence of the SCI subjects. The ISNCSCI protocol was used to assess the NLI as well as the completeness of the lesion (Kirshblum et al., 2011). The Spinal Cord Independence Measure III (SCIM III) was used to assess the level of independence in daily life (Catz and Itzkovich, 2007), and the Graded Redefined Assessment of Strength, Sensibility and Prehension (GRASSP) was used to capture motor and sensory function and functional task performance of the upper extremities. As the GRASSP assesses sensation, strength, qualitative and quantitative grasping through a series of five examinations, the total score and the individual sub-scores of the five examinations were later included separately in the analysis (Kalsi-Ryan et al., 2012a, Kalsi-Ryan et al., 2012b).

6.3.4 Tasks

Each subject had to perform 12 different physical activities out of a set of 24 possible activities. These activities were divided into three activity classes based on measured EE, subjectively perceived exertion, and the amount of distance travelled. The “low-intensity” activity class included the following activities: rest (lying on a bed), watching TV, reading, doing crossword puzzles, playing cards, riding an elevator, playing with a tablet PC, writing, computer work, and passive wheeling (i.e. when the wheelchair was pushed by someone else). The “high intensity” class included the following activities: washing dishes, hanging out the laundry, using a handbike ergometer (30W), playing table tennis, and weight lifting. The last class was called “wheeling” and included activities involving wheelchair self-propulsion. These activities included completing a wheelchair skill parcour (including a slalom with nine cones, four curbs of 3-8cm height, and a ramp with an inclination of 8%), wheeling at different speeds (2km/h, 3.5km/h, 5km/h, 6.5km/h and self-chosen), wheeling uphill (inclination 2.6%), wheeling downhill (inclination 2.6%), and wheeling on a wheelchair ergometer.

Table 6-1: Demographics and assessment scores of the included participants.

Variables	Values
No of participants	30
Sex	
Male	27
Female	3
Age (years)	45.0 ± 11.4
Weight (kg)	74.3 ± 17.1
Height (m)	1.76 ± 0.09
Injury level	
C3 - C8	11
T1 - L1	19
AIS score	
A	17
B	7
C	3
D	3
Reported hours of sport/week	2.5 ± 2.9

6.3.5 Protocol

Participants came to the Balgrist University Hospital for a single session of approximately five hours in the morning after an overnight fast of at least ten hours. First, participants were informed about the experimental procedure, and the twelve pseudo-randomly selected tasks were explained in detail. Subsequently, body composition was assessed by use of BIA, height was measured while the subject was lying on the bed, and weight was measured with a wheelchair scale. Participants were equipped with one sensor module at each wrist, one module was fixed at the chest (approximately at the sternum) and an additional module was fixed to one wheel of the wheelchair. Thereafter, the sensor modules were time-synchronized with the camera, the indirect calorimeter, and the heart rate monitor.

The first part of the experiment consisted of 20min of rest, lying on a bed for assessment of REE, followed by a standardized breakfast equivalent to 30% of a participant's calculated daily EE. The second part of the experiment started at least 90min after the end of breakfast, when EE had returned to baseline values. First, participants lay on a bad for 20min. This was considered the REE measurement under the non-fasted condition (first task). Subsequently, participants performed eleven 8-min tasks, selected pseudo-randomly from the set of 24 tasks, with a minimum of 5min between two consecutive

tasks. The pseudo-random selection ensured that at least two tasks from each activity class were selected and that each task was performed approximately equally often across all subjects. The 8-min activities were ordered according to the expected intensity of the tasks, starting with the least intense task. After each task, subjects were asked to rate their perceived exertion on an 11-point numeric rating scale (0 = “no exertion”, 10 = “maximum exertion”).

Video recordings were taken during the entire experiment (GoPro Hero HD 2, Go Pro Inc., San Mateo, CA, USA) in order to verify all activities retrospectively. In case subjects were unable to start the experiment in the morning, a shortened version of the protocol was provided, i.e. subjects came to the clinic at least two hours after the last food intake. After explanation of the study and signing the consent form, the experiment started with the assessment of body composition, height and weight, followed by 20min of REE measurement in the non-fasted condition. Afterwards, subjects followed the same protocol as described above.

6.3.6 Data analysis

The complete data processing, statistical analysis, as well as the training of the k-nearest neighbours (kNN) classifier and artificial neural networks (ANNs) were performed using MATLAB 2014a (The MathWorks, Natick, MA, USA). All processing steps were conducted offline.

In total, four different algorithms were designed, evaluated and compared against algorithms described in the literature (Figure 6-2). The first algorithm is of low complexity, which requires only limited computational power and could therefore be implemented directly on an activity tracker for on-line analysis and subject feedback. This algorithm consists of a multi-linear regression (MLR) model which uses different statistical features derived from the IMU data and previously estimated REE as predictors. The second algorithm is a more complex approach requiring more computational power. The algorithm consists of an ANN using features derived from the sensor data and the estimated REE as predictors. The third (MLR based with prior classification) and fourth (ANN based with prior classification)

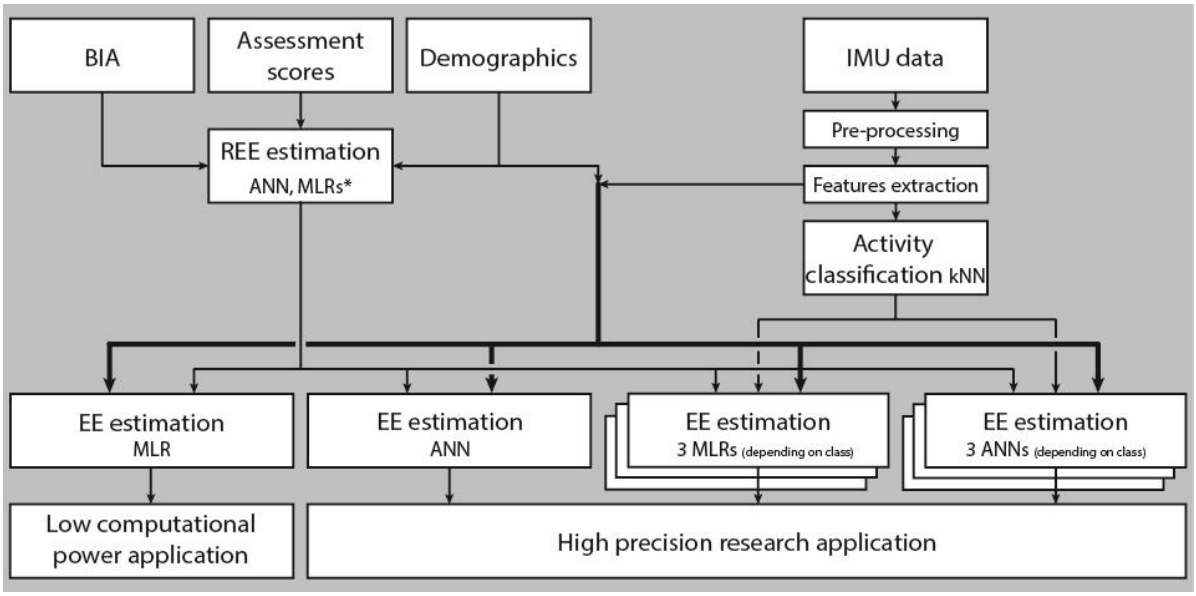

Figure 6-2: Flow chart summarizing the different evaluated algorithms. The first algorithm consists of a multiple linear regression (MLR) model, the second algorithm consists of an artificial neural network (ANN), the third algorithm consists of a k-nearest neighbour (kNN) classifier in combination with different MLRs, and the forth algorithm consist of a kNN classifier in combination with different ANNs. All algorithms are based on features derived from IMU data and on previously estimated REE.

algorithms are motivated by the work of Staudenmayer and colleagues (Staudenmayer et al., 2009). This group showed that prior classification into different activity classes before the EE estimation increases the estimation accuracy significantly. Therefore, the third and fourth algorithms consist of three parts. In the first part, the REE is estimated from demographic data; in the second part the different activities are classified into the three activity classes; in the third part, the EE is estimated using different MLRs or ANNs, respectively, for each of the classes. All processing steps are explained in the following paragraph.

Pre-processing: In order to ensure that all IMU data consisted of the same number of samples and that they were temporally aligned, the recordings from the ReSense modules were resampled at 50Hz using a cubic spline interpolation function. Afterwards, IMU recordings were synchronized with the OxyconMobile data and the video recordings, using time stamps, which were aligned at the beginning of the experiment. The acceleration signals were filtered using a 2nd order Butterworth high-pass filer with a cut-off frequency of 0.25Hz in order to remove the static acceleration component due to gravity. Gyroscope data were filtered with the same high-pass filter. The altitude data was filtered using a 2nd order Butterworth low-pass filter with a cut-off frequency 0.2 Hz.

Labelling and segmentation: Data were labelled using temporal markers from the OxyconMobile, the IMU modules, and from the video recordings. For the REE measurements, the mean of a four-minute window (minutes 14-18) was taken. For each of the individual activities, the last four minutes of each activity were segmented in windows of one minute without overlap. Taking the last four minutes ensured that the EE had reached a steady state. After visual inspection of the data, 1324 windows remained, which were later included in the development of the different models. As HR data was partly missing for some subjects, all analysis involving the HR was only based on 897 windows (67.8%).

Feature calculation: Features were calculated from the processed acceleration signal containing the dynamic component, from the gyroscope data and the altitude signal for each window. All statistical features derived from the accelerometer and gyroscope data were calculated from the respective magnitudes in order to ensure that the orientation of the sensors, and therefore in which orientation the sensor is placed, had no influence on the final algorithm. Statistical features derived from the sensor data were based on previously used features in activity classification studies (Karantonis et al., 2006b, Curone et al., 2010b, Maurer et al., 2006, Bouten et al., 1997b, Ravi et al., 2005, Herren et al., 1999, Baek et al., 2004b, Bao and Intille, 2004a, Stikic et al., 2008a, Leuenberger et al., 2014, Moncada-Torres et al., 2014). Only features from the time domain were taken for further analysis as we have shown that in "real world" applications, frequency domain features usually do not provide useful information (Popp et al., 2016a). In addition, some high level features were included: activity counts (AC) (Leuenberger et al., 2016), total distance travelled and distance travelled actively (Popp et al., 2016a), altitude difference within one epoch, altitude variance within one epoch, and time above acceleration magnitude threshold (empirically chosen). In order to test whether the inclusion of HR improves the overall accuracy of EE estimation, as shown by Nightingale and colleagues (Nightingale et al., 2015), mean HR, resting HR and the difference between mean HR and resting HR were included as additional features. Finally, features extracted from demographics as well as from clinical assessments were included, namely age, height, weight, gender, AIS score (A = 4, D = 1), injury level (C1 = 1, L5 = 25), GRASSP sub-scores and SCIM sub-scores.

REE estimation: Five different multiple linear regression (MLR) models were developed for the estimation of the REE. The different MLR models have all the following basic form:

$$REE = \alpha + \sum_{i=1}^{n} \beta_i \cdot F_i \qquad (6.1)$$

with α representing the intercept, and β_i representing the regression coefficient of the feature F_i. All MLR models included the independent variables height, weight, age and gender. In addition, different clinical scores were also included as independent variables, namely total SCIM III score, completeness, NLI, AIS score, and motor score of the ISNCSCI assessment. The MLR was computed by minimizing the sum of squared relative errors according to the method described by Tofalis (Tofallis, 2009). Moreover, ANNs based on the same features were trained in order to reveal more complex and non-linear relationships. Readers not familiar with ANNs can refer to the work of Basheer and Hajmeer (Basheer and Hajmeer, 2000). As one hidden layer is usually sufficient in most applications, all ANNs had a single hidden layer with five sigmoid neurons (Basheer and Hajmeer, 2000). The initial weights were chosen by the Nguyen-Widrow layer initialization function and the Levenberg-Marquardt backpropagation algorithm was used to train the ANNs (Hagan and Menhaj, 1994, Nguyen and Widrow, 1990). As the actual output can vary depending on the initial weights, 100 ANNs were trained per iteration and the mean outcome was used for further analysis. The performance was analyzed using the leave-one-subject cross-validation, resulting in 30 iterations. The MAE in percent was chosen as criterion for the MLRs and ANNs. A detailed overview of the models and features included in this study can be found in Table 6-2. In addition to the REE estimation models described above, three well established estimation models, which have been developed for the able-bodied population, were evaluated with the data from this study: the Harris-Benedict equation, the updated Harris-Benedict equation and the Mifflin-St. Jeor equation (Mifflin et al., 1990, Harris and Benedict, 1918, Roza and Shizgal, 1984). Finally, the REE was also estimated from the BIA measurement using the BIA software BodyComposition Professional (Medi Cal HealthCare GmbH, Karlsruhe, Germany).

Activity classification: In order to classify the different windows into one of the previously described activity categories “low-intensity”, “high-intensity” and “wheeling”, a kNN classifier with k=10 and a squared inverse distance weight was used. A total of n=1384 windows were used to train the kNN

classifier. Three features were selected for the kNN classifier, namely the AC of the wheel sensor as well as the root mean square (RMS, right wrist) and the median (left wrist) of the angular velocity magnitude. Among all feature combinations, the combination with these three features showed the best classification accuracy. In order to evaluate the performance of the kNN classifier, the leave-one-subject-out cross-validation method was used for the analysis. This resulted in a total of 30 iterations, one per subject. The percentage of correct classified windows was taken as a criterion to optimize the classifier.

EE estimation: In total four different estimation models were designed for the activity dependent EE not including the HR. An MLR model and an ANN model were designed where the activity-dependent EE was estimated using IMU data and the estimated REE as predictors. In order to see if a prior classification into different activity classes increases the estimation accuracy, additional MLR and ANN based models were designed. Thereby each activity class had a separate MLR or ANN estimation model. In order to see how the classification accuracy of the previously mentioned kNN classifier influences the final EE estimation, the MLR and ANN models with prior activity classification were evaluated i) assuming 100% correct classification and ii) with the classes estimated by the kNN classifier. Similar to the REE estimation using MLR, the MLRs for the activity-depended EE estimation were computed using the sum of squared relative errors (Tofallis, 2009). The MLR model without prior classification used seven predictors in total (right wrist IMU: mean acceleration magnitude, kurtosis of the angular velocity magnitude, altitude difference; left wrist IMU: root mean square of the acceleration magnitude; chest IMU: root mean square of the angular velocity magnitude; wheel IMU: variance of the angular velocity magnitude; REE). The MLR model with previous classification used for the MLR of the "low-intensity" class the same features as predictors as mentioned before, the "wheeling" class used one predictor less, specifically, the root mean square of the acceleration magnitude of the left wrist IMU. The "high intensity" class used slightly different features as predictors (right wrist IMU: altitude difference; left wrist IMU: root mean square of the acceleration magnitude; chest IMU: median of the acceleration magnitude, root mean square of the angular velocity magnitude; wheel IMU: kurtosis of the acceleration magnitude, variance of the angular velocity magnitude; REE). The ANNs trained for the estimation of the activity-dependent EE had the same design as the ANNs trained for the REE

estimation. This means that all ANNs had one hidden layer with five sigmoid neurons. The Nguyen-Widrow layer initialization function was used to choose the initial weights and the Levenberg-Marquardt backpropagation algorithm was used to train the ANNs. Here again, 100 ANNs were trained per excluded subject and the mean outcome was used for further analysis. The ANN without prior activity classification used six features as input, namely the mean acceleration magnitude (right wrist IMU), the activity counts (left wrist IMU), activity counts (chest IMU), altitude difference (chest IMU), distance travelled, and REE. The ANN model with prior activity classification had different features as inputs for every ANN. The ANN for the activity class "low intensity" had seven inputs, namely the mean acceleration magnitude (right wrist IMU), kurtosis of the angular velocity magnitude (right wrist IMU), altitude difference (right wrist IMU), root mean square of the angular velocity magnitude (chest IMU), weight, gender, and estimated REE. The ANN for the "high intensity" class used five features as input, namely the activity counts (right wrist IMU), mean acceleration magnitude (left wrist IMU), mean angular velocity magnitude (chest IMU), activity counts (left wrist), and estimated REE. The ANN for the "wheeling" class had six inputs: root mean square of the acceleration magnitude (right wrist IMU and left wrist IMU), activity counts (chest IMU), mean angular velocity magnitude (wheel IMU), activity counts (left wrist), and estimated REE. In order to test if the inclusion of HR improves the estimation, all models (MLR and ANN based) with prior activity classification were trained again but this time including the difference between measured HR and resting HR as additional predictor. Note that only 897 windows were available for the training of the models including HR. All developed models (MLR, ANN, with and without HR) were evaluated using the leave-one-subject-out cross-validation method. This resulted in a total of 30 iterations for each developed model.

Establishing reference values for a healthy lifestyle: For a healthy lifestyle, different reference values exist for the able-bodied population. The most well-known reference value for a healthy lifestyle is probably the 10'000 steps a day reference (equivalent 300kcal/day (Choi et al., 2007, Hatano, 1993)). However, this reference value is controversial and other research groups and institutions have proposed lower daily step-goals (Tudor-Locke and Bassett Jr, 2004). Furthermore, other activity goals, which are not directly related to the number of steps, have been proposed.

The U.S. Department of Health and Human Services for example, suggests 150 min of moderate physical activity per week (e.g. 5x30 min) or 75 min of vigorous physical activity per week (U.S. Department of Health and Human Services 2008). This is similar to what the American College of Sport Medicine (ACSM) suggested in their updated recommendations from 2007, where 30 min of moderate physical activity on five days a week or 20min of vigorous physical activity on 3 days per week is suggested to promote a healthy lifestyle (Haskell et al., 2007). Blair and colleagues stated in their work, that 30min of moderate intensity activity per day provides substantial benefits, but 60 min of moderate intensity activities per day would be ideal (Blair et al., 2004). These 60min of moderate (to vigorous) activity per day are also what is recommended by Wilson and colleagues in order to prevent weight gain (Wilson et al., 2010). 60 min of moderate to vigorous activity per day results in an increase in energy expenditure by 150-200 kcal/day. In order to establish values for a healthy lifestyle in the wheelchair bound SCI population, we therefore investigated which daily distance travelled in wheelchair would result in 150 kcal/day, 200kcal/day, and 300 kcal/day. In order to translate this recommendation for a healthy lifestyle into a daily distance to travel by wheelchair, the daily average speed has to be taken into consideration. Since the average wheeling speed in the SCI population was reported to be 1.7-2.3 km/h (Oyster et al., 2011, Sonenblum et al., 2012b), the EE measured in the wheeling task at 2km/h was used. On the other hand, there are recommendations based on time spent in activities of moderate (to vigorous) intensity. Therefore, we estimated the distance to travel and the corresponding EE based on the recommendation corresponding to 30min and 60min of wheeling at moderate intensity.

Performance analysis & statistics: The performance of the REE and EE estimation models were analyzed in terms of MAE in percent and mean signed error (MSE) in percent. The performance of the kNN classifier was analyzed using overall classification accuracy in percent and in addition the sensitivity of the different classes was computed (Popp et al., 2016a). In order to compare different activities, the metabolic equivalent of task (MET) was calculated using an adapted formula for the SCI population (Collins et al., 2010), where 1 SCI MET is equivalent to 2.7 mL O2·kg-1·min-1 in contrast to the formula for the able-bodied population, where 1 MET is equivalent to 3.5 mL O2·kg-1·min-1 (Ainsworth et al., 2011). In order to demonstrate the relationship between measured SCI MET and

perceived exertion (numeric rating scale), a Spearman rank correlation was used. The significance level for all statistical analyses was set to $p=0.05$.

6.4 Results

An overview of all REE estimation models is presented in Table 6-2. The estimates are compared in terms of MAE, MSE and maximal error. Both Harris-Benedict equations as well as the ANN with height, weight, age, gender and total SCIM III score performed best in terms of MAE (14.2%). Generally, all models overestimated the REE, which is reflected in the positive MSE. Only the estimation with the BIA, the Mifflin-St. Jeor equation and the MLR model including height, weight, age, gender and total SCIM III score showed an underestimation of the true EE value. The MAE in percent for men was always lower than the MAE for women, except for the BIA estimation where an MAE for men of 24.0 ± 11.5 % and MAE for women of 17.8 ± 19.2 % were found. By way of comparison, the MAE resulting from the updated Harris-Benedict equation was 13.0 ± 7.2 % for men and 25.0 ± 7.2 % for women.

Activity classification: The overall classification accuracy of the kNN classifier was 97.9%. An overview of the classification accuracy of each individual activity class can be found in Figure 6-3 B. In addition, a 3D scatter plot (Figure 6-3 A) and two 2D scatter plots (Figure 6-3 C&D) are presented in order to visualize the separation of the different activity classes. The sensitivity for the individual activities was generally high, with a range of 81.8-100% and a median of 100%.

Activity-dependent EE: ANN and MLR models were based on a total of 1324 windows. An overview of the EE estimation accuracy of all models can be found in Table 6-3. Overall, the ANN model where the activity was previously classified into classes by the kNN classifier showed the lowest overall MAE for the EE estimation with 14.4±5.3 % (Figure 6-4). The MAE of the different activity classes for the previously mentioned EE estimation model was 11.8±6.1% for the “low intensity” class, 19.2±11.7% for the “high intensity” class, and 14.4±6.8% for the “wheeling” class. Assuming a classification accuracy of 100% (ANN class known) for the kNN classifier, this would only result in a marginally better overall MAE (14.1±5.4%) for the EE estimation. The MAE for the different activity classes was 11.8±6.0 for the “low intensity” class, 17.6±11.7% for the “high intensity” class, and 14.2±6.9% for the “wheeling” class. The MLR model (with prior kNN classification) profited from the inclusion of the HR. The overall MAE for the EE estimation improved from 16.0±6.2% to 14.9±4.8% when including

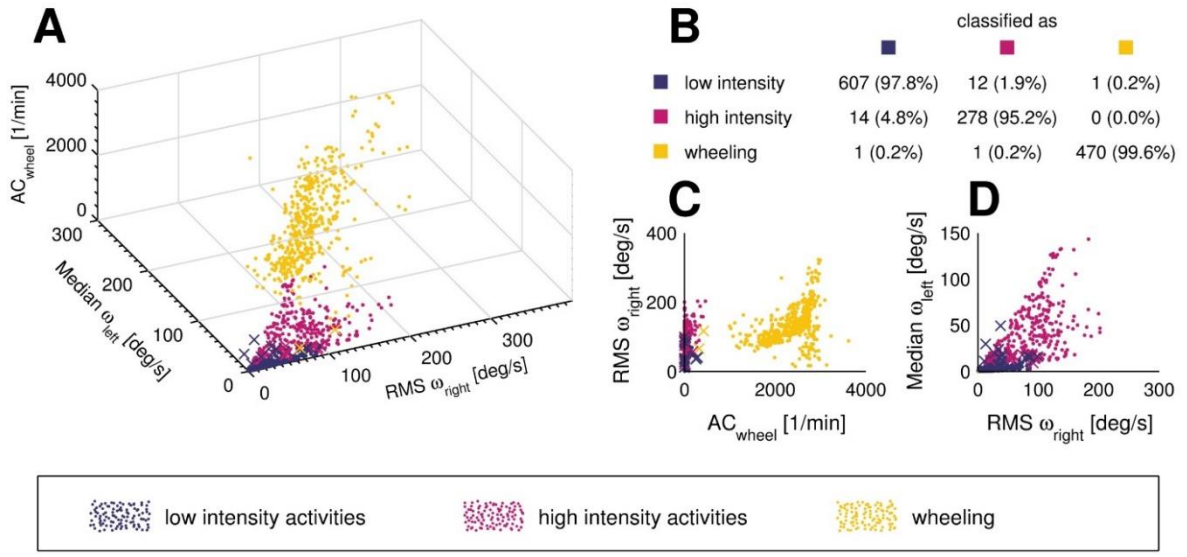

Figure 6-3: 3D scatter plot of the different activity classes for the three features used (A). A point represents a correct prediction and a cross a false prediction. In addition, the confusion matrix for the entire data set (n=1384 windows) is represented in subplot B. The overall classification accuracy was 97.92%. In order to illustrate how the different activity classes can be separated, two additional projections of the 3D scatter plot are presented (C,D).

the HR. The MAE for the different classes was 13.7±6.8% without HR and 13.8±6.1% with HR for the "low intensity" class, 19.0±10.7% without HR and 17.4±9.4% with HR for the "high intensity" class, and 17.9±9.3% without HR and 17.2±10.9% with HR for the "wheeling" class. In contrast to the MLR model, the ANN model (with prior kNN classification) did not benefit from the inclusion of the HR. The overall MAE for the EE estimation with the ANN model was 12.9±4.7% without HR and 13.6±5.4% with inclusion of the HR. Looking at different classes showed that the MAE was 10.8±5.9% without HR and 12.3±6.9% with HR for the "low intensity" class, 18.6±13.2% without HR and 17.3±9.8% with HR for the "high intensity" class, and 14.2±8.6% without HR and 15.1±12.2% with HR for the "wheeling" class.

The evaluation of the two 2.5h-measurements to validate the algorithm under real-world conditions is shown in Figure 6-5. For subject #1, the real EE was underestimated by 23.24 kcal (6.07%) while for subject #2, the real value was overestimated by 12.19 kcal (4.57%).

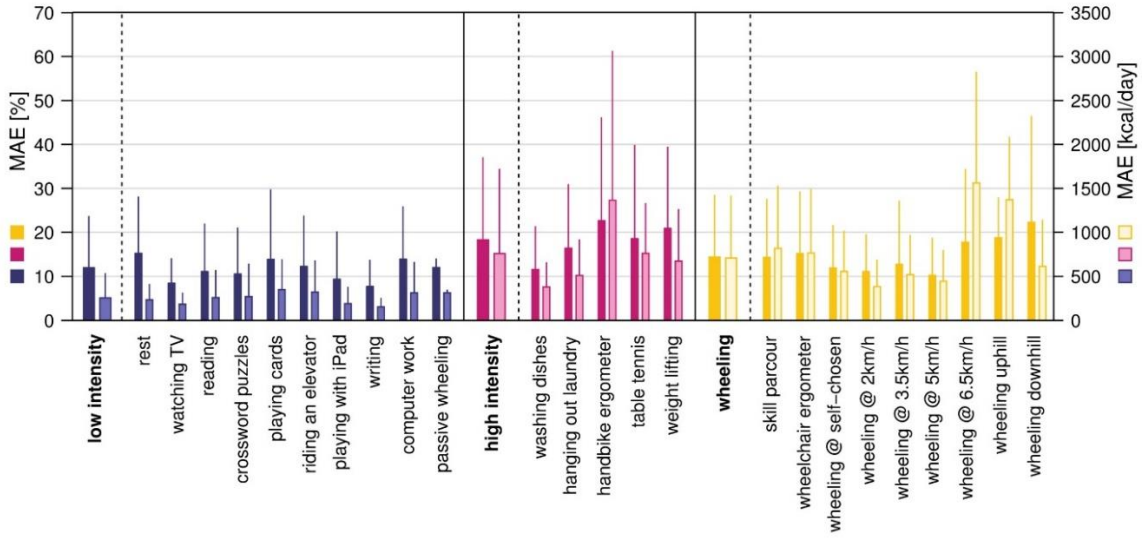

Figure 6-4: Mean absolute error (MAE) for the EE estimation using the ANN model with prior activity classification. The overall MAE was 14.4±5.3%. The MAE in percent for the single activities and classes is presented in dark colours and the MAE in kcal is presented in bright colours.

Energy cost of physical activities: The metabolic cost of each single activity and the three activity classes is presented in Figure 6-6. The mean SCI MET for the "low-intensity" class was 1.60 ± 0.50 and all activities were below 2 SCI MET, which is considered as light intensity activity (Pate et al., 1995). The mean SCI MET for the "high-intensity" class was 3.24 ± 1.45 and three activities of this class are considered as light intensity activities and two as moderate intensity activities. For the "wheeling" class the mean SCI MET was 3.78 ± 1.62 and, according to Pate and co-workers, two activities would be classified as light intensity activities, six as moderate intensity activities, and one as vigorous intensity activity (Pate et al., 1995). In order to show the relationship between measured SCI MET and perceived exertion, a correlation ($R=0.73$, $p<0.001$) is presented in Figure 6-7.

Recommendations of healthy lifestyle: The conversion of the recommendations for a healthy lifestyle in the able-bodied population to daily goals in the wheelchair-bound SCI population can be found in Table 6-4.

Table 6-2: Results of the REE estimation based on BIA measurement, models known from the literature (°), and MLR and ANN models developed in this study.

	Mean absolute error				Mean signed error		Max error	
Model description	[%]	[kcal/day]	tetraplegic [%]	paraplegic [%]	[%]	[kcal/day]	[%]	kcal
BIA*	23.3 ± 12.2	409.7 ± 255.7	23.5 ± 12.2	23.2 ± 12.5	-22.5 ± 13.7	-400.7 ± 270.2	48.3	956.1
Harris-Benedic°	14.2 ± 7.9	229.8 ± 129.1	13.9 ± 7.9	14.5 ± 8.2	1.9 ± 16.4	0.5 ± 267.1	26.7	528.2
updated Harris-Benedict°	14.2 ± 7.8	227.8 ± 123.1	13.5 ± 7.4	14.6 ± 8.2	2.3 ± 16.3	7.0 ± 262.4	25.9	511.4
Mifflin-St.Jeor°	15.1 ± 11.8	256.1 ± 204.9	16.7 ± 12.8	14.1 ± 11.4	-8.1 ± 17.5	-169.5 ± 283.1	34.6	648.8
Multiple linear regression								
h, w, a, g	15.7 ± 12.0	250.3 ± 182.6	15.0 ± 8.6	16.1 ± 13.8	1.3 ± 19.9	63.3 ± 306.7	48.7	810.5
h, w, a, g, SCIM III	16.6 ± 15.5	262.4 ± 227.6	13.2 ± 8.0	18.7 ± 18.5	-0.4 ± 22.9	37.7 ± 348.8	67.8	933.3
h, w, a, g, AIS	16.3 ± 11.3	261.5 ± 175.1	16.2 ± 7.1	16.3 ± 13.5	1.2 ± 20.0	63.2 ± 312.0	48.5	807.3
h, w, a, g, NLI	16.4 ± 11.5	264.2 ± 175.7	15.1 ± 8.4	17.2 ± 13.2	0.9 ± 20.3	57.9 ± 315.7	48.9	814.4
h, w, a, g, motor score	16.6 ± 12.7	264.1 ± 190.8	16.0 ± 9.3	16.9 ± 14.6	1.2 ± 21.0	64.9 ± 322.9	49.2	818.2
Artificial neural network								
h, w, a, g	16.2 ± 12.2	248.9 ± 156.5	14.3 ± 8.3	17.4 ± 14.1	2.7 ± 20.4	-6.6 ± 297.7	32.2	535.7
h, w, a, g, SCIM III	14.2 ± 12.2	215.7 ± 160.0	10.0 ± 5.8	16.7 ± 14.4	2.8 ± 18.7	4.2 ± 271.5	39.7	660.4
h, w, a, g, AIS	17.0 ± 11.0	263.0 ± 137.6	15.4 ± 7.4	18.0 ± 12.9	2.4 ± 20.4	-12.6 ± 300.6	49.7	528.5
h, w, a, g, NLI	16.6 ± 11.0	256.5 ± 136.5	14.6 ± 6.9	17.9 ± 12.9	2.7 ± 20.0	-5.8 ± 294.5	33.3	554.3
h, w, a, g, motor score	15.8 ± 12.3	240.1 ± 155.0	12.2 ± 8.4	17.9 ± 14.0	2.9 ± 20.0	-1.2 ± 289.4	54.4	579.0
h, w, a, g, AIS, NLI	17.4 ± 11.7	266.8 ± 140.5	14.4 ± 8.2	19.2 ± 13.2	2.9 ± 21.0	-5.7 ± 305.6	52.3	557.0

h = height, w = weight, a = age, g = gender, * For the REE estimation based on the BIA measurement only N=28 subjects were included.

Table 6-3: Evaluation of the different models developed as a part of this study. The analysis including the HR was based only on N=897 windows.

	Mean absolute error				Mean signed error		Max error	
Model description	[%]	[kcal/day]	tetraplegic [%]	paraplegic [%]	[%]	[kcal/day]	[%]	kcal
N = 1324								
MLR general	15.3 ± 4.8	592.7 ± 270.9	16.4 ± 4.7	14.6 ± 4.9	-2.9 ± 11.1	-266.2 ± 444.4	27.3	1180.1
MLR class known	15.0 ± 4.7	579.2 ± 255.1	15.9 ± 4.2	14.5 ± 5.1	-2.5 ± 10.5	-233.0 ± 416.7	25.7	1103.8
MLR class estimated	15.2 ± 4.7	584.0 ± 253.6	16.3 ± 4.0	14.5 ± 5.0	-2.5 ± 10.5	-235.0 ± 415.4	25.8	1108.9
ANN general	17.3 ± 6.8	606.5 ± 225.1	18.2 ± 6.6	16.8 ± 7.1	5.4 ± 13.4	20.3 ± 489.9	26.8	1118.0
ANN class known	14.1 ± 5.4	513.6 ± 201.3	14.9 ± 4.7	13.6 ± 5.8	3.3 ± 9.8	2.9 ± 379.8	23.9	980.0
ANN class estimated	14.4 ± 5.3	524.7 ± 205.2	15.5 ± 4.7	13.8 ± 5.7	3.5 ± 9.9	-1.3 ± 384.4	24.4	1011.6
N = 897 (HR analysis)								
MLR class estimated	16.0 ± 6.2	576.9 ± 281.6	16.9 ± 4.7	15.6 ± 7.0	2.9 ± 12.6	-221.8 ± 437.9	35.3	1406.9
MLR class estimated with HR	14.9 ± 4.8	513.9 ± 193.5	16.4 ± 4.5	14.1 ± 4.8	-1.8 ± 12.3	-154.2 ± 426.2	24.6	961.0
ANN class estimated	12.9 ± 4.7	419 ± 141.4	12.8 ± 3.1	12.9 ± 5.4	3.4 ± 8.2	35.1 ± 284.6	19.4	659.7
ANN class estimated with HR	13.6 ± 5.4	445.8 ± 160.7	14.5 ± 5.5	13.0 ± 5.5	3.0 ± 10.2	14.6 ± 336.4	23.0	816

Table 6-4: Recommendation for the able-bodied population translated to the distance to travel for the SCI population or the EE spent during moderate activity. * The activities used for this recommendation cannot always be classified as an activity of moderate intensity.

Recommendation	Reference	EE [kcal]	Speed [km/h]	REE measured [kcal/day]	EE measured [kcal/day]	Extra EE measured [kcal/day]	Distance [km]	Time needed [min]
10'000 steps/day	1	300	2.0	1650	3430	1780	***8.1***	***243***
150 kcal of additional EE	2	150	2.0	1650	3430	1780	***4.0***	***121***
200 kcal of additional EE	2	200	2.0	1650	3430	1780	***5.4***	***162***
30 min of moderate activity	3	***54***	3.5	1644	4255	2611	***1.8***	30
"	3	***61***	5.0	1559	4502	2943	***2.5***	30
60 min of moderate activity	4	***109***	3.5	1644	4255	2611	***3.5***	60
"	4	***123***	5.0	1559	4502	2943	***5.0***	60
Recommendations based on this study (following ASCM recommendation)		**74**	**5.0**	**1559**	**4502**	**2943**	***3.0***	**36**
		74	**5.0**	**1559**	**4502**	**2943**	***6.0***	**72**
	*	**92**	**3.5**	**1644**	**4255**	**2611**	***3.0***	**51**
	*	**111**	**2.0**	**1650**	**3430**	**1780**	***3.0***	**90**

1 (Choi et al., 2007, Hatano, 1993), 2 (Wilson et al., 2010, Perret et al., 2010), 3 (Blair et al., 2004), 4 (Blair et al., 2004)

6.5 Discussion

The main aim of this study was to develop and validate an algorithm for estimating EE from IMU data applicable in a real-world situation in individuals with SCI. We present a highly accurate method to estimate ADL-dependent EE from IMU recordings. Most importantly, we provide reference values for wheelchair-bound SCI subjects to promote and coach a healthy lifestyle, which could be beneficial for reducing the risk of cardiovascular diseases.

REE reflects the energy used to maintain vital functions at room temperature. To account for its large contribution (approximately 65% in the able-bodied population (Buchholz and Pencharz, 2004)) to total daily energy expenditure, it was deemed important to accurately estimate the REE. Also, at a later stage, the estimated REE was used as predictor for the activity-dependent EE estimation models. As expected, the BIA-based model showed the worst REE estimation in terms of MAE, MSE, and maximum error, and is generally known to be very population specific (Lee and Gallagher, 2008). Therefore, a separate BIA estimation model for SCI would be required. The three well-established REE estimation equations, namely the Harris-Benedict equation, the updated Harris-Benedict equation, and the Mifflin-St. Jeor equation performed equally well. The MAE for REE estimation using the updated Harris-Benedict equation has been reported to be around 14% for the able-bodied population (Roza and Shizgal, 1984). This compares favourably to 14.2±7.9% for the SCI data in the present study.

Here, we also investigated whether and how REE estimation models could be improved by considering clinical scores. However, the inclusion of the AIS score did not improve the models and is likely too unspecific in describing the extent of impairment. Also, including the level of injury or the motor scores of the ISNCSCI did not improve the estimation accuracy significantly. The only clinical score improving the MAE of the REE estimation was the SCIM III total score, although it only improved the ANN-based model. In general, all REE estimation models that were developed in this study were based on the data of only 30 subjects. This number is clearly too small to build a general model for this heterogeneous population of SCI subjects. For this reason, subsequent analyses were performed using the updated Harris-Benedict equation for REE estimation.

In the able-bodied population, the type of activity performed by a subject was shown to be of great importance when establishing models to estimate EE (Staudenmayer et al., 2009). In order to obtain a generalizable EE estimation model, we chose to split the different activities into three broader activity classes. The overall classification accuracy of the kNN classifier was slightly better than previous comparable models developed for the SCI population, which can most likely be explained by the fact that we included only three activity classes, whereas Hiremath and co-workers included four and seven activity classes, respectively (Hiremath et al., 2013, Hiremath et al., 2015). The kNN classification has proven to be an appropriate approach for activity classification in the able-bodied population as well as in neurological conditions other than SCI (Bao and Intille, 2004a, Maurer et al., 2006, Moncada-Torres et al., 2014, Leuenberger et al., 2014). The performance of our kNN classifier was excellent, with an overall classification accuracy of 97.9%. The activity class "wheeling" had only 2 out of 472 misclassified events. Already a single feature, namely the activity counts of the wheel sensor, was enough to classify the aforementioned class (Figure 6-3 C). The "low intensity" and "high intensity" class had 13 and 14 misclassified events. In the "low intensity" class, the activity "playing cards" showed the overall worst sensitivity with 85.3%. This result can be explained by the fact that even if playing cards is considered as low intense activity, it can include extended periods of faster and more intense arm movements. However, in only 2 out of 24 activities, the presented kNN classifier had a sensitivity lower than 90%. Thus, the presented kNN classifier is accurate enough to be used for the activity classification of the final EE estimation algorithm. Furthermore, since the kNN classifier classifies activities into activity classes (i.e., groups of activities) and not into single activities, this approach may be generalizable to other activities and applications.

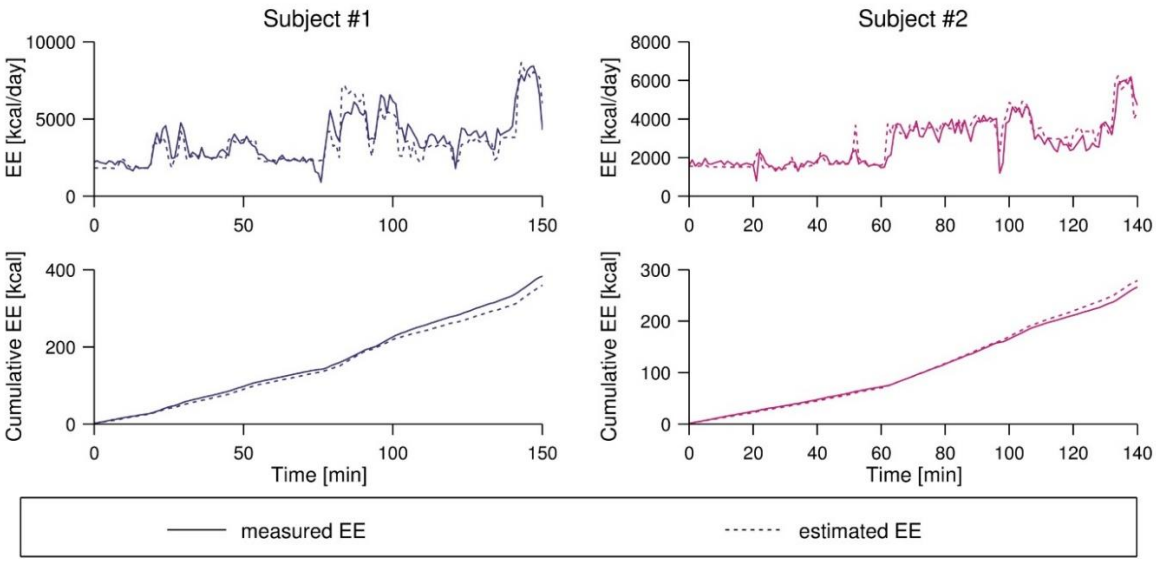

Figure 6-5: Pre-validation of two subjects using the class-dependent ANN algorithm. The two top plots show the measured EE from the indirect calorimetry and the estimate based on the IMU data, and the bottom plots show the cumulative value of the estimated and the measured EE value. At the end of the measurement period, the real EE was underestimated by 6.07% for subject #1 and overestimated by 4.57% for subject #2.

The MAE of the activity-dependent EE estimation ranged from 14.1% up to 17.3%, when the HR information was not included. However, we have to take into account that the model reaching a MAE of 14.1% assumed a perfect classification into the different activity classes. In general, the overall MAE is in the range of other accelerometer or IMU based models developed for the SCI population although those studies included fewer activities (Hiremath et al., 2012, Hiremath et al., 2013, Nightingale et al., 2015). Recently, Hiremath and coworkers presented an EE estimation model which was developed using recordings from 20 different activities, achieving a MAE of 25% (Hiremath et al., 2016). A possible explanation for the different results might be that Hiremath and coworkers used linear regression models, which do not account for non-linear relationships between accelerometer measurements and EE (Hiremath et al., 2016). MAE in the present study was always highest for the "high intensity" class, which can be explained by the fact that weight-loading activities, such as the handbike ergometer and weight lifting, have been included in this class. In fact, a similarly decreased estimation accuracy for activities with external load has already been reported previously in the able-bodied population (Swartz et al., 2000, Brage et al., 2004). In order to obtain the best EE estimate for each class, different features where used for the different classes. Interestingly, all models developed in this study, whether MLR or ANN based, included features derived from the accelerometer data as well as from the gyroscope data.

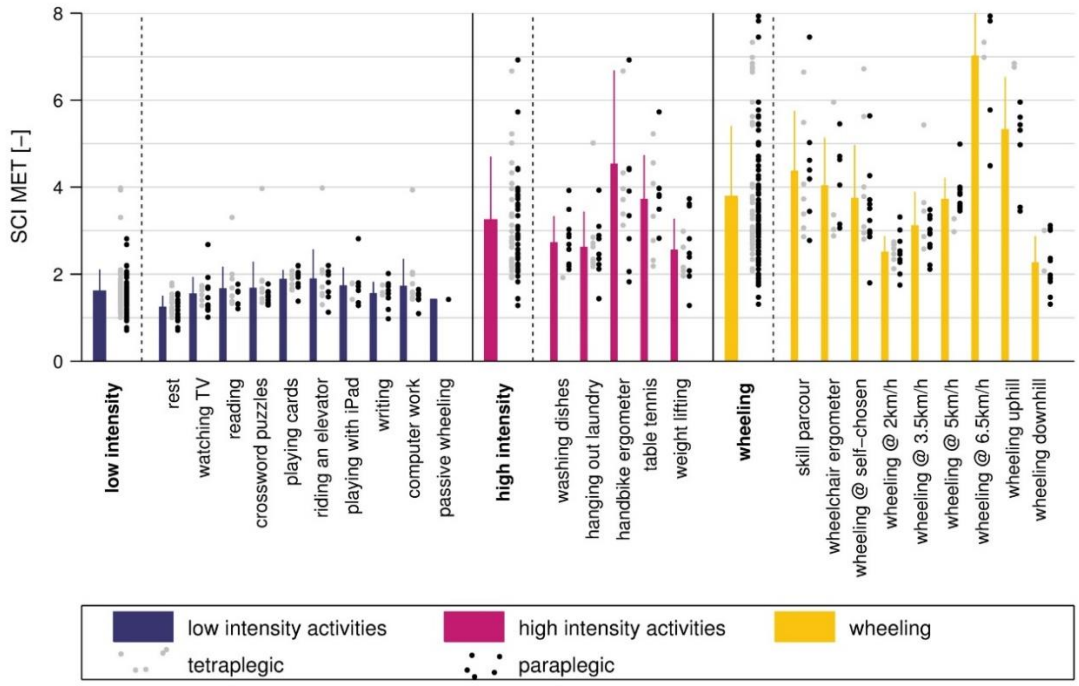

Figure 6-6: SCI MET presented for all activities and classes. The grey dots to the right of each bar represent the values for the tetraplegic subjects and the black dots the values for the paraplegic subjects. The bars represent the mean of the pooled data including paraplegic and tetraplegic subjects.

This is in contrast to what Moncada-Torres and co-workers have shown, where features derived from the gyroscope data did not provide useful information for activity classification (Moncada-Torres et al., 2014). This discrepancy can be explained by the fact that, in our study, the algorithms were used to estimate a continuous value of EE, while in the study by Moncada-Torres the algorithms were used to classify activities (Moncada-Torres et al., 2014). The inclusion of altimeter-based features in the final algorithm was not surprising, as it has already been shown that accelerometer and altimeter are a good combination to estimate EE in activities with altitude changes (Yamazaki et al., 2009). Two features based on demographic data were further included, namely weight and gender. These two features were only selected in the class-dependent model and only for the "low intensity" class. Again, the exclusion of features based on demographic data may be explained by the fact that they are already represented in other features, especially in the REE. The comparison between MLR and ANN-based models showed that the MLR based model performed better when no previous activity classification occurred, and the ANN-based model performed better for the class-dependent model.

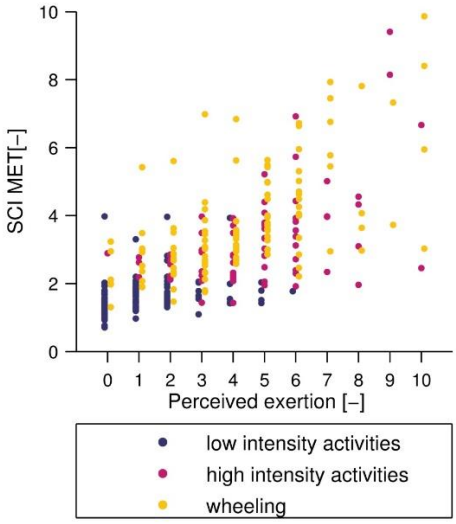

Figure 6-7: Correlation between perceived exertion, assessed with a numeric rating scale, and measured SCI MET. The correlation coefficient was R=0.73 (p<0.001).

The inclusion of the HR showed a slight improvement for the MLR-based model. Thereby, the overall estimation improvement comes mainly from the improvement in the "high intensity" class. This might be due to the fact that the addition of the HR can, to a certain extent, improve the EE estimate of weight loading activities. The validity of combining accelerometer and HR measurements in the SCI population to estimate EE by using linear models has already been shown by Nightingale and coworkers (Nightingale et al., 2015). Our non-linear approach based on the ANNs did not benefit from the inclusion of the HR, and the MAE increased when adding the HR as additional predictor. While the MAE decreased for the "high intensity" class, it increased slightly for the "wheeling" motion class and was negligible for the "low intensity "class. In fact, the change in HR might not necessarily result from a change in the intensity of an activity, especially in the "low intensity" class, as HR is known to be influenced also by emotion, stress or other factors which are most visible at rest and during low intensity exercise (Ainslie et al., 2003). During the assessments in the present study, activity-independent factors potentially influencing HR were minimized. Hence, the application of the ANN model with HR as additional feature would most likely result in even higher estimation errors under 'real-world' conditions. Therefore, we suggest using the class-dependent ANN model without HR for future applications.

Based on the insights from this study and existing literature for the able-bodied population, we seeked to propose activity-related recommendations for a healthy lifestyle in the SCI population. For subjects with SCI, activity recommendations were translated into daily distance travelled in a manual wheelchair. Since translations from able-bodied to SCI are based on the EE recordings of the present study, we assured that the different SCI MET values in the literature matched the SCI MET values of this study. Collins and co-workers investigated the metabolic cost of 27 different physical activities in 170 adults with SCI (Collins et al., 2010). Six activities, namely desk work, laundry, washing dishes, weight lifting, table tennis, and hand bike ergometer were also included in our study. The measured mean SCI MET of these activities was indeed in the same range as was reported previously, except for the hand bike ergometer activity, where mean SCI MET was 4.5 in the present study compared to values between 3.37 and 3.83 reported by Collins and co-workers (Collins et al., 2010). Possibly, this difference can be explained by differing angular velocities of the hand bike ergometer between the two studies. Further agreement between the SCI MET of this study and the literature can be found in the study of Hiremath and coworkers (Hiremath et al., 2016). For the four common activities of both studies, namely arm ergometry, deskwork, resting and propulsion, all activities were within one standard deviation of EE. In the work of Nightingale and co-workers the EE for the propulsion at different wheelchair speeds (on a treadmill) was reported (Nightingale et al., 2015). Although the data cannot be compared directly to the values of our study, due to different protocols, we can see a linear relationship between wheelchair speed and EE in both studies, when excluding the task of wheeling at a speed of 6.5km/h in our study. In conclusion, the SCI MET recorded in this study matches the values reported in the literature well. Therefore, we consider it a valid approach to use the measured EE of the present study for healthy lifestyle recommendations in the SCI population.

The most commonly used recommendation for an active lifestyle in the able-bodied population is the ASCM recommendation suggesting 30min of moderate to vigorous activity per day on at least 5 days per week. For the wheelchair-bound SCI population, the results of our study found wheeling at 3.5km/h or 5km/h to represent an activity of moderate intensity. In order to choose one of the two speeds for the translation of the ASCM recommendation, we further examined the EE at these two wheeling speeds. According to Wilson and co-workers (Wilson et al., 2010), 60min of moderate to vigorous activity per

day should result in approximately 150kcal of increased EE, and 30min of moderate to vigorous physical activity therefore corresponds to an additional 75kcal. Wheeling at 5km/h for 30min was closer to the desired 75kcal than wheeling at 3.5km/h. For this reason, we chose to use 5km/h for the translation of the ASCM guidelines to the wheelchair-bound SCI population. This translation would therefore result in a recommendation to travel a daily distance of approximately 3km at 5km/h in the wheelchair.

There exist, however, also other recommendations for the able-bodied population. For the translation of the 10'000 steps/day (roughly 300kcal/day) to a distance to travel per day in the wheelchair, we selected an average wheeling speed of 2km/h. This value was based on daily averages obtained from long-term recordings in the SCI population (Oyster et al., 2011, Sonenblum et al., 2012b). Based on these values, the recommendation for the SCI population would be to wheel for around 8km per day at this average speed. However, it is likely that this reference distance is far too high. First, the threshold of 10'000 steps/day is controversial in the able-bodied population, and some researchers have suggested lower thresholds for the able-bodied population. Second, the daily EE and the REE of an individual with SCI are lower than those of an able-bodied person, and therefore less than the additional 300 kcal/day (estimated for 10'000 steps) might be sufficient for a health-promoting effect. We further translated other activity recommendations for the able-bodied population such as an additional 150kcal per day and 200kcal per day spent in activities of moderate to vigorous intensity, into daily distance to travel in the wheelchair. As these recommendations are, however, not well established, we therefore did not consider them for our final recommendation.

Therefore, based on data of the present study we recommend to travel for at least 3km at 5km/h on 5 days a week in order to achieve a health-promoting additional daily EE. This recommendation is in line with the recommendations of the U.S. Department of Health and Human Services and the ACSM (U.S. Department of Health and Human Services 2008, Haskell et al., 2007). There are, however, wheelchair users who cannot achieve a wheeling speed of 5km/h and therefore cannot fulfill the proposed combination of extra calories and intensity. Nevertheless, these wheelchair users could try to reach the goal of 3km/day, first, because even at lower speeds they reach the recommended daily goal of additional

75kcal, and second, because 3km per day is more than what an average wheelchair user travels per day (around 2km (Oyster et al., 2011, Sonenblum et al., 2012b, Brogioli et al., 2016a, Brogioli et al., 2016b)).

While our recommendation aims at minimizing the risk for cardiovascular diseases, Blair and co-workers stated in their work that 60min instead of 30min of moderate to vigorous physical activity per day is beneficial for different health outcomes such as, for example, maintaining a lean body mass or improving muscular strength and endurance (Blair et al., 2004). In order to fulfill the 60min recommendation, our results can easily be extrapolated to a daily distance to travel of 6km/day.

We would like to acknowledge some limitations of this study. Firstly, the number of women included in this study (i.e. 3) may be considered too small (although it reflects a typical distribution in traumatic SCI) and, therefore, the sample measured may not be representative for the entire SCI population. Secondly, no individual HR calibration such as the method presented by Spurr and coworkers was used, which might have influenced the models including the HR (Spurr et al., 1988). The classification into different activity classes worked well for the activities included in this study, but a validation in a real-world setting is required. A further limitation of this study concerns the recommendations for a healthy lifestyle made for the SCI population. All values were translated from recommendations from the able-bodied population and it first has to be shown that those values should also be used in the SCI population. Finally, the REE models were based on 30 subjects only (equal to 30 data points), thus the inclusion of more subjects is needed to allow for the design of a more general estimation model.

6.6 Conclusion

The models presented in this study accurately estimate EE in an unprecedented pool of 24 activities and in 3 hours of continuous measurements in wheelchair-bound SCI individuals, making it a powerful tool to be used during continuous and non-obstructive recordings in real-world situations. IMU-based EE estimation is a promising methodology that may be used, together with the proposed wheeling reference value of 3km per day, to promote a healthy lifestyle in SCI individuals at later stages of and/or after rehabilitation. The use of such recordings and recommendations may help to increase physical activity of SCI individuals to an extent allowing to decrease the prevalence of cardiovascular disease and increase quality of life in the long run.

7 General Discussion and Outlook

7.1 Thesis contributions

Clinical assessments such as the FMA, SCIM, GRASSP, or BBT are commonly used in daily clinical routine to quantify the extent of sensorimotor impairment. In research these assessments are typically used to evaluate the effect of a certain intervention. Despite the benefits for clinicians as a tool for stratifying patients and tracking recovery over time, there are a number of major drawbacks of such assessments. They are often subjective and the outcomes are represented on an ordinal scale. Furthermore, such assessments lack sensitivity, and are merely snapshots inside the structured clinical environment (i.e. they measure capacity and not performance), and may not differentiate impairment from compensation (Kitago et al., 2012). Additionally, the capacity of force generation is usually only assessed in a static case, outside of any functional context. The ICF domain "performance" is typically covered by clinical questionnaires such as the FIM and the SCIM and is therefore not assessed in an objective way. Due to the large number of drawbacks, clinical assessments can only be used in a limited way in research. These limitations have, for example, been associated with the failure of showing efficacy of treatment in intervention studies (Duncan et al., 1992).

In order to track functional recovery, level of impairment and degree of compensation during rehabilitation sessions or activities of daily living (ADL), objective and sensitive assessment tools are needed. Theses assessments should on the one hand be able to better cover the ICF domain "capacity" by detecting even small changes in the level of function, and on the other hand cover the ICF domain "performance" in an objective way by tracking and quantifying physical activity over extended periods of time during rehabilitative training as well as outside of the therapy, both in the clinical and home environments. Novel sensing and robotics technologies have created new opportunities for the development of objective and sensitive assessments beyond what is possible with current clinical scales. In the context of this thesis, two new assessment methods based on novel technologies were introduced and evaluated.

The first assessment method is an advanced and detailed evaluation tool intended to measure finger and hand function in laboratory and clinical settings. This objective robot-assisted kinematic and kinetic assessment method allows deeper insights into neuromuscular control of movement and related dysfunctions, beyond what is possible with standard clinical assessments. The second assessment method presented in this thesis is a tool for research and clinical application in daily clinical routine as well as in the home environment, covering the ICF domain "performance". This assessment method is based on the analysis of data provided by wearable IMUs and allows continuous monitoring of physical activity of individuals with neurological injuries over an extended period of time, under natural environmental conditions in the clinic and at home.

These assessment concepts and algorithms were developed, validated and applied on people with specific neurological conditions (stroke and SCI) within this thesis. However, these methods can be adapted and applied to other neurological conditions.

7.1.1 Robotic tools to investigate the neural control of movement and isometric force production

The first part of this thesis aimed at developing a kinematic and kinetic assessment tool based on a robotic wrist manipulandum (ReFlex) for capacity assessment under laboratory settings. With the developed assessment tool, we investigated the interdependence of wrist and finger control in neurologically intact controls and transferred the knowledge to another platform in order to investigate how this control is affected and changed following stroke.

The robotic wrist manipulandum (Chapuis et al., 2010) was developed before the start of this thesis. Therefore the first part of this project consisted in optimizing the robot for a potential application as an assessment tool in neuroscience research. Different low-level interaction controllers used in the ReHapticKnob (Metzger et al., 2011) and the I-SUR platform (Manurung et al., in preparation) were implemented, tested and adapted in order to guarantee high safety and good haptic interaction quality. The next step was to optimize the ergonomic aspects of the interface between the human and the robot. This step was necessary as a non-ergonomic wrist interface could lead to awkward postures, increased

co-activation, formation of altered muscle activation patterns, or result in accelerated muscular fatigue or pain, thus representing a significant confound. Therefore, a study was conducted in which we investigated the effect of different handle designs (i.e. haptic interface) on performance, comfort, fatigue, pain and muscle activation patterns in a wrist flexion task (Popp et al., 2016b). In this study, no effect of any of the handles on task performance or on kinematic and kinetic parameters was found. However, increased levels of co-activation and altered muscle activation patterns were found for the joystick-like handle, which is typically used in robotic manipulanda (Masia et al., 2009, Suminski et al., 2007, Kadivar et al., 2012). In addition, the investigated handles differed in terms of perceived comfort and task difficulty. The findings of this study did not only influence the further design and therefore the optimization of the ReFlex robot, it also extended the general knowledge on how such a physical interface should be designed for robot-assisted rehabilitation, biomechanics and neuroscience research, and also has implications for teleoperation and gaming applications.

Following the improvement of the ergonomic aspects of the ReFlex, we conducted a first study where we investigated the interdependence of wrist and digit control under static conditions. Fifteen healthy subjects were asked to generate maximum precision grip force in different wrist postures and under two wrist stabilization conditions (self- and externally stabilized). The study revealed an optimal wrist flexion-extension angle of around 20-30° of extension for the generation of maximum grip strength, which is in line with findings of other studies. Furthermore, the external stabilization of the wrist led to a significant increase in grip strength. The evaluation of the muscle activation patterns showed no change with the wrist stabilization conditions and only a marginal change with the wrist angle. However, muscle activation patterns strongly varied across subjects, most likely due to multiple potential solutions to produce a two finger precision pinch. Finally, three strong muscle synergies (FCR-FDS, ECU-EDC, and FDS-EDCU) were found in all subjects across all angles and both stabilization conditions. Overall, this study provided novel information about the neural control of intrinsic and extrinsic hand muscles in neurologically intact individuals. Consequently, the ReFlex robot in combination with EMG measurements is a valid and objective tool for capacity assessments under laboratory settings.

Building on this first study, a second, similar study investigating precision grip was conducted with seven chronic stroke patients with moderate hand impairment. As expected, the maximum precision grip strength was significantly lower in the stroke group compared to the neurologically intact group. Surprisingly, the maximum grip strength of the stroke subjects did not depend on the wrist flexion-extension angle. Nevertheless, in terms of produced torque at the level of the wrist, the optimal angle would lie at the neutral wrist flexion-extension position. In addition, stroke survivors were able to benefit from external wrist stabilization for the production of precision grip strength. This finding supports that stroke survivors with weaknesses at the level of the fingers might benefit from a wrist splint. The analysis of the muscle activation pattern revealed that some muscle synergies are preserved following stroke, even though the common cortical drive to these muscle pairs was significantly reduced compared to the neurologically intact controls. A strong muscle synergy of the intrinsic hand muscles was revealed in stroke patients, which was not found in the control group. Together with the relatively high intrinsic muscle activation, this implies that stroke survivors rely more on the intrinsic muscles for generating force in a precision in grip. In conclusion, this study contributed to knowledge on how wrist and finger control as well as muscle activations patterns are altered following stroke. It further demonstrated that ReFlex is a powerful assessment tool for quantifying performance of sensorimotor control in people with neurological conditions that allows the experimenter to gain insights, which are not possible with standardized clinical assessments.

The combination of the implemented low-level interaction controllers and the adapted design of the robot not only makes it an optimal research tool to investigate wrist and finger interdependence (as seen in chapter 3 and 4), but also to investigate human motor control and motor learning, assess proprioception, characterize joint properties, or to test and evaluate novel assessment protocols. A number of other studies in the lab benefited from the groundwork done on the ReFlex. For example, it was used to evaluate psychometric properties of two different assessment procedures for wrist proprioception (Rinderknecht et al., 2016), to investigate the effect of stochastic resonance on wrist proprioception (Master thesis of Anna-Maria Georgarkais), as well as to investigate the role of visual feedback on the modulation of muscle co-activation (Master thesis of Alessandro Schäppi), and to test a novel method for detecting inattention in psychophysical experiments (Rinderknecht et al., in review).

In summary, the ReFlex can be used as an objective kinematic and kinetic assessment tool of wrist and hand function. It is a powerful tool to investigate motor control and motor learning, to characterize joint properties or to investigate proprioception in humans. Furthermore, the robot is also an optimal tool for the validation and testing of new assessment procedures as it can be coupled with neurophysiological measurements.

7.1.2 Wearable sensors for continuous long-term assessment of performance

The specific aim of this part of the thesis was to develop and validate IMU based tools to provide general information about the amount and intensity of upper limb activity, energy expenditure, as well as specific activities such as upper limb activity in the context of wheelchair propulsion (mobility) and activities of daily living.

The first algorithm developed and validated in the context of this thesis allowed monitoring of wheel kinematics and type of wheelchair propulsion within a "real-world" situation (Popp et al., 2016a). Although algorithms have already been proposed in order to track mobility in manual wheelchair users, the development of the current algorithm was indispensable. First, existing methods (Sonenblum et al., 2012a, Coulter et al., 2011, Ojeda and Ding, 2014, Postma et al., 2005) were in fact able to quantify the mobility in terms of, for example, distance travelled, but the "true" contribution in terms of physical activity of the wheelchair user was not detectable, as these methodologies were not able to distinguish between self-propulsion and attendant-propulsion of the wheelchair, leading to an overestimation of physical activity, as our studies have shown. Second, other approaches addressing the activity classification of self-propulsion (Hiremath et al., 2013, Hiremath et al., 2015, Postma et al., 2005) were not applicable for continuous measurement in a "real-world" setting, as they were developed under strict laboratory settings. The algorithm developed within this thesis is a precise and reliable assessment tool for performance assessment of mobility and upper-limb activity in "real-world" situations, which provides continuous measures of wheel kinematics and type of wheelchair propulsion. Furthermore, the algorithm is adaptable to different needs. In combination with ReSense it can range from a high precision assessment tool for assessments of maximally two days where four sensors are required, to an unobtrusive and simple tool for assessments lasting up to two weeks and which only requires one sensor

at the wheel. If allowed by the sensor's battery runtime, the presented algorithm could be also used for longer measurements.

The second algorithm provides an estimation of EE for wheelchair-bound SCI individuals. Different groups have already developed estimation models for EE in manual wheelchair users. Unfortunately, none of the developed algorithms were applicable for continuous long-term assessments of EE, as these algorithms were developed using data from only a few physical activities and were not generalizable to a wide range of activities of daily living (Hiremath et al., 2012, Hiremath et al., 2013). A recently presented EE estimation algorithm included 20 different physical activities (Hiremath et al., 2016) but the resulting mean absolute estimation error of around 25% made this algorithm inappropriate for research purposes. The algorithm, which was developed in the scope of this thesis, allows for accurate continuous EE estimation in "real world" situations with a mean absolute estimation error of 14%. Furthermore, as part of this estimation model, an algorithm for the classification of "low intensity", "high intensity" as well as "wheeling" activities was developed. This algorithm showed an overall classification accuracy of almost 98% and can also be used separately in long-term assessments to classify the physical activity in different activity classes. Using the data from the indirect calorimeter in combination with the ReSense data, recommendations for a healthy and active lifestyle in the wheelchair-bound SCI population were made. The developed algorithm in combination with suggested recommendations for a healthy lifestyle could thus be implemented on an activity tracker in order to promote an active lifestyle in the SCI population, thereby reducing the risk for secondary diseases.

In addition to the methods presented in Chapter 5 (mobility) and Chapter 6 (EE), we validated an algorithm for the assessment of limb-use laterality (Brogioli et al., 2016a), which together provide an overall assessment of a patients abilities and activity level. This algorithm was necessary, as no specific assessment of laterality in the field of SCI existed, even though a strong laterality can significantly affect many activities of daily living. As part of this algorithm validation, laterality during activities of daily living was assessed and correlated to different clinical scores in 12 tetraplegic individuals. The laterality measured with the IMUs during activities of daily living positively correlated with the laterality measured clinically (GRASSP sub-test: manual muscle testing). Furthermore, we found a positive

correlation between laterality measured with the IMUs and the independence measured with the SCIM. Overall, this study showed that limb-use laterality occurs during activities of daily living in cervical SCI patients and that the proposed methodology is a valid tool to assess limb-use laterality during activities of daily living.

The three algorithms assessing mobility, energy expenditure and limb-use laterality build a basis for an evaluation framework for upper-limb activity of wheelchair-bound individuals with SCI. We also included activity counts (AC) as additional outcome measure for the amount of upper-limb activity and applied this assessment framework to demonstrate the feasibility, validity and sensitivity of this tool. In this study (Brogioli et al., 2017), we equipped 11 paraplegic and 19 tetraplegic patients at the acute stage (70-98 days post injury) with four sensor modules for the duration of three consecutive days. In addition, we collected clinical assessment scores from the GRASSP, the SCIM and the ISNCSCI. The result of this study showed that wearable sensors are a valid and sensitive assessment tool to measure overall performance and independence in people with a SCI. Furthermore, the study suggested that the assessments with wearable sensors complement the clinical assessments.

The last study which was performed within the timeline of this thesis used the sensors in combination with the developed algorithms to monitor upper-limb activity in cervical SCI individuals during the initial rehabilitation phase (Brogioli et al., 2016b). 31 patients (12 paraplegic and 19 tetraplegic) were assessed during rehabilitation at one, three and six months post injury in three different clinics across Switzerland. The assessments at each time point included continuous ReSense measurements for up to seven days and three clinical assessments, namely the ISNCSCI, the GRASSP and the SCIM. We found that tetraplegic patients improve upper-limb activity over the duration of the initial rehabilitation. At six months post injury the level of upper limb activity in tetraplegic patients reached the same values as in the paraplegic subjects. Limb-use laterality was not present in all tetraplegic patients. In the patients showing lateralization at the beginning of the rehabilitation, limb-use laterality significantly reduced but remained significantly different at the six-month time-point compared to the patients without initial lateralization. Interestingly, the peak velocity during wheeling increased slightly over the duration of

the rehabilitation in both groups, but did not differ between the groups. This study demonstrated that sensor-based assessments can provide additional insights to the clinical assessment scores.

In summary, it can be stated that, within the scope of this thesis, a powerful and objective performance assessment framework was developed and validated. In contrast to many other existing methodologies for the SCI population, the developed algorithms were introduced in observational studies in the clinical environment. Thereby, these objective performance assessments have shown to be a powerful tool in combination with standardized clinical assessments covering the ICF domains “body function and structure” and “capacity”, to get new insights into functional recovery following SCI. Last but not least, all algorithms presented within the context of this thesis were developed in a way that they can potentially be implemented in a future activity tracker for the SCI population, requiring only a single sensor and low computational power.

7.2 Outlook

7.2.1 Ongoing and planned studies using the ReFlex manipulandum

Within the scope of this thesis, we conducted two studies investigating the interdependence of wrist and digit control in neurologically intact controls as well as in stroke survivors. While, the two studies provided new insights into force production at the level of the fingers as well as new insights into changes in muscle activation patterns and muscle synergies following stroke, the study was conducted under static conditions. However, the simultaneous performance of two dynamic tasks with the wrist and fingers may challenge the motor control and may expand the already gained knowledge on the interdependence of wrist and digit control in healthy as well as in stroke survivors. Therefore we plan du conduct two additional studies using the ReFlex robot:

In a first study participants will have to maintain the precision grip at 20% of the maximum voluntary force. Simultaneously, they will be asked to move their wrist according to a given trajectory. The study will be conducted under four different conditions with varying resistance to wrist movement. In the first condition the wrist will be moved by the robot, in the second condition no external force will be applied, in the third condition a velocity dependent resistance will be applied, and the in the fourth condition subjects will have to generate wrist torque to move the cursor on the screen while the wrist is held in place by the robot. To examine the effect on grip, periodic trials with sudden small position perturbation to the wrist movement will be included. We hypothesize that the variation in grip force will increase as the required wrist torque increases (depending on the resistance provided through the robot) and that the variation in grip force will be greater in wrist flexion than in extension. Furthermore, we assume that the activity level of the finger flexors will only show limited correlation with wrist angle until the required wrist torque rises above a certain threshold level.

In the second study participants will have to move their wrist while varying the precision grip force. Both patterns, namely the wrist position and the force profile will be of a sinusoidal shape and will be performed independent from each other. Three experimental conditions will be examined. First, no force will be applied by the robot. Second, the robot will apply a velocity-dependent resistance to the wrist,

and third, the wrist is moved by the robot. We hypothesize that task performance (grip force and wrist position error) will degrade and coherence between muscles will increase as wrist movement frequency increases. Overall, with these two additional experiments we hope to extend the gained knowledge from the previous experiments with additional insights into the interdependence of wrist and digit control under dynamic conditions.

7.2.2 Wearable sensors for long-term monitoring in acute and chronic SCI

Expanding the current evaluation framework

Although the developed analysis framework already provides a large number of outcome measures (e.g. amount of upper-limb movement, limb-use laterality, wheeling speed and distance, EE, or activity classification), it can only be applied to wheelchair-bound patients. The extension of the current framework to pedestrians is of particular importance as incomplete SCI individuals may transition from wheelchair-bound to walking during the rehabilitation process. Therefore, it is important to have outcome measures on gait and walking. In a first step, an algorithm identifying walking phases in continuous measurements should be developed and validated. A possible approach based on a multi-sensor setup has already been presented for stroke subjects (Leuenberger et al., 2014). However, for an application in SCI individuals, this algorithm will need modifications and validation. At the same time, the development of an additional EE estimation algorithm for incomplete SCI walkers is needed, as the existing algorithm (Chapter 6) cannot be applied to this population.

The current outcome measures only provide information about duration, intensity, or amount of upper-limb activity, but not about the quality of the performed movement or activity. Yet, providing measures about the quality of the movement could be beneficial for clinical research as it might help, for example, to detect compensatory movements. It is obvious that for manual wheelchair users such an assessment of movement quality could focus on wheelchair propulsion. As Leuenberger (Leuenberger, 2015) has suggested, the hand trajectory during wheelchair propulsion could be tracked using a zero-velocity update method. Thereby different wheelchair propulsion patterns could be analyzed and the outcomes could be correlated to, for example, distance or velocity, but also to the energy expenditure. The

additional outcome could not only provide information about the movement quality but also about its efficiency (ergonomics).

Wearable sensors for clinical applications

In the context of this thesis we have shown that assessments with wearable sensors are a powerful tool in SCI research. However, wearable sensors could also enter the daily clinical routine in SCI, similar to what is already done in sleep medicine for example (Sadeh, 2011, Spivak et al., 2007). These wearable sensors could be used as a performance assessment tool, similar to how it is applied in research, or as objective assessment tool for capacity measurements, especially when outcome measures of movement quality are available. The biggest potential of wearable sensors for the daily clinical routine, however, lies in the application as a therapy tool. Since patients in the initial SCI rehabilitation phase receive only a few hours of therapy per day, it would be optimal to use the sensors to augment the therapy time as well as promote activity outside of therapy sessions. With a sensor, which can provide a feedback to the patients, a therapist could set daily activity goals, depending on the physical and mental condition as well as the impairments of a patient. In a second step, the goal-setting could be automated, according to the past achievements of patients, similar to the assessment-driven therapy concept implemented on a rehabilitation robot (Metzger et al., 2014b).

Energy expenditure estimation in elderly using IMU recordings

In an ongoing study we are currently collecting data from 15 younger (18-35 years) as well as from 15 older subjects (50-80 years) in order to develop an energy expenditure estimation model valid for a wide age range. Within this study, subjects are equipped with 6 ReSense modules as they perform 12 randomly selected activities of daily living. Besides the development of the EE estimation model, this study should provide novel information about how IMU recordings change within different age groups and how algorithms have to be developed if the target group includes elderly people. Furthermore, this study should reveal which sensor locations are important for activity classification and EE estimation. Even though this algorithm cannot be directly embedded as such into the current analysis framework, findings resulting from this study may support the design of novel algorithms, the adaptation of current algorithms, and the interpretation of results in the SCI population.

Development of a new sensor: JUMP

Over the last six years, ReSense has shown to be a reliable and robust tool for the design and validation of algorithms and also for the application in clinical studies. However, during these six years, improvements in sensor technologies have led to a significant drop in power consumption, theoretically allowing for longer recording durations and higher sampling rates. Therefore, a new sensor module (Joint Universities Motion Platform, JUMP) has been developed by the ETH Zurich (Rehabilitation Engineering Lab & Laboratory of Movement Biomechanics) and the Zurich University of Applied Sciences (ZHAW). This JUMP module has similar sensing capabilities as ReSense, but the recording duration should be doubled and the implemented Bluetooth LE communication between sensors allows for a better synchronization of sensors. The development of the sensors was part of the ZurichMOVE project which aims at developing an IMU-based platform for clinical use. Together with the algorithms developed within this thesis, this assessment framework has the potential to be widely applied in clinics and to generate a significant impact on clinical SCI research and beyond. It is already planned that the presented evaluation framework and the novel JUMP modules will be used in a phase 2 clinical trial of anti-Nogo A antibody treatment following acute spinal cord injury, as a secondary endpoint.

7.2.3 Potential for combining robotic and wearable sensor-based assessments

The combination of a robotic capacity assessments and wearable sensor-based performance assessment has a vast potential for the application in clinical trials. First, the robotic assessment can provide kinematic and kinetic performance measures of sensorimotor impairment in a well-controlled and reproducible task. Simultaneously, the robot can be coupled to additional systems to measure brain activity (fNIRS, EEG) or muscle activity (EMG). The combination of robotic devices with additional measurement systems could potentially allow one to distinguish between "true" recovery and compensation. Furthermore, such robotic assessments allow the detection of subtle changes in task performance, trajectories, force and torque production as well as muscle activation patterns. For this reason, robotic capacity assessments are well suited for application in intervention studies, as they can provide information beyond to what is possible with conventional clinical assessments. A nice secondary effect of such robotic assessments is the fact that the outcome measures are presented on a continuous scale, which increases the statistical power of studies, compared to when standard clinical assessments are used, as their outcomes are typically presented on ordinal or even nominal scales.

Performance assessments based on wearable sensors are the optimal complement to the robotic capacity assessments. First, wearable sensor-based assessments provide outcome measures on the level of physical activity within a "real world" situation. This allows the investigation of how improvements in capacity as a result of a specific intervention are transferred to activities of daily living. Second, wearable sensors can be used to identify and quantify potentially confounding factors such as, e.g., the amount of activity outside of the therapy. This can be very important in intervention studies as it might help for the analysis and interpretation of results.

In conclusion, the combination of robotic systems, such as the ReFlex, and sensor based assessments, as presented within this thesis, can be used to quantify improvements in function due to a certain intervention, and provide information on how and whether an intervention has an impact on the behavior of a patient in his/her natural environment (outside the clinic).

References

ABELA, E., MISSIMER, J., WIEST, R., FEDERSPIEL, A., HESS, C., STURZENEGGER, M. & WEDER, B. 2012. Lesions to primary sensory and posterior parietal cortices impair recovery from hand paresis after stroke. *PLoS One,* 7**,** e31275.

ADAMS, M. & HICKS, A. 2005. Spasticity after spinal cord injury. *Spinal cord,* 43**,** 577-586.

AINSLIE, P. N., REILLY, T. & WESTERTERP, K. R. 2003. Estimating human energy expenditure. *Sports Medicine,* 33**,** 683-698.

AINSWORTH, B. E., HASKELL, W. L., HERRMANN, S. D., MECKES, N., BASSETT JR, D. R., TUDOR-LOCKE, C., GREER, J. L., VEZINA, J., WHITT-GLOVER, M. C. & LEON, A. S. 2011. 2011 Compendium of Physical Activities: a second update of codes and MET values. *Medicine and science in sports and exercise,* 43**,** 1575-1581.

ANASTASOPOULOU, P., TANSELLA, M., STUMPP, J., SHAMMAS, L. & HEY, S. Classification of human physical activity and energy expenditure estimation by accelerometry and barometry. 2012 Annual International Conference of the IEEE Engineering in Medicine and Biology Society, 2012. IEEE, 6451-6454.

ANDERSON, K. D. 2004. Targeting recovery: priorities of the spinal cord-injured population. *Journal of neurotrauma,* 21**,** 1371-1383.

ANNEKEN, V., HANSSEN-DOOSE, A., HIRSCHFELD, S., SCHEUER, T. & THIETJE, R. 2010. Influence of physical exercise on quality of life in individuals with spinal cord injury. *Spinal Cord,* 48**,** 393-399.

AYOUB, M. & PRESTI, P. L. 1971. The determination of an optimum size cylindrical handle by use of electromyography. *Ergonomics,* 14**,** 509-518.

BAEK, J., LEE, G., PARK, W. & YUN, B.-J. Accelerometer signal processing for user activity detection. Knowledge-Based Intelligent Information and Engineering Systems, 2004a. Springer, 610-617.

BAEK, J., LEE, G., PARK, W. & YUN, B.-J. Accelerometer signal processing for user activity detection. International Conference on Knowledge-Based and Intelligent Information and Engineering Systems, 2004b. Springer, 610-617.

BAILEY, R. R., KLAESNER, J. W. & LANG, C. E. 2014. An accelerometry-based methodology for assessment of real-world bilateral upper extremity activity. *PloS one,* 9**,** e103135.

BAILEY, R. R., KLAESNER, J. W. & LANG, C. E. 2015. Quantifying real-world upper-limb activity in nondisabled adults and adults with chronic stroke. *Neurorehabilitation and neural repair,* 29**,** 969-978.

BALASUBRAMANIAN, V., DUTT, A. & RAI, S. 2011. Analysis of muscle fatigue in helicopter pilots. *Applied ergonomics,* 42**,** 913-918.

BAO, L. & INTILLE, S. S. Activity recognition from user-annotated acceleration data. International Conference on Pervasive Computing, 2004a. Springer, 1-17.

BAO, L. & INTILLE, S. S. 2004b. Activity recognition from user-annotated acceleration data. *Pervasive computing.* Springer.

BARDORFER, A., MUNIH, M., ZUPAN, A. & PRIMOZIC, A. 2001. Upper limb motion analysis using haptic interface. *IEEE/ASME transactions on Mechatronics,* 6**,** 253-260.

BARRECA, S. R., STRATFORD, P. W., LAMBERT, C. L., MASTERS, L. M. & STREINER, D. L. 2005. Test-retest reliability, validity, and sensitivity of the Chedoke arm and hand activity inventory: a new measure of upper-limb function for survivors of stroke. *Archives of physical medicine and rehabilitation,* 86**,** 1616-1622.

BASHEER, I. & HAJMEER, M. 2000. Artificial neural networks: fundamentals, computing, design, and application. *Journal of microbiological methods,* 43**,** 3-31.

BEEKHUIZEN, K. S. & FIELD-FOTE, E. C. 2005. Massed practice versus massed practice with stimulation: effects on upper extremity function and cortical plasticity in individuals with incomplete cervical spinal cord injury. *Neurorehabilitation and neural repair,* 19**,** 33-45.

BEEKHUIZEN, K. S. & FIELD-FOTE, E. C. 2008. Sensory stimulation augments the effects of massed practice training in persons with tetraplegia. *Archives of physical medicine and rehabilitation,* 89**,** 602-608.

BHARDWAJ, P., NAYAK, S. S., KISWAR, A. M. & SABAPATHY, S. R. 2011. Effect of static wrist position on grip strength. *Indian journal of plastic surgery: official publication of the Association of Plastic Surgeons of India,* 44**,** 55.

BLAIR, S. N., LAMONTE, M. J. & NICHAMAN, M. Z. 2004. The evolution of physical activity recommendations: how much is enough? *The American journal of clinical nutrition,* 79**,** 913S-920S.

BLENNERHASSETT, J. M., CAREY, L. M. & MATYAS, T. A. 2006. Grip force regulation during pinch grip lifts under somatosensory guidance: comparison between people with stroke and healthy controls. *Archives of physical medicine and rehabilitation,* 87**,** 418-429.

BLENNERHASSETT, J. M., CAREY, L. M. & MATYAS, T. A. 2008. Clinical measures of handgrip limitation relate to impaired pinch grip force control after stroke. *Journal of Hand Therapy,* 21**,** 245-253.

BLENNERHASSETT, J. M., MATYAS, T. A. & CAREY, L. M. 2007. Impaired discrimination of surface friction contributes to pinch grip deficit after stroke. *Neurorehabilitation and Neural Repair,* 21**,** 263-272.

BOISSY, P., BOURBONNAIS, D., CARLOTTI, M. M., GRAVEL, D. & ARSENAULT, B. A. 1999. Maximal grip force in chronic stroke subjects and its relationship to global upper extremity function. *Clinical Rehabilitation,* 13**,** 354-362.

BONATO, P. 2005. Advances in wearable technology and applications in physical medicine and rehabilitation. *Journal of NeuroEngineering and Rehabilitation,* 2**,** 1.

BOSECKER, C., DIPIETRO, L., VOLPE, B. & KREBS, H. I. 2009. Kinematic robot-based evaluation scales and clinical counterparts to measure upper limb motor performance in patients with chronic stroke. *Neurorehabilitation and neural repair*.

BOUTEN, C. V., KOEKKOEK, K. T., VERDUIN, M., KODDE, R. & JANSSEN, J. D. 1997a. A triaxial accelerometer and portable data processing unit for the assessment of daily physical activity. *Biomedical Engineering, IEEE Transactions on,* 44**,** 136-147.

BOUTEN, C. V., KOEKKOEK, K. T., VERDUIN, M., KODDE, R. & JANSSEN, J. D. 1997b. A triaxial accelerometer and portable data processing unit for the assessment of daily physical activity. *IEEE Transactions on Biomedical Engineering,* 44**,** 136-147.

BRAGE, S., BRAGE, N., FRANKS, P. W., EKELUND, U., WONG, M.-Y., ANDERSEN, L. B., FROBERG, K. & WAREHAM, N. J. 2004. Branched equation modeling of simultaneous accelerometry and heart rate monitoring improves estimate of directly measured physical activity energy expenditure. *Journal of Applied Physiology,* 96**,** 343-351.

BROGIOLI, M., POPP, W. L., ALBISSER, U., BRUST, A. K., FROTZLER, A., GASSERT, R., CURT, A. & STARKEY, M. L. 2016a. Novel Sensor Technology to Assess Independence and Limb-Use Laterality in Cervical Spinal Cord Injury. *Journal of Neurotrauma,* 33**,** 1950-1957.

BROGIOLI, M., POPP, W. L., SCHNEIDER, S., ALBISSER, U., BRUST, A. K., FROTZLER, A., GASSERT, R., CURT, A. & STARKEY, M. L. 2017. Multi-day recordings of wearable sensors are valid and sensitive measures of function and independence in human spinal cord injury. *Journal of Neurotrauma,* 34**,** 1141-1148.

BROGIOLI, M., SCHNEIDER, S., POPP, W. L., ALBISSER, U., BRUST, A. K., VELSTRA, I.-M., GASSERT, R., CURT, A. & STARKEY, M. L. 2016b. Monitoring Upper limb recovery after cervical spinal cord injury: insights beyond assessment scores. *Frontiers in Neurology,* 7.

BUCHHOLZ, A. C., MARTIN GINIS, K. A., BRAY, S. R., CRAVEN, B. C., HICKS, A. L., HAYES, K. C., LATIMER, A. E., MCCOLL, M. A., POTTER, P. J. & WOLFE, D. L. 2009. Greater daily leisure time physical activity is associated with lower chronic disease risk in adults with spinal cord injury. *Applied Physiology, Nutrition, and Metabolism,* 34**,** 640-647.

BUCHHOLZ, A. C. & PENCHARZ, P. B. 2004. Energy expenditure in chronic spinal cord injury. *Current Opinion in Clinical Nutrition & Metabolic Care,* 7**,** 635-639.

BUDHOTA, A., HUSSAIN, A., HUGHES, C., HANSEN, C., KAGER, S., VISHWANATH, D. A., KUAH, C. W. K., CHUA, K. & CAMPOLO, D. Role of EMG as a complementary tool for assessment of motor impairment. Biomedical Robotics and Biomechatronics (BioRob), 2016 6th IEEE International Conference on, 2016. IEEE, 692-697.

BULTHAUP, S., CIPRIANI, D. J. & THOMAS, J. J. 1999. An electromyography study of wrist extension orthoses and upper-extremity function. *American Journal of Occupational Therapy,* 53**,** 434-440.

BURDET, E. & MILNER, T. 1998. Quantization of human motions and learning of accurate movements. *Biological cybernetics,* 78**,** 307-318.

BURDET, E., OSU, R., FRANKLIN, D. W., MILNER, T. E. & KAWATO, M. 2001. The central nervous system stabilizes unstable dynamics by learning optimal impedance. *Nature,* 414**,** 446-449.

BUTTON, K. S., IOANNIDIS, J. P., MOKRYSZ, C., NOSEK, B. A., FLINT, J., ROBINSON, E. S. & MUNAFÒ, M. R. 2013. Power failure: why small sample size undermines the reliability of neuroscience. *Nature Reviews Neuroscience,* 14**,** 365-376.

CAMERON, B. D., FRANKS, I. M., INGLIS, J. T. & CHUA, R. 2010. Implicit motor learning from target error during explicit reach control. *Experimental Brain Research,* 206**,** 99-104.

CANNING, C. G., ADA, L. & O'DWYER, N. J. 2000. Abnormal muscle activation characteristics associated with loss of dexterity after stroke. *Journal of the neurological sciences,* 176**,** 45-56.

CAPPELLO, L., ELANGOVAN, N., CONTU, S., KHOSRAVANI, S., KONCZAK, J. & MASIA, L. 2015. Robot-aided assessment of wrist proprioception. *Frontiers in human neuroscience,* 9.

CAREY, L. M. 1995. Somatosensory loss after stroke. *Critical Reviews™ in Physical and Rehabilitation Medicine,* 7.

CATZ, A. & ITZKOVICH, M. 2007. Spinal Cord Independence Measure: comprehensive ability rating scale for the spinal cord lesion patient. *Journal of rehabilitation research and development,* 44**,** 65.

CATZ, A., ITZKOVICH, M., AGRANOV, E., RING, H. & TAMIR, A. 1997. SCIM—spinal cord independence measure. *Spinal cord,* 35**,** 850-856.

CHAO, E. Y. 1989. *Biomechanics of the hand: a basic research study*, World Scientific.

CHAPUIS, D., DE GRAVE, R. B., LAMBERCY, O. & GASSERT, R. ReFlex, a haptic wrist interface for motor learning and rehabilitation. Haptics Symposium, 2010 IEEE, 2010. IEEE, 417-424.

CHEN, H.-M., CHEN, C. C., HSUEH, I.-P., HUANG, S.-L. & HSIEH, C.-L. 2009. Test-retest reproducibility and smallest real difference of 5 hand function tests in patients with stroke. *Neurorehabilitation and neural repair*.

CHEUNG, V. C., TUROLLA, A., AGOSTINI, M., SILVONI, S., BENNIS, C., KASI, P., PAGANONI, S., BONATO, P. & BIZZI, E. 2012. Muscle synergy patterns as physiological markers of motor cortical damage. *Proceedings of the National Academy of Sciences,* 109**,** 14652-14656.

CHOI, B. C., PAK, A. W. & CHOI, J. C. 2007. Daily step goal of 10,000 steps: a literature review. *Clinical & Investigative Medicine,* 30**,** 146-151.

CIRSTEA, M. & LEVIN, M. F. 2000. Compensatory strategies for reaching in stroke. *Brain,* 123**,** 940-953.

COLLINS, E. G., GATER, D., KIRATLI, J., BUTLER, J., HANSON, K. & LANGBEIN, W. E. 2010. Energy cost of physical activities in persons with spinal cord injury. *Medicine and science in sports and exercise,* 42**,** 691-700.

COULTER, E. H., DALL, P. M., ROCHESTER, L., HASLER, J. P. & GRANAT, M. H. 2011. Development and validation of a physical activity monitor for use on a wheelchair. *Spinal Cord,* 49**,** 445-450.

COWAN, R. E., BONINGER, M. L., SAWATZKY, B. J., MAZOYER, B. D. & COOPER, R. A. 2008. Preliminary outcomes of the SmartWheel Users' Group database: a proposed framework for clinicians to objectively evaluate manual wheelchair propulsion. *Archives of Physical Medicine and Rehabilitation,* 89**,** 260-268.

CRAMER, S. C., SUR, M., DOBKIN, B. H., O'BRIEN, C., SANGER, T. D., TROJANOWSKI, J. Q., RUMSEY, J. M., HICKS, R., CAMERON, J. & CHEN, D. 2011. Harnessing neuroplasticity for clinical applications. *Brain,* 134**,** 1591-1609.

CRAWFORD, J. O., WANIBE, E. & NAYAK, L. 2002. The interaction between lid diameter, height and shape on wrist torque exertion in younger and older adults. *Ergonomics,* 45**,** 922-933.

CROUTER, S. E. & BASSETT, D. R. 2008. A new 2-regression model for the Actical accelerometer. *British journal of sports medicine,* 42**,** 217-224.

CRUZ, E., WALDINGER, H. & KAMPER, D. 2005. Kinetic and kinematic workspaces of the index finger following stroke. *Brain,* 128**,** 1112-1121.

CURONE, D., BERTOLOTTI, G. M., CRISTIANI, A., SECCO, E. L. & MAGENES, G. 2010a. A real-time and self-calibrating algorithm based on triaxial accelerometer signals for the detection of human posture and activity. *Information Technology in Biomedicine, IEEE Transactions on,* 14**,** 1098-1105.

CURONE, D., BERTOLOTTI, G. M., CRISTIANI, A., SECCO, E. L. & MAGENES, G. 2010b. A real-time and self-calibrating algorithm based on triaxial accelerometer signals for the detection of human posture and activity. *IEEE transactions on information technology in biomedicine,* 14**,** 1098-1105.

CURT, A., VAN HEDEL, H. J., KLAUS, D. & DIETZ, V. 2008. Recovery from a spinal cord injury: significance of compensation, neural plasticity, and repair. *Journal of neurotrauma,* 25**,** 677-685.

DANNA-DOS SANTOS, A., POSTON, B., JESUNATHADAS, M., BOBICH, L. R., HAMM, T. M. & SANTELLO, M. 2010. Influence of fatigue on hand muscle coordination and EMG-EMG coherence during three-digit grasping. *Journal of neurophysiology,* 104**,** 3576-3587.

DANNECKER, K. L., SAZONOVA, N. A., MELANSON, E. L., SAZONOV, E. S. & BROWNING, R. C. 2013. A comparison of energy expenditure estimation of several physical activity monitors. *Medicine and science in sports and exercise,* 45**,** 2105.

DE LOS REYES-GUZMÁN, A., DIMBWADYO-TERRER, I., TRINCADO-ALONSO, F., MONASTERIO-HUELIN, F., TORRICELLI, D. & GIL-AGUDO, A. 2014. Quantitative assessment based on kinematic measures of functional impairments during upper extremity movements: A review. *Clinical Biomechanics,* 29**,** 719-727.

DEMPSEY, P. G. & AYOUB, M. 1996. The influence of gender, grasp type, pinch width and wrist position on sustained pinch strength. *International Journal of Industrial Ergonomics,* 17**,** 259-273.

DEWALD, J., BEER, R. F., GIVEN, J. D., MCGUIRE, J. R. & RYMER, W. Z. 1999. Reorganization of flexion reflexes in the upper extremity of hemiparetic subjects. *Muscle & nerve,* 22**,** 1209-1221.

DEWALD, J. P., POPE, P. S., GIVEN, J. D., BUCHANAN, T. S. & RYMER, W. Z. 1995. Abnormal muscle coactivation patterns during isometric torque generation at the elbow and shoulder in hemiparetic subjects. *Brain,* 118**,** 495-510.

DEWALD, J. P. & SCHMIT, B. D. Stretch reflex gain and threshold changes as a function of elbow stretch velocity in hemiparetic stroke. Engineering in medicine and biology society, 2003. proceedings of the 25th annual international conference of the IEEE, 2003. IEEE, 1464-1467.

DI DOMIZIO, J., MOGK, J. P. & KEIR, P. J. 2008. Wrist splint effects on muscle activity and force during a handgrip task. *Journal of applied biomechanics,* 24**,** 298-303.

DIETZ, V. & SINKJAER, T. 2007. Spastic movement disorder: impaired reflex function and altered muscle mechanics. *The Lancet Neurology,* 6**,** 725-733.

DIETZ, V., TRIPPEL, M. & BERGER, W. 1991. Reflex activity and muscle tone during elbow movements in patients with spastic paresis. *Annals of neurology,* 30**,** 767-779.

DIPIETRO, L., KREBS, H. I., FASOLI, S. E., VOLPE, B. T., STEIN, J., BEVER, C. & HOGAN, N. 2007. Changing motor synergies in chronic stroke. *Journal of neurophysiology,* 98**,** 757-768.

DOBKIN, B. H. & DORSCH, A. 2011. The promise of mHealth daily activity monitoring and outcome assessments by wearable sensors. *Neurorehabilitation and neural repair,* 25**,** 788-798.

DONG, H., LOOMER, P., BARR, A., LAROCHE, C., YOUNG, E. & REMPEL, D. 2007. The effect of tool handle shape on hand muscle load and pinch force in a simulated dental scaling task. *Applied ergonomics,* 38**,** 525-531.

DOVAT, L., LAMBERCY, O., SALMAN, B., JOHNSON, V., GASSERT, R., BURDET, E., TEO, C. L. & MILNER, T. Post-stroke training of a pick and place activity in a virtual environment. 2008 Virtual Rehabilitation, 2008. IEEE, 28-34.

DOWLING, A. V., EBERLY, V., MANEEKOBKUNWONG, S., MULROY, S. J., REQUEJO, P. S. & GWIN, J. T. 2016. Telehealth monitor to measure physical activity and pressure relief maneuver performance in wheelchair users. *Assistive Technology***,** 1-8.

DUKELOW, S. P., HERTER, T. M., MOORE, K. D., DEMERS, M. J., GLASGOW, J. I., BAGG, S. D., NORMAN, K. E. & SCOTT, S. H. 2010. Quantitative assessment of limb position sense following stroke. *Neurorehabilitation and Neural Repair,* 24**,** 178-187.

DUNCAN, P. W., BODE, R. K., LAI, S. M., PERERA, S. & INVESTIGATORS, G. A. I. N. A. 2003. Rasch analysis of a new stroke-specific outcome scale: the Stroke Impact Scale. *Archives of physical medicine and rehabilitation,* 84**,** 950-963.

DUNCAN, P. W., GOLDSTEIN, L. B., MATCHAR, D., DIVINE, G. W. & FEUSSNER, J. 1992. Measurement of motor recovery after stroke. Outcome assessment and sample size requirements. *Stroke,* 23**,** 1084-1089.

ERVILHA, U., GRAVEN-NIELSEN, T. & DUARTE, M. 2012. A simple test of muscle coactivation estimation using electromyography. *Brazilian Journal of Medical and Biological Research,* 45**,** 977-981.

EUVING, E. J., GURARI, N., DROGOS, J. M., TRAXEL, S., STIENEN, A. H. & DEWALD, J. P. Individuals with Chronic Hemiparetic Stroke Correctly Match Forearm Position Within a Single Arm: Preliminary Findings. International Conference on Human Haptic Sensing and Touch Enabled Computer Applications, 2016. Springer, 122-133.

FEIGIN, V. L., LAWES, C. M., BENNETT, D. A. & ANDERSON, C. S. 2003. Stroke epidemiology: a review of population-based studies of incidence, prevalence, and case-fatality in the late 20th century. *The Lancet Neurology,* 2**,** 43-53.

FEYS, P., ALDERS, G., GIJBELS, D., DE BOECK, J., DE WEYER, T., CONINX, K., RAYMAEKERS, C., TRUYENS, V., GROENEN, P. & MEIJER, K. Arm training in Multiple Sclerosis using Phantom: clinical relevance of robotic outcome measures. 2009 IEEE International Conference on Rehabilitation Robotics, 2009. IEEE, 576-581.

FLUET, M.-C., LAMBERCY, O. & GASSERT, R. Upper limb assessment using a virtual peg insertion test. 2011 IEEE International Conference on Rehabilitation Robotics, 2011. IEEE, 1-6.

FREEDSON, P. S., LYDEN, K., KOZEY-KEADLE, S. & STAUDENMAYER, J. 2011. Evaluation of artificial neural network algorithms for predicting METs and activity type from accelerometer data: validation on an independent sample. *Journal of Applied Physiology,* 111**,** 1804-1812.

FREEDSON, P. S., MELANSON, E. & SIRARD, J. 1998. Calibration of the Computer Science and Applications, Inc. accelerometer. *Medicine and science in sports and exercise,* 30**,** 777-781.

FUGL-MEYER, A. R., JÄÄSKÖ, L., LEYMAN, I., OLSSON, S. & STEGLIND, S. 1974. The post-stroke hemiplegic patient. 1. a method for evaluation of physical performance. *Scandinavian journal of rehabilitation medicine,* 7**,** 13-31.

GARCIA-MASSO, X., SERRA-ANO, P., GARCIA-RAFFI, L., SANCHEZ-PEREZ, E., LÓPEZ-PASCUAL, J. & GONZALEZ, L. 2013. Validation of the use of Actigraph GT3X accelerometers to estimate energy expenditure in full time manual wheelchair users with spinal cord injury. *Spinal cord,* 51**,** 898-903.

GASSERT, R., MOSER, R., BURDET, E. & BLEULER, H. 2006. MRI/fMRI-compatible robotic system with force feedback for interaction with human motion. *IEEE ASME TRANSACTIONS ON MECHATRONICS,* 11**,** 216.

GEBRUERS, N., VANROY, C., TRUIJEN, S., ENGELBORGHS, S. & DE DEYN, P. P. 2010. Monitoring of physical activity after stroke: a systematic review of accelerometry-based measures. *Archives of physical medicine and rehabilitation,* 91**,** 288-297.

GELBER, D. A., JOSEFCZYK, B., HERRMAN, D., GOOD, D. C. & VERHULST, S. J. 1995. Comparison of two therapy approaches in the rehabilitation of the pure motor hemiparetic stroke patient. *Neurorehabilitation and Neural Repair,* 9**,** 191-196.

GIRGIS, J., MERRETT, D., KIRKLAND, S., METZ, G., VERGE, V. & FOUAD, K. 2007. Reaching training in rats with spinal cord injury promotes plasticity and task specific recovery. *Brain,* 130**,** 2993-3003.

GLADSTONE, D. J., DANELLS, C. J. & BLACK, S. E. 2002. The Fugl-Meyer assessment of motor recovery after stroke: a critical review of its measurement properties. *Neurorehabilitation and neural repair,* 16**,** 232-240.

GLINSKY, J., HARVEY, L., VAN ES, P., CHEE, S. & GANDEVIA, S. C. 2009. The addition of electrical stimulation to progressive resistance training does not enhance the wrist strength of people with tetraplegia: a randomized controlled trial. *Clinical rehabilitation*.

GONZALEZ, A. G., SALGADO, D. R. & MORUNO, L. G. 2015. Optimisation of a laparoscopic tool handle dimension based on ergonomic analysis. *International Journal of Industrial Ergonomics,* 48**,** 16-24.

GONZALEZ, R. V., BUCHANAN, T. S. & DELP, S. L. 1997. How muscle architecture and moment arms affect wrist flexion-extension moments. *Journal of biomechanics,* 30**,** 705-712.

GONZENBACH, R. R., GASSER, P., ZÖRNER, B., HOCHREUTENER, E., DIETZ, V. & SCHWAB, M. E. 2010. Nogo-A antibodies and training reduce muscle spasms in spinal cord-injured rats. *Annals of neurology,* 68**,** 48-57.

GOWLAND, C., STRATFORD, P., WARD, M., MORELAND, J., TORRESIN, W., VAN HULLENAAR, S., SANFORD, J., BARRECA, S., VANSPALL, B. & PLEWS, N. 1993. Measuring physical impairment and disability with the Chedoke-McMaster Stroke Assessment. *Stroke,* 24**,** 58-63.

GRANT, K. A., HABES, D. J. & STEWARD, L. L. 1992. An analysis of handle designs for reducing manual effort: the influence of grip diameter. *International Journal of Industrial Ergonomics,* 10**,** 199-206.

HAGAN, M. T. & MENHAJ, M. B. 1994. Training feedforward networks with the Marquardt algorithm. *IEEE transactions on Neural Networks,* 5**,** 989-993.

HALLIDAY, D., ROSENBERG, J., AMJAD, A., BREEZE, P., CONWAY, B. & FARMER, S. 1995. A framework for the analysis of mixed time series/point process data—theory and application to the study of physiological tremor, single motor unit discharges and electromyograms. *Progress in biophysics and molecular biology,* 64**,** 237-278.

HALPERN, C. A. & FERNANDEZ, J. E. 1996. The effect of wrist and arm postures on peak pinch strength. *Journal of human ergology,* 25**,** 115-130.

HARRIS, J. A. & BENEDICT, F. G. 1918. A biometric study of human basal metabolism. *Proceedings of the National Academy of Sciences,* 4**,** 370-373.

HASKELL, W. L., LEE, I.-M., PATE, R. R., POWELL, K. E., BLAIR, S. N., FRANKLIN, B. A., MACERA, C. A., HEATH, G. W., THOMPSON, P. D. & BAUMAN, A. 2007. Physical activity and public health: updated recommendation for adults from the American College of Sports Medicine and the American Heart Association. *Circulation,* 116**,** 1081.

HATANO, Y. 1993. Use of the pedometer for promoting daily walking exercise. *International Council for Health, Physical Education, and Recreation,* 29**,** 4-8.

HAZELTON, F. T., SMIDT, G. L., FLATT, A. E. & STEPHENS, R. I. 1975. The influence of wrist position on the force produced by the finger flexors. *Journal of biomechanics,* 8**,** 301IN1303-302IN3306.

HELLIER, J. 2014. *The Brain, the Nervous System, and Their Diseases* Greenwood.

HERMSDÖRFER, J., HAGL, E., NOWAK, D. & MARQUARDT, C. 2003. Grip force control during object manipulation in cerebral stroke. *Clinical Neurophysiology,* 114**,** 915-929.

HERMSDÖRFER, J., MARQUARDT, C., WACK, S. & MAI, N. 1999. Comparative analysis of diadochokinetic movements. *Journal of Electromyography and Kinesiology,* 9**,** 283-295.

HERREN, R., SPARTI, A., AMINIAN, K. & SCHUTZ, Y. 1999. The prediction of speed and incline in outdoor running in humans using accelerometry. *Medicine and science in sports and exercise,* 31**,** 1053-1059.

HERRING, S. R., CASTILLEJOS, P. & HALLBECK, M. S. 2011. User-centered evaluation of handle shape and size and input controls for a neutron detector. *Applied ergonomics,* 42**,** 919-928.

HERTENSTEIN, M. J. & WEISS, S. J. 2011. *The handbook of touch: Neuroscience, behavioral, and health perspectives*, Springer Publishing Company.

HICKS, A., MARTIN, K., DITOR, D., LATIMER, A., CRAVEN, C., BUGARESTI, J. & MCCARTNEY, N. 2003. Long-term exercise training in persons with spinal cord injury: effects on strength, arm ergometry performance and psychological well-being. *Spinal cord,* 41**,** 34-43.

HIREMATH, S., DING, D., FARRINGDON, J., VYAS, N. & COOPER, R. 2013. Physical activity classification utilizing SenseWear activity monitor in manual wheelchair users with spinal cord injury. *Spinal cord,* 51**,** 705-709.

HIREMATH, S. V. & DING, D. 2011. Evaluation of activity monitors in manual wheelchair users with paraplegia. *The journal of spinal cord medicine,* 34**,** 110-117.

HIREMATH, S. V., DING, D., FARRINGDON, J. & COOPER, R. A. 2012. Predicting energy expenditure of manual wheelchair users with spinal cord injury using a multisensor-based activity monitor. *Archives of physical medicine and rehabilitation,* 93**,** 1937-1943.

HIREMATH, S. V., INTILLE, S. S., KELLEHER, A., COOPER, R. A. & DING, D. 2014. Detection of physical activities using a physical activity monitor system for wheelchair users. *Medical engineering & physics*.

HIREMATH, S. V., INTILLE, S. S., KELLEHER, A., COOPER, R. A. & DING, D. 2015. Detection of physical activities using a physical activity monitor system for wheelchair users. *Medical engineering & physics,* 37**,** 68-76.

HIREMATH, S. V., INTILLE, S. S., KELLEHER, A., COOPER, R. A. & DING, D. 2016. Estimation of Energy Expenditure for Wheelchair Users Using a Physical Activity Monitoring System. *Archives of physical medicine and rehabilitation*.

HOGAN, N. 1984a. Adaptive control of mechanical impedance by coactivation of antagonist muscles. *Automatic Control, IEEE Transactions on,* 29**,** 681-690.

HOGAN, N. 1984b. An organizing principle for a class of voluntary movements. *The Journal of Neuroscience,* 4**,** 2745-2754.

HOGAN, N., KREBS, H. I., SHARON, A. & CHARNNARONG, J. 1995. Interactive robotic therapist. Google Patents.

HOLDEFER, R. & MILLER, L. 2002. Primary motor cortical neurons encode functional muscle synergies. *Experimental Brain Research,* 146**,** 233-243.

HORSFALL, I., WATSON, C., CHAMPION, S., PROSSER, P. & RINGROSE, T. 2005. The effect of knife handle shape on stabbing performance. *Applied ergonomics,* 36**,** 505-511.

HUANG, V. S. & KRAKAUER, J. W. 2009. Robotic neurorehabilitation: a computational motor learning perspective. *Journal of neuroengineering and rehabilitation,* 6**,** 1.

IMBACH, L. L., SOMMERAUER, M., LEUENBERGER, K., SCHREGLMANN, S. R., MAIER, O., UHL, M., GASSERT, R. & BAUMANN, C. R. 2014. Dopamine-responsive pattern in tremor patients. *Parkinsonism & related disorders,* 20**,** 1283-1286.

IMRHAN, S. N. 1991. The influence of wrist position on different types of pinch strength. *Applied Ergonomics,* 22**,** 379-384.

IMRHAN, S. N. & RAHMAN, R. 1995. The effects of pinch width on pinch strengths of adult males using realistic pinch-handle coupling. *International Journal of Industrial Ergonomics,* 16**,** 123-134.

ITZKOVICH, M., GELERNTER, I., BIERING-SORENSEN, F., WEEKS, C., LARAMEE, M., CRAVEN, B., TONACK, M., HITZIG, S., GLASER, E. & ZEILIG, G. 2007a. The Spinal Cord Independence Measure (SCIM) version III: reliability and validity in a multi-center international study. *Disability and rehabilitation,* 29**,** 1926-1933.

ITZKOVICH, M., GELERNTER, I., BIERING-SORENSEN, F., WEEKS, C., LARAMEE, M., CRAVEN, B., TONACK, M., HITZIG, S., GLASER, E. & ZEILIG, G. 2007b. The Spinal Cord Independence Measure (SCIM) version III: reliability and validity in a multi-center international study. *Disability & Rehabilitation,* 29**,** 1926-1933.

JOHANSSON, L., BJÖRING, G. & HÄGG, G. M. 2004. The effect of wrist orthoses on forearm muscle activity. *Applied ergonomics,* 35**,** 129-136.

JØRGENSEN, K., FALLENTIN, N., KROGH-LUND, C. & JENSEN, B. 1988. Electromyography and fatigue during prolonged, low-level static contractions. *European journal of applied physiology and occupational physiology,* 57**,** 316-321.

KADIVAR, Z., SULLIVAN, J., ENG, D., PEHLIVAN, A., MALLEY, M., YOZBATIRAN, N., BERLINER, J., BOAKE, C. & FRANCISCO, G. 2012. RiceWrist Robotic Device for Upper Limb Training: Feasibility Study and Case Report of Two Tetraplegic Persons with Spinal Cord Injury. *International Journal of Biological Engineering,* 2**,** 27-38.

KALRA, M., RAKHEJA, S., MARCOTTE, P., DEWANGAN, K. & ADEWUSI, S. 2015. Measurement of coupling forces at the power tool handle-hand interface. *International Journal of Industrial Ergonomics,* 50**,** 105-120.

KALSI-RYAN, S., BEATON, D., CURT, A., DUFF, S., POPOVIC, M. R., RUDHE, C., FEHLINGS, M. G. & VERRIER, M. C. 2012a. The graded redefined assessment of strength sensibility and prehension: reliability and validity. *Journal of neurotrauma,* 29**,** 905-914.

KALSI-RYAN, S., CURT, A., VERRIER, M. C. & FEHLINGS, M. G. 2012b. Development of the Graded Redefined Assessment of Strength, Sensibility and Prehension (GRASSP): reviewing measurement specific to the upper limb in tetraplegia. *Journal of Neurosurgery: Spine,* 17**,** 65-76.

KAMPER, D., HARVEY, R., SURESH, S. & RYMER, W. 2003. Relative contributions of neural mechanisms versus muscle mechanics in promoting finger extension deficits following stroke. *Muscle & nerve,* 28**,** 309-318.

KAMPER, D. G., FISCHER, H. C., CONRAD, M. O., TOWLES, J. D., RYMER, W. Z. & TRIANDAFILOU, K. M. 2014. Finger-thumb coupling contributes to exaggerated thumb flexion in stroke survivors. *Journal of neurophysiology,* 111**,** 2665-2674.

KAMPER, D. G., FISCHER, H. C., CRUZ, E. G. & RYMER, W. Z. 2006. Weakness is the primary contributor to finger impairment in chronic stroke. *Archives of physical medicine and rehabilitation,* 87**,** 1262-1269.

KARANTONIS, D. M., NARAYANAN, M. R., MATHIE, M., LOVELL, N. H. & CELLER, B. G. 2006a. Implementation of a real-time human movement classifier using a triaxial accelerometer for ambulatory monitoring. *Information Technology in Biomedicine, IEEE Transactions on,* 10**,** 156-167.

KARANTONIS, D. M., NARAYANAN, M. R., MATHIE, M., LOVELL, N. H. & CELLER, B. G. 2006b. Implementation of a real-time human movement classifier using a triaxial accelerometer for ambulatory monitoring. *IEEE transactions on information technology in biomedicine,* 10**,** 156-167.

KELLER, U., SCHÖLCH, S., ALBISSER, U., RUDHE, C., CURT, A., RIENER, R. & KLAMROTH-MARGANSKA, V. 2015. Robot-assisted arm assessments in spinal cord injured patients: A consideration of concept study. *PloS one,* 10**,** e0126948.

KIRSHBLUM, S. C., BURNS, S. P., BIERING-SORENSEN, F., DONOVAN, W., GRAVES, D. E., JHA, A., JOHANSEN, M., JONES, L., KRASSIOUKOV, A. & MULCAHEY, M. 2011. International standards for neurological classification of spinal cord injury (revised 2011). *The journal of spinal cord medicine,* 34**,** 535-546.

KITAGO, T., LIANG, J., HUANG, V. S., HAYES, S., SIMON, P., TENTEROMANO, L., LAZAR, R. M., MARSHALL, R. S., MAZZONI, P. & LENNIHAN, L. 2012. Improvement after constraint-induced movement therapy recovery of normal motor control or task-specific compensation? *Neurorehabilitation and neural repair***,** 1545968312452631.

KLAMROTH-MARGANSKA, V., BLANCO, J., CAMPEN, K., CURT, A., DIETZ, V., ETTLIN, T., FELDER, M., FELLINGHAUER, B., GUIDALI, M. & KOLLMAR, A. 2014. Three-dimensional, task-specific robot therapy of the arm after stroke: a multicentre, parallel-group randomised trial. *The Lancet Neurology,* 13**,** 159-166.

KLIPPEL, N. J. & HEIL, D. P. 2003. Validation of energy expenditure prediction algorithms in adults using the Actical electronic activity monitor. *Medicine & Science in Sports & Exercise,* 35**,** S284.

KLOOSTERMAN, M., SNOEK, G. & JANNINK, M. 2009. Systematic review of the effects of exercise therapy on the upper extremity of patients with spinal-cord injury. *Spinal Cord,* 47**,** 196-203.

KONG, Y. K. & LOWE, B. D. 2005. Optimal cylindrical handle diameter for grip force tasks. *International Journal of Industrial Ergonomics,* 35**,** 495-507.

KONG, Y. K., LOWE, B. D., LEE, S. J. & KRIEG, E. F. 2008. Evaluation of handle shapes for screwdriving. *Applied ergonomics,* 39**,** 191-198.

KONONENKO, I. Estimating attributes: analysis and extensions of RELIEF. Machine Learning: ECML-94, 1994. Springer, 171-182.

KOWALCZEWSKI, J., CHONG, S. L., GALEA, M. & PROCHAZKA, A. 2011. In-home tele-rehabilitation improves tetraplegic hand function. *Neurorehabilitation and neural repair,* 25**,** 412-422.

KREBS, H. I., AISEN, M. L., VOLPE, B. T. & HOGAN, N. 1999. Quantization of continuous arm movements in humans with brain injury. *Proceedings of the National Academy of Sciences,* 96**,** 4645-4649.

KWAKKEL, G., KOLLEN, B. J. & KREBS, H. I. 2007. Effects of robot-assisted therapy on upper limb recovery after stroke: a systematic review. *Neurorehabilitation and neural repair*.

KWAKKEL, G., KOLLEN, B. J., VAN DER GROND, J. & PREVO, A. J. 2003. Probability of regaining dexterity in the flaccid upper limb impact of severity of paresis and time since onset in acute stroke. *Stroke,* 34**,** 2181-2186.

LAMBERCY, O., DOVAT, L., GASSERT, R., BURDET, E., TEO, C. L. & MILNER, T. 2007. A haptic knob for rehabilitation of hand function. *IEEE Transactions on Neural Systems and Rehabilitation Engineering,* 15**,** 356-366.

LAMBERCY, O., LÜNENBURGER, L., GASSERT, R. & BOLLIGER, M. 2012. Robots for measurement/clinical assessment. *Neurorehabilitation Technology.* Springer.

LAMBERCY, O., MAGGIONI, S., LÜNENBURGER, L., GASSERT, R. & BOLLIGER, M. 2016. Robotic and wearable sensor technologies for measurements/clinical assessments. *Neurorehabilitation Technology.* Springer.

LAMBERCY, O., METZGER, J.-C., SANTELLO, M. & GASSERT, R. 2015. A method to study precision grip control in viscoelastic force fields using a robotic gripper. *IEEE Transactions on Biomedical Engineering,* 62**,** 39-48.

LAMBERCY, O., ROBLES, A. J., KIM, Y. & GASSERT, R. Design of a robotic device for assessment and rehabilitation of hand sensory function. 2011 IEEE International Conference on Rehabilitation Robotics, 2011. IEEE, 1-6.

LANG, C. E., STRUBE, M. J., BLAND, M. D., WADDELL, K. J., CHERRY-ALLEN, K. M., NUDO, R. J., DROMERICK, A. W. & BIRKENMEIER, R. L. 2016. Dose response of task-specific upper limb training in people at least 6 months poststroke: A phase II, single-blind, randomized, controlled trial. *Annals of Neurology,* 80**,** 342-354.

LASTAYO, P. & HARTZEL, J. 1999. Dynamic versus static grip strength: how grip strength changes when the wrist is moved, and why dynamic grip strength may be a more functional measurement. *Journal of Hand Therapy,* 12**,** 212-218.

LAWRENCE, B., BONINGER, M., COOPER, R. & SHIMADA, S. Effect of start-up kinetics on wheelchair pushrim dynamic analysis. Engineering in Medicine and Biology Society, 1997. Proceedings of the 19th Annual International Conference of the IEEE, 1997. IEEE, 1877-1879.

LEE, J.-A. & SECHACHALAM, S. 2016. The Effect of Wrist Position on Grip Endurance and Grip Strength. *The Journal of Hand Surgery,* 41**,** e367-e373.

LEE, J. & RIM, K. 1991. Measurement of finger joint angles and maximum finger forces during cylinder grip activity. *Journal of Biomedical Engineering,* 13**,** 152-162.

LEE, S. Y. & GALLAGHER, D. 2008. Assessment methods in human body composition. *Current opinion in clinical nutrition and metabolic care,* 11**,** 566.

LEMMENS, R. J., TIMMERMANS, A. A., JANSSEN-POTTEN, Y. J., PULLES, S. A., GEERS, R. P., BAKX, W. G., SMEETS, R. J. & SEELEN, H. A. 2014. Accelerometry measuring the outcome of robot-supported upper limb training in chronic stroke: a randomized controlled trial. *PloS one,* 9**,** e96414.

LEMMENS, R. J., TIMMERMANS, A. A., JANSSEN-POTTEN, Y. J., SMEETS, R. J. & SEELEN, H. A. 2012. Valid and reliable instruments for arm-hand assessment at ICF activity level in persons with hemiplegia: a systematic review. *BMC neurology,* 12**,** 1.

LEUENBERGER, K. & GASSERT, R. Low-power sensor module for long-term activity monitoring. 2011 Annual International Conference of the IEEE Engineering in Medicine and Biology Society, 2011. IEEE, 2237-2241.

LEUENBERGER, K., GONZENBACH, R., WACHTER, S., LUFT, A. & GASSERT, R. 2016. A method to qualitatively assess arm use in stroke survivors in the home environment. *Medical & biological engineering & computing***,** 1-10.

LEUENBERGER, K., GONZENBACH, R., WIEDMER, E., LUFT, A. & GASSERT, R. Classification of stair ascent and descent in stroke patients. Wearable and Implantable Body Sensor Networks Workshops (BSN Workshops), 2014 11th International Conference on, 2014. IEEE, 11-16.

LEUENBERGER, K., HOFMANN, R., BRUGGER, P. & GASSERT, R. 2015. Measurement of human rotation behavior for psychological and neuropsychological investigations. *Behavior research methods,* 47**,** 1425-1435.

LEUENBERGER, K. D. 2015. *Long-term activity and movement monitoring in neurological patients.* Dissertation, ETH-Zürich, 2015, Nr. 23116.

LI, Z.-M. 2002. The influence of wrist position on individual finger forces during forceful grip. *The Journal of hand surgery,* 27**,** 886-896.

LINCOLN, N. B., PARRY, R. H. & VASS, C. D. 1999. Randomized, controlled trial to evaluate increased intensity of physiotherapy treatment of arm function after stroke. *Stroke,* 30**,** 573-579.

LLOYD-JONES, D., ADAMS, R., CARNETHON, M., DE SIMONE, G., FERGUSON, T. B., FLEGAL, K., FORD, E., FURIE, K., GO, A. & GREENLUND, K. 2009. Heart disease and stroke statistics—2009 update a report from the American Heart Association Statistics Committee and Stroke Statistics Subcommittee. *Circulation,* 119**,** e21-e181.

LONG, C., CONRAD, P., HALL, E. & FURLER, S. 1970. Intrinsic-extrinsic muscle control of the hand in power grip and precision handling. *J Bone Joint Surg Am,* 52**,** 853-867.

LU, X., BATTISTUZZO, C. R., ZOGHI, M. & GALEA, M. P. 2015. Effects of training on upper limb function after cervical spinal cord injury: a systematic review. *Clinical rehabilitation,* 29**,** 3-13.

LUM, P. S., GODFREY, S. B., BROKAW, E. B., HOLLEY, R. J. & NICHOLS, D. 2012. Robotic approaches for rehabilitation of hand function after stroke. *American Journal of Physical Medicine & Rehabilitation,* 91**,** S242-S254.

MAIER, I. C., BAUMANN, K., THALLMAIR, M., WEINMANN, O., SCHOLL, J. & SCHWAB, M. E. 2008. Constraint-induced movement therapy in the adult rat after unilateral corticospinal tract injury. *The Journal of Neuroscience,* 28**,** 9386-9403.

MAIER, M. A. & HEPP-REYMOND, M.-C. 1995. EMG activation patterns during force production in precision grip. *Experimental Brain Research,* 103**,** 108-122.

MASIA, L., CASADIO, M., GIANNONI, P., SANDINI, G. & MORASSO, P. 2009. Performance adaptive training control strategy for recovering wrist movements in stroke patients: a preliminary, feasibility study. *Journal of neuroengineering and rehabilitation,* 6**,** 44.

MATHIOWETZ, V., FEDERMAN, S. & WIEMER, D. 1985a. Box and block test of manual dexterity: norms for 6–19 year olds. *Canadian Journal of Occupational Therapy,* 52**,** 241-245.

MATHIOWETZ, V., KASHMAN, N., VOLLAND, G., WEBER, K., DOWE, M. & ROGERS, S. 1985b. Grip and pinch strength: normative data for adults. *Arch Phys Med Rehabil,* 66**,** 69-74.

MATHIOWETZ, V., RENNELLS, C. & DONAHOE, L. 1985c. Effect of elbow position on grip and key pinch strength. *The Journal of hand surgery,* 10**,** 694-697.

MAURER, U., ROWE, A., SMAILAGIC, A. & SIEWIOREK, D. 2006. Location and activity recognition using eWatch: A wearable sensor platform. *Ambient Intelligence in Everyday Life.* Springer.

MCCOLL, M. A., WALKER, J., STIRLING, P., WILKINS, R. & COREY, P. 1997. Expectations of life and health among spinal cord injured adults. *Spinal cord,* 35**,** 818-828.

MCDONNELL, M. N., HILLIER, S. L., RIDDING, M. C. & MILES, T. S. 2006. Impairments in precision grip correlate with functional measures in adult hemiplegia. *Clinical Neurophysiology,* 117**,** 1474-1480.

MCDOWELL, I. 2006. *Measuring health: a guide to rating scales and questionnaires*, Oxford university press.

MELENDEZ-CALDERON, A., MASIA, L., GASSERT, R., SANDINI, G. & BURDET, E. 2011. Force field adaptation can be learned using vision in the absence of proprioceptive error. *IEEE Transactions on Neural Systems and Rehabilitation Engineering,* 19**,** 298-306.

MESKERS, C. G., SCHOUTEN, A. C., DE GROOT, J. H., DE VLUGT, E., VAN HILTEN, B. J., VAN DER HELM, F. C. & ARENDZEN, H. J. 2009. Muscle weakness and lack of reflex gain adaptation predominate during post-stroke posture control of the wrist. *Journal of neuroengineering and rehabilitation,* 6**,** 1.

METOKI, N., SATO, Y., SATOH, K., OKUMURA, K. & IWAMOTO, J. 2003. Muscular atrophy in the hemiplegic thigh in patients after stroke. *American journal of physical medicine & rehabilitation,* 82**,** 862-865.

METZGER, J.-C., LAMBERCY, O., CALIFFI, A., CONTI, F. M. & GASSERT, R. 2014a. Neurocognitive robot-assisted therapy of hand function. *IEEE transactions on haptics,* 7**,** 140-149.

METZGER, J.-C., LAMBERCY, O., CALIFFI, A., DINACCI, D., PETRILLO, C., ROSSI, P., CONTI, F. M. & GASSERT, R. 2014b. Assessment-driven selection and adaptation of exercise difficulty in robot-assisted therapy: a pilot study with a hand rehabilitation robot. *Journal of neuroengineering and rehabilitation,* 11**,** 1.

METZGER, J.-C., LAMBERCY, O., CHAPUIS, D. & GASSERT, R. Design and characterization of the ReHapticKnob, a robot for assessment and therapy of hand function. 2011 IEEE/RSJ International Conference on Intelligent Robots and Systems, 2011. IEEE, 3074-3080.

MEYER, K., SIMMET, A., ARNOLD, M., MATTLE, H. & NEDELTCHEV, K. 2009. Stroke events and case fatalities in Switzerland based on hospital statistics and cause of death statistics. *Swiss medical weekly,* 139**,** 65.

MIFFLIN, M. D., ST JEOR, S. T., HILL, L. A., SCOTT, B. J., DAUGHERTY, S. A. & KOH, Y. 1990. A new predictive equation for resting energy expenditure in healthy individuals. *The American journal of clinical nutrition,* 51**,** 241-247.

MILNER, T. E. & CLOUTIER, C. 1993. Compensation for mechanically unstable loading in voluntary wrist movement. *Experimental Brain Research,* 94**,** 522-532.

MILNER, T. E. & CLOUTIER, C. 1998. Damping of the wrist joint during voluntary movement. *Experimental Brain Research,* 122**,** 309-317.

MILOT, M. H., MARCHAL-CRESPO, L., GREEN, C. S., CRAMER, S. C. & REINKENSMEYER, D. J. 2010. Comparison of error-amplification and haptic-guidance training techniques for learning of a timing-based motor task by healthy individuals. *Experimental Brain Research,* 201**,** 119-131.

MOHAMMAD, Y. A. A. 2005. Anthropometric characteristics of the hand based on laterality and sex among Jordanian. *International Journal of Industrial Ergonomics,* 35**,** 747-754.

MONCADA-TORRES, A., LEUENBERGER, K., GONZENBACH, R., LUFT, A. & GASSERT, R. 2014. Activity classification based on inertial and barometric pressure sensors at different anatomical locations. *Physiological measurement,* 35**,** 1245.

MORSE, J. L., JUNG, M. C., BASHFORD, G. R. & HALLBECK, M. S. 2006. Maximal dynamic grip force and wrist torque: The effects of gender, exertion direction, angular velocity, and wrist angle. *Applied ergonomics,* 37**,** 737-742.

MOTL, R. W., MCAULEY, E., SNOOK, E. M. & GLIOTTONI, R. C. 2009. Physical activity and quality of life in multiple sclerosis: intermediary roles of disability, fatigue, mood, pain, self-efficacy and social support. *Psychology Health and Medicine,* 14**,** 111-124.

MOZAFFARIAN, D., BENJAMIN, E. J., GO, A. S., ARNETT, D. K., BLAHA, M. J., CUSHMAN, M., DE FERRANTI, S., DESPRES, J., FULLERTON, H. & HOWARD, V. 2015. Heart disease and stroke statistics--2015 update: A report from the American Heart Association. *Circulation,* 131**,** e29.

MULTON, S., FRANZEN, R., POIRRIER, A.-L., SCHOLTES, F. & SCHOENEN, J. 2003. The effect of treadmill training on motor recovery after a partial spinal cord compression-injury in the adult rat. *Journal of neurotrauma,* 20**,** 699-706.

MYERS, J., LEE, M. & KIRATLI, J. 2007. Cardiovascular disease in spinal cord injury: an overview of prevalence, risk, evaluation, and management. *American journal of physical medicine & rehabilitation,* 86**,** 142-152.

NASH, M. S. 2005. Exercise as a Health-Promoting Activity Following Spinal Cord Injury. *Journal of Neurologic Physical Therapy,* 29**,** 87-103,106.

NG, P. K., BEE, M. C., SAPTARI, A. & MOHAMAD, N. A. 2014. A review of different pinch techniques. *Theoretical Issues in Ergonomics Science,* 15**,** 517-533.

NGUYEN, D. & WIDROW, B. Improving the learning speed of 2-layer neural networks by choosing initial values of the adaptive weights. Neural Networks, 1990., 1990 IJCNN International Joint Conference on, 1990. IEEE, 21-26.

NIGHTINGALE, T., WALHIN, J., THOMPSON, D. & BILZON, J. 2015. Predicting physical activity energy expenditure in wheelchair users with a multisensor device. *BMJ Open Sport & Exercise Medicine,* 1**,** bmjsem-2015-000008.

NIJLAND, R. H., VAN WEGEN, E. E., HARMELING-VAN DER WEL, B. C., KWAKKEL, G. & INVESTIGATORS, E. 2010. Presence of finger extension and shoulder abduction within 72 hours after stroke predicts functional recovery early prediction of functional outcome after stroke: the EPOS cohort study. *Stroke,* 41**,** 745-750.

NILSEN, T., HERMANN, M., ERIKSEN, C. S., DAGFINRUD, H., MOWINCKEL, P. & KJEKEN, I. 2012. Grip force and pinch grip in an adult population: reference values and factors associated with grip force. *Scandinavian journal of occupational therapy,* 19**,** 288-296.

NOOIJEN, C. F., DE GROOT, S., POSTMA, K., BERGEN, M. P., STAM, H. J., BUSSMANN, J. & VAN DEN BERG-EMONS, R. 2012. A more active lifestyle in persons with a recent spinal cord injury benefits physical fitness and health. *Spinal Cord,* 50**,** 320-323.

NORTON, J. A. & GORASSINI, M. A. 2006. Changes in cortically related intermuscular coherence accompanying improvements in locomotor skills in incomplete spinal cord injury. *Journal of neurophysiology,* 95**,** 2580-2589.

NSCISC 2010. Annual report for the spinal cord injury model systems. *National Spinal Cord Injury Statistical Center, Birmingham, Alabama, which is funded by grant*.

O'DRISCOLL, S. W., HORII, E., NESS, R., CAHALAN, T. D., RICHARDS, R. R. & AN, K.-N. 1992. The relationship between wrist position, grasp size, and grip strength. *The Journal of hand surgery,* 17**,** 169-177.

O'DWYER, N., ADA, L. & NEILSON, P. 1996. Spasticity and muscle contracture following stroke. *Brain,* 119**,** 1737-1749.

OJEDA, M. & DING, D. 2014. Temporal Parameters Estimation for Wheelchair Propulsion Using Wearable Sensors. *BioMed research international,* 2014.

OLANOW, C. W., STERN, M. B. & SETHI, K. 2009. The scientific and clinical basis for the treatment of Parkinson disease (2009). *Neurology,* 72**,** S1-S136.

OSU, R., FRANKLIN, D. W., KATO, H., GOMI, H., DOMEN, K., YOSHIOKA, T. & KAWATO, M. 2002. Short-and long-term changes in joint co-contraction associated with motor learning as revealed from surface EMG. *Journal of Neurophysiology,* 88**,** 991-1004.

OYSTER, M. L., KARMARKAR, A. M., PATRICK, M., READ, M. S., NICOLINI, L. & BONINGER, M. L. 2011. Investigation of factors associated with manual wheelchair mobility in persons with spinal cord injury. *Archives of physical medicine and rehabilitation,* 92**,** 484-490.

PARVATIKAR, V. & MUKKANNAVAR, P. 2009. Comparative study of grip strength in different positions of shoulder and elbow with wrist in neutral and extension positions. *Journal of Exercise Science and Physiotherapy,* 5**,** 67.

PATE, R. R., PRATT, M., BLAIR, S. N., HASKELL, W. L., MACERA, C. A., BOUCHARD, C., BUCHNER, D., ETTINGER, W., HEATH, G. W. & KING, A. C. 1995. Physical activity and public health: a recommendation from the Centers for Disease Control and Prevention and the American College of Sports Medicine. *Jama,* 273**,** 402-407.

PERREAULT, E. J., KIRSCH, R. F. & CRAGO, P. E. 2004. Multijoint dynamics and postural stability of the human arm. *Experimental brain research,* 157**,** 507-517.

PERRET, C., BERRY, H., HUNT, K. J., DONALDSON, N. & KAKEBEEKE, T. H. 2010. Feasibility of functional electrical stimulated cycling in subjects with spinal cord injury: an energetics assessment. *Journal of rehabilitation medicine,* 42**,** 873-875.

PHILLIPS, W. T., KIRATLI, B. J., SARKARATI, M., WERAARCHAKUL, G., MYERS, J., FRANKLIN, B. A., PARKASH, I. & FROELICHER, V. 1998. Effect of spinal cord injury on the heart and cardiovascular fitness. *Current problems in cardiology,* 23**,** 641-716.

PLATZ, T., PINKOWSKI, C., VAN WIJCK, F., KIM, I.-H., DI BELLA, P. & JOHNSON, G. 2005. Reliability and validity of arm function assessment with standardized guidelines for the Fugl-Meyer Test, Action Research Arm Test and Box and Block Test: a multicentre study. *Clinical Rehabilitation,* 19**,** 404-411.

PLEWA, K., POTVIN, J. R. & DICKEY, J. P. 2016. Wrist rotations about one or two axes affect maximum wrist strength. *Applied ergonomics,* 53**,** 152-160.

POPP, W. L., BROGIOLI, M., LEUENBERGER, K., ALBISSER, U., FROTZLER, A., CURT, A., GASSERT, R. & STARKEY, M. L. 2016a. A novel algorithm for detecting active propulsion in wheelchair users following spinal cord injury. *Medical engineering & physics,* 38**,** 267-274.

POPP, W. L., LAMBERCY, O., MÜLLER, C. & GASSERT, R. 2016b. Effect of Handle Design on Movement Dynamics and Muscle Co-activation in a Wrist Flexion Task. *Int J Ind Ergon,* 56**,** 170-180.

POSTMA, K., BUSSMANN, J., SLUIS, T., BERGEN, M. & STAM, H. 2005. Validity of the detection of wheelchair propulsion as measured with an Activity Monitor in patients with spinal cord injury. *Spinal Cord,* 43**,** 550-557.

POSTON, B., DANNA-DOS SANTOS, A., JESUNATHADAS, M., HAMM, T. M. & SANTELLO, M. 2010. Force-independent distribution of correlated neural inputs to hand muscles during three-digit grasping. *Journal of neurophysiology,* 104**,** 1141-1154.

PRANGE, G. B., JANNINK, M. J., GROOTHUIS-OUDSHOORN, C. G., HERMENS, H. J. & IJZERMAN, M. J. 2006. Systematic review of the effect of robot-aided therapy on recovery of the hemiparetic arm after stroke. *Journal of rehabilitation research and development,* 43**,** 171.

PRYCE, J. C. 1980. The wrist position between neutral and ulnar deviation that facilitates the maximum power grip strength. *Journal of biomechanics,* 13**,** 505-511.

RAGHAVAN, P. 2007. The nature of hand motor impairment after stroke and its treatment. *Current treatment options in cardiovascular medicine,* 9**,** 221-228.

RAGHAVAN, P., PETRA, E., KRAKAUER, J. W. & GORDON, A. M. 2006. Patterns of impairment in digit independence after subcortical stroke. *Journal of neurophysiology,* 95**,** 369-378.

RATHORE, S. S., HINN, A. R., COOPER, L. S., TYROLER, H. A. & ROSAMOND, W. D. 2002. Characterization of incident stroke signs and symptoms findings from the atherosclerosis risk in communities study. *Stroke,* 33**,** 2718-2721.

RAUCH, A., HINRICHS, T., OBERHAUSER, C., CIEZA, A. & GROUP, S. S. 2016. Do people with spinal cord injury meet the WHO recommendations on physical activity? *International journal of public health,* 61**,** 17-27.

RAVI, N., DANDEKAR, N., MYSORE, P. & LITTMAN, M. L. Activity recognition from accelerometer data. AAAI, 2005. 1541-1546.

RINDERKNECHT, M. D., POPP, W. L., LAMBERCY, O. & GASSERT, R. Experimental validation of a rapid, adaptive robotic assessment of the MCP joint angle difference threshold. International Conference on Human Haptic Sensing and Touch Enabled Computer Applications, 2014. Springer, 3-10.

RINDERKNECHT, M. D., POPP, W. L., LAMBERCY, O. & GASSERT, R. 2016. Reliable and Rapid Robotic Assessment of Wrist Proprioception Using a Gauge Position Matching Paradigm. *Frontiers in Human Neuroscience,* 10.

ROH, J., RYMER, W. Z., PERREAULT, E. J., YOO, S. B. & BEER, R. F. 2013. Alterations in upper limb muscle synergy structure in chronic stroke survivors. *Journal of neurophysiology,* 109**,** 768-781.

ROSENBERG, J., AMJAD, A., BREEZE, P., BRILLINGER, D. & HALLIDAY, D. 1989. The Fourier approach to the identification of functional coupling between neuronal spike trains. *Progress in biophysics and molecular biology,* 53**,** 1-31.

ROZA, A. M. & SHIZGAL, H. M. 1984. The Harris Benedict equation reevaluated: resting energy requirements and the body cell mass. *The American journal of clinical nutrition,* 40**,** 168-182.

RUDHE, C. & VAN HEDEL, H. J. 2009. Upper extremity function in persons with tetraplegia: Relationships between strength, capacity and the Spinal Cord Independence Measure. *Neurorehabilitation and neural repair*.

RUDICK, R. A. & MILLER, D. M. 2008. Health-related quality of life in multiple sclerosis. *CNS drugs,* 22**,** 827-839.

SADEH, A. 2011. The role and validity of actigraphy in sleep medicine: an update. *Sleep medicine reviews,* 15**,** 259-267.

SAMSA, G. P., PATRICK, C. H. & FEUSSNER, J. R. 1993. Long-term survival of veterans with traumatic spinal cord injury. *Archives of Neurology,* 50**,** 909-914.

SANGANI, S. G., STARSKY, A. J., MCGUIRE, J. R. & SCHMIT, B. D. 2007. Multijoint reflexes of the stroke arm: neural coupling of the elbow and shoulder. *Muscle & nerve,* 36**,** 694-703.

SANTOS-CARRERAS, L., HAGEN, M., GASSERT, R. & BLEULER, H. 2012. Survey on Surgical Instrument Handle Design Ergonomics and Acceptance. *Surgical Innovation,* 19**,** 50-59.

SAVIC, G., BERGSTRÖM, E., FRANKEL, H., JAMOUS, M. & JONES, P. 2007. Inter-rater reliability of motor and sensory examinations performed according to American Spinal Injury Association standards. *Spinal cord,* 45**,** 444-451.

SEO, N. J., ARMSTRONG, T. J., ASHTON-MILLER, J. A. & CHAFFIN, D. B. 2007. The effect of torque direction and cylindrical handle diameter on the coupling between the hand and a cylindrical handle. *Journal of biomechanics,* 40**,** 3236-3243.

SEO, N. J., RYMER, W. Z. & KAMPER, D. G. 2010. Altered digit force direction during pinch grip following stroke. *Experimental brain research,* 202**,** 891-901.

SHADMEHR, R. & MUSSA-IVALDI, F. A. 1994. Adaptive representation of dynamics during learning of a motor task. *The Journal of Neuroscience,* 14**,** 3208-3224.

SHIVERS, C. L., MIRKA, G. A. & KABER, D. B. 2002. Effect of grip span on lateral pinch grip strength. *Human Factors: The Journal of the Human Factors and Ergonomics Society,* 44**,** 569-577.

SINDALL, P., LENTON, J. P., WHYTOCK, K., TOLFREY, K., OYSTER, M. L., COOPER, R. A. & GOOSEY-TOLFREY, V. L. 2013. Criterion validity and accuracy of global positioning satellite and data logging devices for wheelchair tennis court movement. *The journal of spinal cord medicine,* 36**,** 383-393.

SONENBLUM, S. E., SPRIGLE, S., CASPALL, J. & LOPEZ, R. 2012a. Validation of an accelerometer-based method to measure the use of manual wheelchairs. *Medical engineering & physics,* 34**,** 781-786.

SONENBLUM, S. E., SPRIGLE, S. & LOPEZ, R. A. 2012b. Manual wheelchair use: bouts of mobility in everyday life. *Rehabilitation research and practice,* 2012.

SPIVAK, E., OKSENBERG, A. & CATZ, A. 2007. The feasibility of sleep assessment by actigraph in patients with tetraplegia. *Spinal Cord,* 45**,** 765-770.

SPOOREN, A., JANSSEN-POTTEN, Y., KERCKHOFS, E., BONGERS, H. & SEELEN, H. 2011. ToCUEST: a task-oriented client-centered training module to improve upper extremity skilled performance in cervical spinal cord-injured persons. *Spinal cord,* 49**,** 1042-1048.

SPURR, G., PRENTICE, A., MURGATROYD, P., GOLDBERG, G., REINA, J. & CHRISTMAN, N. 1988. Energy expenditure from minute-by-minute heart-rate recording: comparison with indirect calorimetry. *The American journal of clinical nutrition,* 48**,** 552-559.

STARKEY, M. L., BLEUL, C., KASPER, H., MOSBERGER, A. C., ZÖRNER, B., GIGER, S., GULLO, M., BUSCHMANN, F. & SCHWAB, M. E. 2014. High-impact, self-motivated training within an enriched environment with single animal tracking dose-dependently promotes motor skill acquisition and functional recovery. *Neurorehabilitation and neural repair***,** 1545968314520721.

STAUDENMAYER, J., POBER, D., CROUTER, S., BASSETT, D. & FREEDSON, P. 2009. An artificial neural network to estimate physical activity energy expenditure and identify physical activity type from an accelerometer. *Journal of Applied Physiology,* 107**,** 1300-1307.

STIKIC, M., HUYNH, T., VAN LAERHOVEN, K. & SCHIELE, B. ADL recognition based on the combination of RFID and accelerometer sensing. 2008 Second International Conference on Pervasive Computing Technologies for Healthcare, 2008a. IEEE, 258-263.

STIKIC, M., HUYNH, T., VAN LAERHOVEN, K. & SCHIELE, B. ADL recognition based on the combination of RFID and accelerometer sensing. Pervasive Computing Technologies for Healthcare, 2008. PervasiveHealth 2008. Second International Conference on, 2008b. IEEE, 258-263.

STINEAR, C. M., BARBER, P. A., PETOE, M., ANWAR, S. & BYBLOW, W. D. 2012. The PREP algorithm predicts potential for upper limb recovery after stroke. *Brain,* 135**,** 2527-2535.

STOVER, S. & FINE, P. 1987. The epidemiology and economics of spinal cord injury. *Spinal Cord,* 25**,** 225-228.

STROHRMANN, C., LABRUYÈRE, R., GERBER, C. N., VAN HEDEL, H. J., ARNRICH, B. & TRÖSTER, G. 2013. Monitoring motor capacity changes of children during rehabilitation using body-worn sensors. *Journal of neuroengineering and rehabilitation,* 10**,** 1.

SULLIVAN, J. E. & HEDMAN, L. D. 2015. Sensory dysfunction following stroke: incidence, significance, examination, and intervention. *Topics in stroke rehabilitation*.

SUMINSKI, A. J., ZIMBELMAN, J. L. & SCHEIDT, R. A. 2007. Design and validation of a MR-compatible pneumatic manipulandum. *Journal of neuroscience methods,* 163**,** 255-266.

SUNDERLAND, A., TINSON, D., BRADLEY, L. & HEWER, R. L. 1989. Arm function after stroke. An evaluation of grip strength as a measure of recovery and a prognostic indicator. *Journal of Neurology, Neurosurgery & Psychiatry,* 52**,** 1267-1272.

SWARTZ, A. M., STRATH, S. J., BASSETT, D. R., O BRIEN, W. L., KING, G. A. & AINSWORTH, B. E. 2000. Estimation of energy expenditure using CSA accelerometers at hip and wrist sites. *Medicine and Science in Sports and Exercise,* 32**,** S450-S456.

TAKAHASHI, C. D. & REINKENSMEYER, D. J. 2003. Hemiparetic stroke impairs anticipatory control of arm movement. *Experimental brain research,* 149**,** 131-140.

TAUB, E., MILLER, N., NOVACK, T., COOK 3RD, E., FLEMING, W., NEPOMUCENO, C., CONNELL, J. & CRAGO, J. 1993. Technique to improve chronic motor deficit after stroke. *Archives of physical medicine and rehabilitation,* 74**,** 347-354.

TAUB, E., USWATTE, G., BOWMAN, M. H., MARK, V. W., DELGADO, A., BRYSON, C., MORRIS, D. & BISHOP-MCKAY, S. 2013. Constraint-induced movement therapy combined with conventional neurorehabilitation techniques in chronic stroke patients with plegic hands: a case series. *Archives of physical medicine and rehabilitation,* 94**,** 86-94.

TEASELL, R. W., FOLEY, N. C., BHOGAL, S. K. & SPEECHLEY, M. R. 2015. An evidence-based review of stroke rehabilitation. *Topics in stroke Rehabilitation*.

THRANE, G., EMAUS, N., ASKIM, T. & ANKE, A. 2011. Arm use in patients with subacute stroke monitored by accelerometry: association with motor impairment and influence on self-dependence. *Journal of rehabilitation medicine,* 43**,** 299-304.

TOFALLIS, C. 2009. Least squares percentage regression. *Journal of Modern Applied Statistical Methods*.

TOMATIS, L., NAKASEKO, M. & LÄUBLI, T. 2009. Co-activation and maximal EMG activity of forearm muscles during key tapping. *International Journal of Industrial Ergonomics,* 39**,** 749-755.

TUDOR-LOCKE, C. & BASSETT JR, D. R. 2004. How many steps/day are enough? *Sports medicine,* 34**,** 1-8.

TWITCHELL, T. E. 1951. The restoration of motor function following hemiplegia in man. *Brain,* 74**,** 443-480.

U.S. DEPARTMENT OF HEALHT AND HUMAN SERVICES 2008. Physical activity guidelines for Americans.

USWATTE, G., GIULIANI, C., WINSTEIN, C., ZERINGUE, A., HOBBS, L. & WOLF, S. L. 2006. Validity of accelerometry for monitoring real-world arm activity in patients with subacute stroke: evidence from the extremity constraint-induced therapy evaluation trial. *Archives of physical medicine and rehabilitation,* 87**,** 1340-1345.

USWATTE, G., MILTNER, W. H., FOO, B., VARMA, M., MORAN, S. & TAUB, E. 2000. Objective measurement of functional upper-extremity movement using accelerometer recordings transformed with a threshold filter. *Stroke,* 31**,** 662-667.

USWATTE, G., TAUB, E., MORRIS, D., VIGNOLO, M. & MCCULLOCH, K. 2005. Reliability and validity of the upper-extremity Motor Activity Log-14 for measuring real-world arm use. *Stroke,* 36**,** 2493-2496.

VAN DEN BERG-EMONS, R. J., BUSSMANN, J. B., HAISMA, J. A., SLUIS, T. A., VAN DER WOUDE, L. H., BERGEN, M. P. & STAM, H. J. 2008. A prospective study on physical activity levels after spinal cord injury during inpatient rehabilitation and the year after discharge. *Archives of physical medicine and rehabilitation,* 89**,** 2094-2101.

VAN DER PAS, S. C., VERBUNT, J. A., BREUKELAAR, D. E., VAN WOERDEN, R. & SEELEN, H. A. 2011. Assessment of arm activity using triaxial accelerometry in patients with a stroke. *Archives of physical medicine and rehabilitation,* 92**,** 1437-1442.

VAN PEPPEN, R. P., KWAKKEL, G., WOOD-DAUPHINEE, S., HENDRIKS, H. J., VAN DER WEES, P. J. & DEKKER, J. 2004. The impact of physical therapy on functional outcomes after stroke: what's the evidence? *Clinical rehabilitation,* 18**,** 833-862.

VANHEES, L., LEFEVRE, J., PHILIPPAERTS, R., MARTENS, M., HUYGENS, W., TROOSTERS, T. & BEUNEN, G. 2005. How to assess physical activity? How to assess physical fitness? *European Journal of Cardiovascular Prevention & Rehabilitation,* 12**,** 102-114.

VIGARU, B., SULZER, J. & GASSERT, R. 2016. Design and Evaluation of a Cable-Driven fMRI-Compatible Haptic Interface to Investigate Precision Grip Control. *IEEE transactions on haptics,* 9**,** 20-32.

VLAAR, M., SOLIS-ESCALANTE, T., VARDY, A., VAN DER HELM, F. & SCHOUTEN, A. 2016. Quantifying Nonlinear Contributions to Cortical Responses Evoked by Continuous Wrist Manipulation.

WARBURTON, D. E., NICOL, C. W. & BREDIN, S. S. 2006. Health benefits of physical activity: the evidence. *Canadian medical association journal,* 174**,** 801-809.

WARMS, C. A., WHITNEY, J. D. & BELZA, B. 2008. Measurement and description of physical activity in adult manual wheelchair users. *Disability and health journal,* 1**,** 236-244.

WASHBURN, R. & HEDRICK, B. 1997. Descriptive epidemiology of physical activity in university graduates with locomotor disabilities. *International Journal of Rehabilitation Research,* 20**,** 275-288.

WELK, G. 2002. *Physical activity assessments for health-related research*, Human Kinetics.

WESTERTERP, K. R. 2009. Assessment of physical activity: a critical appraisal. *European journal of applied physiology,* 105**,** 823-828.

WHO 2013. International Classification of Functioning, Disability and Health: ICF. Geneva: WHO; 2001. *Also available from: URL: http://www. who. int/classifications/icf/en [cited 2014 Jan 9]*.

WILLIAMSON, A. & HOGGART, B. 2005. Pain: a review of three commonly used pain rating scales. *Journal of clinical nursing,* 14**,** 798-804.

WILSON, T., BRAY, G. A., TEMPLE, N. J. & STRUBLE, M. B. 2010. *Nutrition guide for physicians*, Springer.

WOLPERT, D. M. & FLANAGAN, J. R. 2010. Q&A: Robotics as a tool to understand the brain. *BMC biology,* 8**,** 92.

WREN, T. A. L., PATRICK DO, K., RETHLEFSEN, S. A. & HEALY, B. 2006. Cross-correlation as a method for comparing dynamic electromyography signals during gait. *Journal of biomechanics,* 39**,** 2714-2718.

WYNDAELE, M. & WYNDAELE, J.-J. 2006. Incidence, prevalence and epidemiology of spinal cord injury: what learns a worldwide literature survey? *Spinal cord,* 44**,** 523-529.

YAMAZAKI, T., GEN-NO, H., KAMIJO, Y., OKAZAKI, K., MASUKI, S. & NOSE, H. 2009. A new device to estimate VO2 during incline walking by accelerometry and barometry. *Medicine and science in sports and exercise,* 41**,** 2213-2219.

YOSHII, Y., YUINE, H., KAZUKI, O., TUNG, W.-L. & ISHII, T. 2015. Measurement of wrist flexion and extension torques in different forearm positions. *BioMedical Engineering OnLine,* 14**,** 115.

YOUNG, J. G., WOOLLEY, C., ARMSTRONG, T. J. & ASHTON-MILLER, J. A. 2009. Hand-handhold coupling: effect of handle shape, orientation, and friction on breakaway strength. *Human Factors: The Journal of the Human Factors and Ergonomics Society,* 51**,** 705-717.

ZARIFFA, J., KAPADIA, N., KRAMER, J., TAYLOR, P., ALIZADEH-MEGHRAZI, M., ZIVANOVIC, V., WILLMS, R., TOWNSON, A., CURT, A. & POPOVIC, M. 2012. Feasibility and efficacy of upper limb robotic rehabilitation in a subacute cervical spinal cord injury population. *Spinal Cord,* 50**,** 220-226.

ZEILER, S. R. & KRAKAUER, J. W. 2013. The interaction between training and plasticity in the post-stroke brain. *Current opinion in neurology,* 26**,** 609.

ZENNARO, D., LÄUBLI, T., KREBS, D., KLIPSTEIN, A. & KRUEGER, H. 2003. Continuous, intermitted and sporadic motor unit activity in the trapezius muscle during prolonged computer work. *Journal of Electromyography and Kinesiology,* 13**,** 113-124.